

“Analysis, Design & Implementation of Reduced Complexity & Near Optimal Performance Semi-Blind Channel Estimation Techniques for Wireless MIMO Communication System”

A thesis submitted
for the award of the degree of

DOCTOR OF PHILOSOPHY

in

Electrical Engineering

By

Jaymin Kantilal Bhalani



DEPARTMENT OF ELECTRICAL ENGINEERING
FACULTY OF TECHNOLOGY & ENGINEERING
THE MAHARAJA SAYAJIRAO UNIVERSITY OF BARODA
VADODARA – 390 001 GUJARAT, INDIA
JULY 2012

ACKNOWLEDGEMENTS

This thesis could not have been completed without the help and support of many people. My utmost gratitude to the omnipresent God, for providing me inspiration, strength, energy and patience to start and accomplish my goal. First and foremost, I would like to express my sincere thanks with deep sense of gratitude to my guide **Prof. A. I. Trivedi**, for his guidance, support, and encouragement throughout the course of this work. He has given me excellent guidance, yet allowed me ample freedom in my research. The direction, advice, discussions and constant motivation given by him have been so helpful that it enabled me to complete work successfully. He created and pointed to the path and helped in every way to reach this final destination. It has truly been an honor to work under his supervision. My special thanks to my co-guide **Dr. Yogesh P. Kosta** for his valuable and excellent guidance.

I express my profound thanks to **Prof. S.K. Shah**, Head of Electrical Engineering Department, Faculty of Technology & Engineering, M.S. University of Baroda, for his kind support and guidance throughout of my work. I am also very thankful to **Prof. S. K. Joshi** and all the faculty members and supporting staff of Electrical Engineering Department, Faculty of Technology and Engineering, M.S. University of Baroda.

I express my sincere thanks to **CHARUSAT** management, **Provost, Registrar, Advisors, Principal (C.S.P.I.T.)** and **Dean (Faculty of Technology & Engineering)** for their kind support and continuous motivation to get my work done. My special thanks to my colleague friends **Mr. Brijesh Shah, Mr. Sarman Hadia, Mr. Dharmendra Chauhan, Mr. Sagar Patel,** and **Mr. Trushit Upadhyay** for their help and support. I am also very thankful to **Prof. J. C. Prajapati** and **Prof. Vymoesh Nandurbarkar**, for their guidance in the subjects of Mathematics and Linear Algebra for the mathematical modeling of algorithms.

I would like to thank some senior professors **Prof. J. V. Dave, Prof. K. R. Parmar, Prof. K. G. Maradia, Prof. M. V. Shah, Prof. Usha Nilkanthan** and **Prof. R.A. Thakkar** for their inspirations.

With immense affection, I am very thankful to my **parents**, who showered love and affection on me. They guided me through my first steps to this milestone in my life and always supported me. They taught me to read, think and analyze.

I express my special thanks to my dearest wife **Amruta** and my son **Saumya** for all the support, inspiration and love given to me despite of all inconvenience caused to them due to my preoccupation with Ph.D. work. I am also thankful to my sisters **Urvi** and **Dhara** for their support.

Last but not the least; I am very thankful to all who helped me directly or indirectly in progressing towards my goal.

July, 2012

Jaymin Kantilal Bhalani

CERTIFICATE

This is to certify that the thesis titled “**Analysis, Design & Implementation of Reduced Complexity & Near Optimal Performance Semi-Blind Channel Estimation Techniques for Wireless MIMO Communication System**” submitted by “**JAYMIN KANTILAL BHALANI**” in fulfillment of the degree of **DOCTOR OF PHILOSOPHY** in Electrical Engineering Department, Faculty of Technology & Engineering, The M. S. University of Baroda, Vadodara is a bonafide record of investigations carried out by him in the Department of Electrical Engineering, Faculty of Technology & Engineering, M. S. University of Baroda, Vadodara under my guidance and supervision. In my opinion this has attained the standard fulfilling the requirements of the Ph.D. Degree as prescribed in the regulations of the University.

July, 2012

Guide:

Prof. A. I. Trivedi

Department of Electrical Engineering,
Faculty of Technology & Engineering,
The Maharaja Sayajirao University of Baroda
Vadodara – 390 001

Head:

Prof. S.K. Shah

Department of Electrical Engineering,
Faculty of Technology & Engineering,
The Maharaja Sayajirao University of
Baroda
Vadodara – 390 001

Dean:

Prof. A. N. Misra

Faculty of Technology & Engineering,
The Maharaja Sayajirao University of
Baroda.
Vadodara – 390 001

DECLARATION

I, **Jaymin Kantilal Bhalani** hereby declare that the work reported in this thesis titled, “**Analysis, Design & Implementation of Reduced Complexity & Near Optimal Performance Semi-Blind Channel Estimation Techniques for Wireless MIMO Communication System**” submitted for the award of the degree of **DOCTOR OF PHILOSOPHY** in Electrical Engineering Department, Faculty of Technology & Engineering, The M. S. University of Baroda, Vadodara is original and was carried out in the Department of Electrical Engineering, Faculty of Technology & Engineering, M. S. University of Baroda, Vadodara. I further declare that this thesis is not substantially the same as one, which has already been submitted in part or in full for the award of any degree or academic qualification of this University or any other Institution or examining body in India or abroad.

July, 2012

Jaymin Kantilal Bhalani

Dedicated
To
My Parents, My Wife Amruta
&
My Son Saumya

ABSTRACT

Multiple-Input Multiple-Output (MIMO) systems play a vital role in fourth generation (4G) wireless systems by exploiting spatial diversity, higher data rate, greater coverage and improved link robustness without increasing total transmission power or bandwidth. Channel State Information (CSI) provides key information for the operation of MIMO wireless communication systems and hence need to be estimated accurately for efficient data detection at receiver. Therefore accurate and robust estimation of wireless channel is of crucial importance for coherent demodulation in MIMO system.

MIMO channel estimation methods can be classified into three classes: training based, blind and semi-blind. Semi-blind channel estimation as a combination of training based method and pure blind method is considered to be a feasible solution of channel estimation for good performance with low complexity.

This thesis work aims to explore and design novel matrix decomposition based semi-blind channel estimation techniques with data detection for reduced complexity and near optimal performance. Matrix decomposition based channel estimation techniques avoid explicit matrix inversions and convert full rank channel matrix in to simpler form for low complexity and they show near optimal performance by achieving a performance nearer to known Channel State Information (CSI) at the receiver. Conventional LS, MMSE and MAP based training channel estimation techniques have been studied and compared with SVD-OPML (Whitening Rotation) and SVD-ROML based semi-blind channel estimation techniques. Initially five novel semi-blind channel estimation techniques (proposed techniques) have been designed with their mathematical models and implemented using MATLAB .Computer simulations have been carried out for $M \times N$ MIMO channel using flat fading Rayleigh and Rician models (where $M=2$ transmitters and $N=2,4,6,8$ receivers) using source

symbols derived from m-PSK ($m = 2,4,8$) modulation schemes with orthogonal pilot symbols. Performance evaluations in terms of BER analysis of proposed semi-blind channel estimation techniques compared with above mentioned conventional techniques have been taken to verify the utility of the thesis work.

CONTENTS

ACKNOWLEDGEMENTS	I
CERTIFICATE.....	III
DECLARATION.....	IV
DEDICATION.....	V
ABSTRACT.....	VI
CONTENTS.....	VIII
LIST OF FIGURES.....	XI
LIST OF TABLES.....	XV
NOMENCLATURE.....	XVII
LIST OF ABBREVIATIONS.....	XX
1. INTRODUCTION	1
1.1 INTRODUCTION	1
1.2 MOTIVATION	2
1.3 OBJECTIVES AND SCOPE OF WORKS	4
1.4 THESIS OUTLINE	5
2. MULTIPLE INPUT MULTIPLE OUTPUT SPACE TIME BLOCK CODING SYSTEM	7
2.1 PROPERTIES OF WIRELESS CHANNEL	7
2.1.1 Fading	8
2.1.1.1 <i>Statistical Models for Fading Channels</i>	15
2.1.1.2 <i>Rayleigh Fading Model</i>	15
2.1.1.3 <i>Rician Fading Model</i>	17
2.1.1.4 <i>Frequency Selective Fading Models</i>	17
2.2 MIMO BACKGROUND	18
2.3 THE MIMO CHANNEL	20
2.4 DEFINITION OF MIMO SYSTEMS	21
2.4.1 Single Input Single Output Channel	21
2.4.2 Single Input Multiple Output (SIMO) system	22
2.4.3 Multiple Input Single Output (MISO) system	23
2.4.4 Multiple-Input, Multiple-Output (MIMO)	23
2.4.5 MIMO Systems with One Modulator/Demodulator	25
2.4.6 MIMO Systems with Multiple Modulators/Demodulators	25

2.5	SPACE TIME BLOCK CODING	26
2.5.1	Array Gain	27
2.5.2	Interference Reduction	28
2.5.3	Spatial Multiplexing Gain	28
2.5.4	Diversity Gain	29
2.6	ALAMOUTI SCHEME	31
2.6.1	Maximum Ratio Combining and Decoding	34
2.6.2	Alamouti Schemes FOR 2×N Structure	35
2.7	ADVANTAGE & DISADVANTAGE OF MIMO	37
2.7.1	Advantages of MIMO	37
2.7.2	Disadvantages and Limitations of MIMO	38
2.8	SUMMARY	39
3.	CHANNEL ESTIMATION	40
3.1	INTRODUCTION	40
3.2	SYSTEM MODEL	41
3.2.1	Simplified Form for System Model	44
3.3	ESTIMATION PHILOSOPHIES	45
3.3.1	Pilot based Estimation	45
3.3.2	Blind Estimation	46
3.3.3	Semi-Blind Philosophy	47
3.4	CHANNEL ESTIMATION TECHNIQUES	47
3.4.1	LS and MMSE	48
3.4.1.1	<i>Least-Squares (LS) Channel Estimation</i>	49
3.4.1.2	<i>Minimum Mean Square Error Channel Estimation</i>	49
3.4.1.3	<i>Maximum A Posteriori (MAP) Channel Estimation</i>	51
3.4.2	Block-Type Pilot vs. Comb-Type Pilot	51
3.4.2.1	<i>Estimation with Block-Type Pilot</i>	52
3.4.2.2	<i>Estimation with Comb-Type Pilot</i>	52
3.5	SUMMARY	54
4.	PROPOSED SEMI-BLIND CHANNEL ESTIMATION TECHNIQUES	55
4.1	INTRODCUTION	55
4.2	SYSTEM MODEL	56
4.3	SVD-OPML BASED SEMI-BLIND CHANNEL ESTIMATION	57
4.4	SVD-ROML BASED SEMI-BLIND CHANNEL ESTIMATION	60

4.5	PROPOSED NOVEL SEMI-BLIND CHANNEL ESTIMATION TECHNIQUES	62
4.5.1	Joint Channel Estimation and Data Detection QR-NEW (Proposed Technique-I)	62
4.5.2	Householder QR-OPML (Proposed Technique-II)	64
4.5.3	Householder QR-OPML-NEW (Proposed Technique-III)	67
4.5.4	Householder QR-OPML- Joint Semi-Blind Channel Estimation and Data Detection (JSBCDE) (Proposed Technique-IV)	70
4.5.5	Modified Whitening Rotation (SVD-OPML) based Joint Semi-Blind Channel Estimation and Data Detection (Proposed Technique-V)	73
4.6	SUMMARY	75
5.	SIMULATION RESULTS	77
5.1	SIMULATIONS OVERVIEW	77
5.2	SIMULATION STEPS	79
5.3	SIMULATIONS RESULTS	81
5.4	OBSERVATIONS OF SIMULATION RESULTS	142
5.5	SUMMARY	142
6.	CONCLUSION & FUTURE SCOPE	144
6.1	CONCLUSIONS	144
6.2	FUTURE SCOPE OF THE WORK	146
	BIBLIOGRAPHY	148
	APENDIX- A	152
	APENDIX- B	153
	APENDIX- C	165

LIST OF FIGURES

Fig 1.1	MIMO Communication System	2
Fig 2.1	Different Paths in Wireless Channel	7
Fig 2.2	Modelling a Multipath Channel with a Linear time-varying Impulse Response	9
Fig 2.3	Flat Fading	10
Fig 2.4	Frequency Selective Fading	12
Fig 2.5	An Approximated Impulse Response for a Frequency Selective Fading	13
Fig 2.6	MIMO Channel	20
Fig 2.7	Single Input Single Output Channel	21
Fig 2.8	Single Input Multiple Output (SIMO) System	22
Fig 2.9	Multiple Input Single Output (MISO) System	23
Fig 2.10	2 x 2 Multi Input Multi Output channel	24
Fig 2.11	One-Modulator/Demodulator MIMO System with n Transmit and m Receive Antennas	25
Fig 2.12	Multiple-Modulator/Demodulator MIMO system with n Transmit and m Receive Antennas	26
Fig 2.13	Single Transmit and Multiple Receive Antenna System	27
Fig 2.14	Multiplexing Gain 2X2 MIMO System	28
Fig 2.15	Alamouti Transmitter	32
Fig 2.16	Receivers for Alamouti Scheme	32
Fig 2.17	2XN MIMO System Using Combiner	36
Fig 2.18	Schematic Representation of a Basic Spatial Multiplexing Scheme with 3 Transmit and 3 Receive Antennas	38
Fig 3.1	Schematic Representation of a MIMO Frame	44
Fig 3.2	Pictorial Representation of Pilot Vs Blind Tradeoff	46
Fig 3.3	Block Diagram of a Noise-corrupted System with LS Estimation	50
Fig 3.4	Block-type Pilot	52
Fig 3.5	Comb Type Pilot	53
Fig 3.6	Pilot Tones in Two Dimension	53
Fig 5.1	Channel Estimation For 2 Transmitter And 6 Receivers MIMO-STBC Using 4PSK (4 Pilots, 100 Blind) For Rayleigh Fading Channel Model	82
Fig 5.2	Channel Estimation For 2 Transmitter And 8 Receivers MIMO-STBC Using 4PSK (4 Pilots, 100 Blind) For Rayleigh Fading Channel Model	84
Fig 5.3	Channel Estimation For 2 Transmitter And 4 Receivers MIMO-STBC Using 4PSK (4 Pilots, 100 Blind) For Rayleigh Fading Channel Model	86
Fig 5.4	Channel Estimation For 2 Transmitter And 2 Receivers MIMO-	88

	STBC Using 4PSK (4 Pilots, 100 Blind) For Rayleigh Fading Channel Model	
Fig 5.5	Channel Estimation For 2 Transmitters And 2 Receivers MIMO-STBC Using 2-PSK (4 Pilots, 100 Blind) For Rayleigh Fading Channel Model	90
Fig 5.6	Channel Estimation For 2 Transmitters And 4 Receivers MIMO-STBC Using 2-PSK (4 Pilots, 100 Blind) For Rayleigh Fading Channel Model	92
Fig 5.7	Channel Estimation For 2 Transmitters And 6 Receivers MIMO-STBC Using 2-PSK (4 Pilots, 100 Blind) For Rayleigh Fading Channel Model	94
Fig 5.8	Channel Estimation For 2 Transmitters And 8 Receivers MIMO-STBC Using 8-PSK (4 Pilots, 100 Blind) For Rayleigh Fading Channel Model	96
Fig 5.9	Channel Estimation For 2 Transmitters And 6 Receivers MIMO-STBC Using 8-PSK (4 Pilots, 100 Blind) For Rayleigh Fading Channel Model	98
Fig 5.10	Channel Estimation For 2 Transmitters And 6 Receivers MIMO-STBC Using 4-PSK (8 Pilots, 100 Blind) For Rayleigh Fading Channel Model	100
Fig 5.11	Channel Estimation For 2 Transmitters And 8 Receivers MIMO-STBC Using 4-PSK (8 Pilots, 100 Blind) For Rayleigh Fading Channel Model	102
Fig 5.12	Channel Estimation For 2 Transmitters And 4 Receivers MIMO-STBC Using 4-PSK (8 Pilots, 100 Blind) For Rayleigh Fading Channel Model	104
Fig 5.13	Channel Estimation For 2 Transmitters And 2 Receivers MIMO-STBC Using 4-PSK (8 Pilots, 100 Blind) For Rayleigh Fading Channel Model	106
Fig 5.14	Channel Estimation For 2 Transmitters And 6 Receivers MIMO-STBC Using 2-PSK (8 Pilots, 100 Blind) For Rayleigh Fading Channel Model	108
Fig 5.15	Channel Estimation For 2 Transmitters And 4 Receivers MIMO-STBC Using 2-PSK (8 Pilots, 100 Blind) For Rayleigh Fading Channel Model	110
Fig 5.16	Channel Estimation For 2 Transmitters And 2 Receivers MIMO-STBC Using 2-PSK (8 Pilots, 100 Blind) For Rayleigh Fading Channel Model	112
Fig 5.17	Channel Estimation For 2 Transmitters And 2 Receivers MIMO-STBC Using 2-PSK (16 Pilots, 100 Blind) For Rayleigh Fading Channel Model	114
Fig 5.18	Channel Estimation For 2 Transmitters And 4 Receivers MIMO-STBC Using 2-PSK (16 Pilots, 100 Blind) For Rayleigh Fading Channel Model	116

	Channel Model	
Fig 5.19	Channel Estimation For 2 Transmitters And 6 Receivers MIMO-STBC Using 2-PSK (16 Pilots, 100 Blind) For Rayleigh Fading Channel Model	118
Fig 5.20	Channel Estimation For 2 Transmitters And 6 Receivers MIMO-STBC Using 4-PSK (16 Pilots, 100 Blind) For Rayleigh Fading Channel Model	120
Fig 5.21	Channel Estimation For 2 Transmitters And 4 Receivers MIMO-STBC Using 4-PSK (16 Pilots, 100 Blind) For Rayleigh Fading Channel Model	122
Fig 5.22	Channel Estimation For 2 Transmitters And 8 Receivers MIMO-STBC Using 4-PSK (16 Pilots, 100 Blind) For Rayleigh Fading Channel Model	124
Fig 5.23	Channel Estimation For 2 Transmitters And 2 Receivers MIMO-STBC Using 4-PSK (16 Pilots, 100 Blind) For Rayleigh Fading Channel Model	126
Fig 5.24	Channel Estimation Of QR-NEW (P.T.-I) For 2x4 MIMO-STBC Presented Under 4-PSK (4 Pilots, 100 Blind) For Different Rice Factor Presented Using Rician Fading Channel Model	127
Fig 5.25	Channel Estimation Of HQR-OPML (P.T.-II) For 2x4 MIMO-STBC Presented Under 4-PSK (4 Pilots, 100 Blind) For Different Rice Factor Presented Using Rician Fading Channel Model	128
Fig 5.26	Channel Estimation Of HQR-OPML-NEW (P.T.-III) For 2x4 MIMO-STBC Presented Under 4-PSK (4 Pilots, 100 Blind) For Different Rice Factor Presented Using Rician Fading Channel Model	129
Fig 5.27	Channel Estimation Of HQR-OPML-JSBCDE (P.T.-IV) For 2x4 MIMO-STBC Presented Under 4-PSK (4 Pilots, 100 Blind) For Different Rice Factor Presented Using Rician Fading Channel Model	130
Fig 5.28	Channel Estimation Of WR-NEW-JSBCDE (P.T.-V) For 2x4 MIMO-STBC Presented Under 4-PSK (4 Pilots, 100 Blind) For Different Rice Factor Presented Using Rician Fading Channel Model	131
Fig 5.29	Channel Estimation Of QR-NEW (P.T.-I) For 2x6 MIMO-STBC Presented Under 4-PSK (4 Pilots, 100 Blind) For Different Rice Factor Presented Using Rician Fading Channel Model	132
Fig 5.30	Channel Estimation Of HQR-OPML (P.T.-II) For 2x6 MIMO-STBC Presented Under 4-PSK (4 Pilots, 100 Blind) For Different Rice Factor Presented Using Rician Fading Channel Model	133
Fig 5.31	Channel Estimation Of HQR-OPML-NEW (P.T.-III) For 2x6 MIMO-STBC Presented Under 4-PSK (4 Pilots, 100 Blind) For Different Rice Factor Presented Using Rician Fading Channel	134

	Model	
Fig 5.32	Channel Estimation Of HQR-OPML-JSBCDE (P.T.-IV) For 2x6 MIMO-STBC Presented Under 4-PSK (4 Pilots, 100 Blind) For Different Rice Factor Presented Using Rician Fading Channel Model	135
Fig 5.33	Channel Estimation Of WR-NEW-JSBCDE (P.T.-V) For 2x6 MIMO-STBC Presented Under 4-PSK (4 Pilots, 100 Blind) For Different Rice Factor Presented Using Rician Fading Channel Model	136
Fig 5.34	Channel Estimation Of QR-NEW (P.T.-I) For 2x8 MIMO-STBC Presented Under 4-PSK (4 Pilots, 100 Blind) For Different Rice Factor Presented Using Rician Fading Channel Model	137
Fig 5.35	Channel Estimation Of HQR-OPML (P.T.-II) For 2x8 MIMO-STBC Presented Under 4-PSK (4 Pilots, 100 Blind) For Different Rice Factor Presented Using Rician Fading Channel Model	138
Fig 5.36	Channel Estimation Of HQR-OPML-NEW (P.T.-III) For 2x8 MIMO-STBC Presented Under 4-PSK (4 Pilots, 100 Blind) For Different Rice Factor Presented Using Rician Fading Channel Model	139
Fig 5.37	Channel Estimation Of HQR-OPML-JSBCDE (P.T.-IV) For 2x8 MIMO-STBC Presented Under 4-PSK (4 Pilots, 100 Blind) For Different Rice Factor Presented Using Rician Fading Channel Model	140
Fig 5.38	Channel Estimation Of WR-NEW-JSBCDE (P.T.-V) For 2x8 MIMO-STBC Presented Under 4-PSK (4 Pilots, 100 Blind) For Different Rice Factor Presented Using Rician Fading Channel Model	141

LIST OF TABLES

Table 5.0	Simulation Parameters for MIMO-STBC System.	78
Table 5.1	Channel Estimation for 2x6 MIMO-STBC using 4-PSK (4pilots,100 blind)	81
Table 5.2	Channel Estimation for 2x8 MIMO-STBC using 4-PSK (4pilots,100 blind)	83
Table 5.3	Channel Estimation for 2x4 MIMO-STBC using 4-PSK (4pilots,100 blind)	85
Table 5.4	Channel Estimation for 2x2 MIMO-STBC using 4-PSK (4pilots,100 blind)	87
Table 5.5	Channel Estimation for 2x2 MIMO-STBC using 2-PSK (4pilots,100 blind)	89
Table 5.6	Channel Estimation for 2x4 MIMO-STBC using 2-PSK (4pilots,100 blind)	91
Table 5.7	Channel Estimation for 2x4 MIMO-STBC using 2-PSK (4pilots,100 blind)	93
Table 5.8	Channel Estimation for 2x8 MIMO-STBC using 8-PSK (4pilots,100 blind)	95
Table 5.9	Channel Estimation for 2x6 MIMO-STBC using 8-PSK (4pilots,100 blind)	97
Table 5.10	Channel Estimation for 2x6 MIMO-STBC using 4-PSK (8 pilots,100 blind)	99
Table 5.11	Channel Estimation for 2x8 MIMO-STBC using 4-PSK (8 pilots,100 blind)	101
Table 5.12	Channel Estimation for 2x4 MIMO-STBC using 4-PSK (8 pilots,100 blind)	103
Table 5.13	Channel Estimation for 2x2 MIMO-STBC using 4-PSK (8 pilots,100 blind)	105
Table 5.14	Channel Estimation for 2x6 MIMO-STBC using 2-PSK (8 pilots,100 blind)	107
Table 5.15	Channel Estimation for 2x4 MIMO-STBC using 2-PSK (8 pilots,100 blind)	109
Table 5.16	Channel Estimation for 2x2 MIMO-STBC using 2-PSK (8 pilots,100 blind)	111
Table 5.17	Channel Estimation for 2x2 MIMO-STBC using 2-PSK(16 pilots,100 blind)	113
Table 5.18	Channel Estimation for 2x4 MIMO-STBC using 2-PSK (16 pilots,100 blind)	115
Table 5.19	Channel Estimation for 2x6 MIMO-STBC using 2-PSK (16 pilots,100 blind)	117
Table 5.20	Channel Estimation for 2x6 MIMO-STBC using 4-PSK (16 pilots,100 blind)	119
Table 5.21	Channel Estimation for 2x4 MIMO-STBC using 4-PSK (16 pilots,100 blind)	121
Table 5.22	Channel Estimation for 2x8 MIMO-STBC using 4-PSK (16 pilots,100 blind)	123
Table 5.23	Channel Estimation for 2x2 MIMO-STBC using 4-PSK (16 pilots,100 blind)	125
Table 5.24	Channel Estimation of QR-NEW (P.T.-I) for 2x4 MIMO-STBC using 4-PSK (4 pilots, 100 blind) for different Rice factors	127

Table 5.25	Channel Estimation of HQR-OPML (P.T.-II) for 2x4 MIMO-STBC using 4-PSK (4 pilots, 100 blind) for different Rice factors	128
Table 5.26	Channel Estimation of HQR-OPML-NEW (P.T.-III) for 2x4 MIMO-STBC using 4-PSK (4 pilots, 100 blind) for different Rice factors	129
Table 5.27	Channel Estimation of HQR-OPML-JSBCDE (P.T.-IV) for 2x4 MIMO-STBC using 4-PSK (4 pilots, 100 blind) for different Rice factors	130
Table 5.28	Channel Estimation of WR-NEW-JSBCDE (P.T.-V) for 2x4 MIMO-STBC using 4-PSK (4 pilots, 100 blind) for different Rice factors	131
Table 5.29	Channel Estimation of QR-NEW (P.T.-I) for 2x6 MIMO-STBC using 4-PSK (4 pilots, 100 blind) for different Rice factors	132
Table 5.30	Channel Estimation of HQR-OPML (P.T.-II) for 2x6 MIMO-STBC using 4-PSK (4 pilots, 100 blind) for different Rice factors	133
Table 5.31	Channel Estimation of HQR-OPML-NEW (P.T.-III) for 2x6 MIMO-STBC using 4-PSK (4 pilots, 100 blind) for different Rice factors	134
Table 5.32	Channel Estimation of HQR-OPML-JSBCDE (P.T.-IV) for 2x6 MIMO-STBC using 4-PSK (4 pilots, 100 blind) for different Rice factors	135
Table 5.33	Channel Estimation of WR-NEW-JSBCDE (P.T.-V) for 2x6 MIMO-STBC using 4-PSK (4 pilots, 100 blind) for different Rice factors	136
Table 5.34	Channel Estimation of QR-NEW (P.T.-I) for 2x8 MIMO-STBC using 4-PSK (4 pilots, 100 blind) for different Rice factors	137
Table 5.35	Channel Estimation of HQR-OPML (P.T.-II) for 2x8 MIMO-STBC using 4-PSK (4 pilots, 100 blind) for different Rice factors	138
Table 5.36	Channel Estimation of HQR-OPML-NEW (P.T.-III) for 2x8 MIMO-STBC using 4-PSK (4 pilots, 100 blind) for different Rice factors	139
Table 5.37	Channel Estimation of HQR-OPML-JSBCDE (P.T.-IV) for 2x8 MIMO-STBC using 4-PSK (4 pilots, 100 blind) for different Rice factors	140
Table 5.38	Channel Estimation of WR-NEW-JSBCDE (P.T.-V) for 2x8 MIMO-STBC using 4-PSK (4 pilots, 100 blind) for different Rice factors	141

NOMENCLATURE

Symbol	Meaning
$\delta(\cdot)$	Dirac delta Function
p_i	Power of i-th path
τ_i	Delay of i-th path
$\bar{\tau}$	Weighted average delay
σ_τ	Delay spread
B_c	Coherence bandwidth
$h(t, \tau)$	Impulse response of channel
f_d	Doppler shift
T_c	Coherence time
$f_R(r)$	Rayleigh or Rician random variable
f_s	Maximum Doppler shift
D	Peak amplitude of dominant signal
C	Channel capacity
$H(k)$	Channel matrix
S	Transmit matrix
$y(k), y_d(k)$	Received signal
$X(k), X_d(k), x$	Transmitted data signal
$\eta(k), n(k)$	Noise signal
M	No of transmitter antennas
N	No of Receiver antennas
K	Total transmitted symbols
L	Length of pilot symbols
a_{im}^d, a_{jm}^p	Amplitudes of data and pilot symbols
d_{im}^d	Unit-variance circularly symmetric complex data symbol

d_{jm}^p	Pilot symbols
S_i^d	Temporal signature of data waveform
S_{jm}^p	Temporal signature of pilot symbols
$p(k)$	Pilot vector
r_n	Received signal vector
n_n	noise signal vector
\hat{h}, \hat{H}	Estimated channel matrix
$(\bullet)^H$	Complex conjugate transpose of matrix
$(\bullet)^T$	Transpose of matrix
M	Training data sequence matrix
R_{hh}, C_H	Auto covariance matrix of channel matrix
R_{hY}	Cross covariance matrix of channel and output
R_{YY}	Auto covariance matrix of output
σ_n^2	Noise variance
σ_s^2	Normalized source power
X_p	Training (pilot) data
Y_p	Received training output
X_b	Blind data
Y_b	Received blind output
W	Whitening matrix
U, Q^H	Unitary rotation matrix of SVD decomposition
Σ	Diagonal matrix (scaling matrix) of SVD decomposition
L	Symbol length
I	Identity matrix
tr	Trace of the matrix

ε	Error function
V, β	Householder transformation vector
Q_p	Hermitan matrix of QR decomposition
R_{YY}, \tilde{R}_{YY}	Output auto-correlation matrix.
\tilde{W}_{MMSE}	Pre-equalizing filter using MMSE.
\tilde{W}_{ZF}	Pre-equalizing filter using Zero-forcing algorithm.
R_p, R	Upper triangular matrix of QR decomposition
$(\cdot)^\dagger$	Pseudo inverse of matrix
\Re_h, \Re_i, \Re_j	Error covariance factors
$\ \cdot\ _2$	Matrix 2 norms
$\ \cdot\ _F$	Matrix Frobenius norms
$E[\cdot]$	Expectation of matrix
C_n	Noise covariance matrix

LIST OF ABBREVIATIONS

WLAN	Wireless local Area Network
WMAN	Wireless Metropolitan Area Network
MIMO	Multiple Input Multiple Output
MISO	Multi Input Single Output
SIMO	Single Input Multiple Output
SISO	Single Input Single Output
STC	Space Time Coding
STBC	Space Time Block Code
OSTBC	Orthogonal Space Time Block Code
STTC	Space Time Trellis Code
V-BLAST	Vertical Bell Laboratories Layered Space time
D-BLAST	Diagonal Bell Laboratories Layered Space time
2G	Second Generation
3G	Third Generation
4G	Fourth Generation
CSI	Channel State Information
LS	Least Square
MMSE	Minimum Mean Square Error
MAP	Maximum a Posteriori
ML	Maximum Likelihood
SOS	Second Order Statistics
HOS	Higher Order Statistics
WR	Whitening Rotation
BER	Bit Error Rate
PSK	Phase Shift Keying
OPML	Orthogonal Pilot Maximum Likelihood Estimator
ROML	Rotation Optimization Maximum Likelihood Estimator
SVD	Singular Value Decomposition
EVD	Eigen Value Decomposition

QRD	QR decomposition
LOS	Line of Sight
AWGN	Adaptive White Gaussian Noise
GTD	Geometrical theory of Diffraction
UTD	Uniform theory of Diffraction
ISI	Inter symbol Interference
PDF	Probability density function
CDMA	Code Division Multiple Access
WCDMA	Wide – band Code Division Multiple Access
SM	Spatial Multiplexing
SE	Spatial Efficiency
BWA	Broadband Wireless Access
CCI	Co channel Interference
MRC	Maximum Ratio Combining
CSI	Channel State Information
i.i.d	Independent and identically distributed
BLUE	Best Linear Unbiased Estimate
MSE	Mean Square Error
PSAM	Pilot Symbol Aided Modulation
P.T.	Proposed Technique
ACF	Autocorrelation Function
ZF	Zero Forcing
H-QRD	Householder QR Decomposition
OFDM	Orthogonal Frequency Division Multiplexing
TBCE	Training (pilot) based channel estimation
SBCE	Semi-blind Channel Estimation
JSBCDE	Joint Semi-Blind Channel Estimation and Data Detection
SNR	Signal to Noise Ratio

CHAPTER 1

INTRODUCTION

1.1 INTRODUCTION

Wireless communications have expanded enormously over the last decade. The expectation is that the growth will continue. Future wireless communication systems are expected to support high-speed and high-quality multimedia services. To increase the quality and capacity of wireless communications by means of higher data throughput and simultaneous increase in range and reliability, Multiple-Input Multiple-Output (MIMO) systems have been proposed to exploit signals from multiple antennas at both the transmitter and receiver [1]-[4]. Even as a relatively new technique, MIMO has already been employed by the third generation (3G) wireless standards in the form of space-time coding, and it is regarded as an essential component of the fourth generation (4G) and other future systems. Current industry trends suggest that large-scale deployment of MIMO wireless systems will initially be seen in WLANs and in wireless metropolitan area networks (WMANs). Corresponding standards currently under definition include the IEEE 802.11n WLAN and IEEE 802.16 WMAN standards.

MIMO systems have been recently under active consideration because of their potential for achieving higher data rate and providing more reliable reception performance compared with traditional single-antenna systems for wireless communications. A space-time (ST) code is a bandwidth-efficient method that can improve the reliability of data transmission in MIMO systems [2], [5]. It encodes a data stream across different transmit antennas and time slots, so that multiple redundant copies of the data stream can be transmitted through independent fading channels and by doing so more reliable detection can be obtained at the receiver. A MIMO system takes advantage of the spatial diversity that is obtained by spatially separated antennas in a dense multipath scattering environment. Further that may be implemented in a number of different ways to obtain either a diversity gain to combat

signal fading or to obtain a capacity gain. To maximize spatial diversity, the same information can be transmitted from multiple transmit antennas and received at multiple antennas simultaneously hence the probability that the information is detected accurately is increased. The simplest way of achieving diversity is through repetition coding that sends the same information symbol in different time slots from different transmit antennas. Examples include delay diversity, Space-Time Block Code (STBC) and Space-Time Trellis Code (STTC), Orthogonal Space-Time Block Code (OSTBC). MIMO systems provide more spatial freedoms or spatial multiplexing so that different information can be transmitted simultaneously over multiple antennas, thereby boosting the system throughput. Examples include Vertical-Bell Laboratories Layered Space-Time (V-BLAST) and Diagonal - Bell Laboratories Layered Space-Time (D-BLAST).

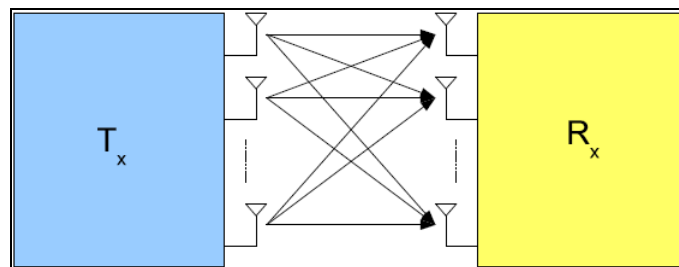


Figure 1.1: MIMO Communication System

1.2 MOTIVATION

MIMO system has the potential to meet the increasing high speed and reliability demands of the future. However for this technology to truly succeed in commercial deployments, there are still several technical obstacles that must be tackled. A major impediment in MIMO is the complicated receiver signal processing. The simultaneous emission of the signals from the multiple transmit antennas increases the mutual interference imposed on the signals, therefore much more complex detection schemes are required to extract the transmitted signals. For example, the complexity of a maximum likelihood detector increases exponentially

with the number of transmit antennas. Spatial equalizers and space-time coding has been proposed to simplify the detection for MIMO systems. Further coherent detection requires knowledge of the channel; therefore accurate channel estimation is crucial in realizing the full potential of MIMO system. In order to attain advantages of MIMO system, the receiver and/or transmitter should have access to channel state information (CSI). Hence effective channel estimation algorithms are needed to guarantee the performance of MIMO communication system.

Several channel estimation algorithms have been developed in recent years. In the literature [6]-[15] MIMO channel estimation methods can be classified into three classes: training (pilot) based channel estimation, blind channel estimation and semi-blind channel estimation. For pure training based scheme, a long training is necessary in order to obtain a reliable channel estimate, which considerably reduces system bandwidth efficiency. Least square (LS), Minimum mean square error (MMSE), Maximum likelihood (ML), Maximum a posteriori (MAP) estimator are popular method [7], [9], [12], [15]-[18]. In Blind methods, no training symbols are used and channel state information is acquired by relying on the received signal statistics [19]-[22] so these techniques are bandwidth efficient but more computationally complex with slow convergence. Blind channel estimation can be classified as second order statistics (SOS) based techniques [23]-[26] and higher order statistics (HOS) based techniques [27],[28] which achieve high system throughput but require high computational complexity. Semi-blind channel estimation approaches are combination of the two aforementioned procedures [29]-[35]. With use of few training symbols along with blind statistical information, such techniques can overcome the convergence problems and high complexity associated with blind estimators and they also have bandwidth efficiency.

The least square (LS), Minimum Mean Square Error (MMSE), Maximum a Posteriori (MAP) are the common methods for training-based channel estimation. Those solutions are relative simple compared to other channel estimation techniques such as blind estimation. However, they still require complex matrix inversions, which are undesirable in real time implementation when number of transmitters and receivers are more. Blind techniques give good results but they are inherently

complex. As compromise matrix decomposition based semi-blind techniques, which eliminates direct complex matrix inversion operations may be good solution for finding channel unknowns. Whitening Rotation (WR)-Orthogonal Pilot Maximum Likelihood (OPML) based semi-blind channel estimation technique [37]-[44] shows very good performance compared to other conventional techniques.

Still there is also scope to find novel semi-blind channel estimation technique(s) with data detection which may outperform conventional techniques. So here main motivation of thesis is to analyze, design and implement novel semi-blind channel estimation techniques which give near optimal performance.

1.3 OBJECTIVES AND SCOPE OF WORKS

The project is based on theoretical research, mathematical modeling, simulations and implementation using MATLAB. The main objectives behind the present work is to design and develop novel semi-blind channel estimation technique(s) /joint semi-blind channel estimation and data detection technique(s) which outperform conventional techniques by giving near optimal performance. Further to investigate the performance of newly developed novel semi-blind estimation technique(s) for Rician flat fading MIMO channel using different Rice factors ($K=5, 10$ and 15). Computer simulations have been carried out to validate the proposed work. In order to attain these objectives and enable a comparison, a detailed comparative study of various conventional methods was carried out, involving the following investigations:

- To implement $2 \times N$ (where 2 shows number of transmitter antennas and N shows number of receiver antennas like $N=2, 4, 6, 8$) MIMO communication system using m-PSK (where $m=2, 4, 8$) modulation constellations in MATLAB, having Space Time Block Code (STBC) based Alamouti code structure. MIMO Channel was assumed as quasi-static Rayleigh flat fading channel with additive white Gaussian noise with zero mean and variance one.
- To investigate BER performance of above MIMO systems with space time block coding.

- To implement and simulate conventional training based channel estimation techniques like Least Square (LS), Minimum Mean Square Error (MMSE) and Maximum a Posteriori (MAP) using orthogonal pilots. BER analysis is taken using MATLAB simulations.
- To implement and simulate matrix decomposition based Whitening Rotation - Orthogonal Pilot Maximum Likelihood (SVD-OPML) and Rotation Optimization Maximum Likelihood (SVD-ROML) semi-blind channel estimation techniques using orthogonal pilots (training) symbols and blind symbols which derived from m-PSK modulation constellations. For different combinations of receiver antennas and orthogonal pilot symbols and modulations constellations (like BPSK, 4-PSK and 8-PSK), BER analysis have been taken to investigate the performance.

1.4 THESIS OUTLINE

The Thesis is organized in the following six chapters:

- | | |
|-----------|--|
| Chapter 1 | This chapter provides basic Introduction overview with literature survey, Motivation, Objectives and Scope of the work and Thesis outline. |
| Chapter 2 | This chapter mainly focuses on “MIMO-STBC system”, which includes wireless channel properties, basic principles of MIMO system, concept of array gain, diversity gain and spatial multiplexing gain, statistical models for fading Channels like Rayleigh fading and Rician fading, fundamentals of space-time block coding (STBC), Alamouti code structure , Alamouti scheme for 2xN structures , receiver structure, MIMO systems model development, MIMO system advantages and its application etc. |
| Chapter 3 | This chapter mainly focuses on “Channel Estimation” part of MIMO systems, which includes introduction, general |

overview of channel estimation techniques and its philosophies like training based channel estimation, blind channel estimation and semi-blind channel estimation, different MIMO channel estimation techniques like LS, MMSE, MAP etc.

Chapter 4 This chapter includes basic MIMO system model and problem formulations for semi-blind channel estimation. It also includes analysis and implementation of conventional semi-blind channel estimation techniques like SVD-OPML and SVD-ROML. Finally it includes design, development and analysis of proposed novel semi-blind channel estimation and data detection techniques

Chapter 5 This chapter includes simulation overview, simulation parameters, and steps of simulations, comparative simulation results of proposed novel semi-blind channel estimation and data detection techniques with conventional channel estimation techniques. Finally discussion on results has been carried out.

Chapter 6 This chapter Presents the authors conclusions from the aforementioned, and discusses directions for future work.

CHAPTER 2

MULTIPLE INPUT MULTIPLE OUTPUT SPACE TIME BLOCK CODING SYSTEM

2.1 PROPERTIES OF WIRELESS CHANNEL

One of the distinguishing characteristics of wireless channels is the fact that there are many different paths between the transmitter and the receiver. The existence of various paths results in receiving different versions of the transmitted signal at the receiver. These separate versions experience different path loss and phases. Figure 2.1 demonstrates the trajectory of different paths in a typical example.

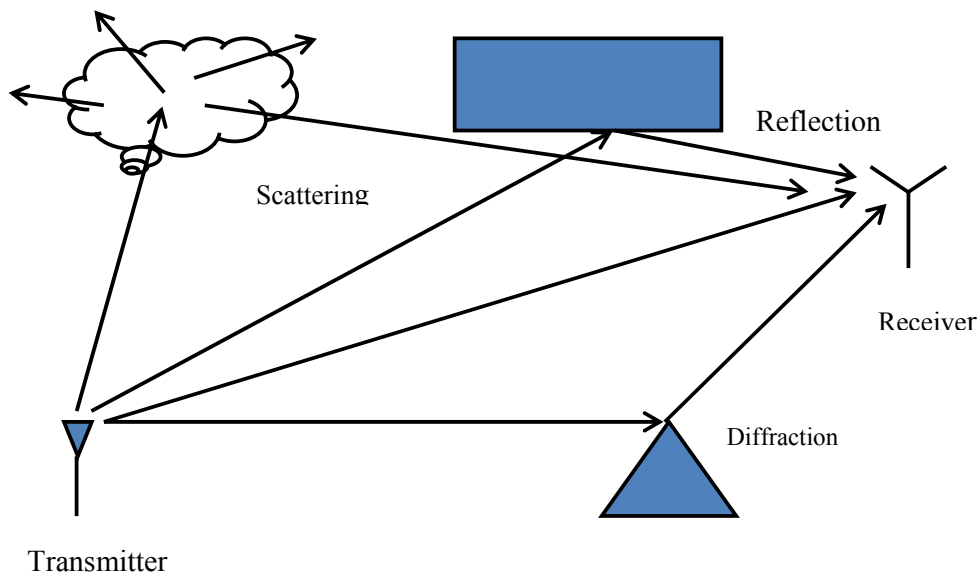


Figure 2.1: Different Paths in Wireless Channel

If there is a direct path between the transmitter and the receiver, it is called the line of sight (LOS). A LOS does not exist when large objects obstruct the line between the transmitter and the receiver. If LOS exists, the corresponding signal received through the LOS is usually the strongest and the dominant signal. At least, the signal from the LOS is more deterministic. While its strength and phase may change due to mobility,

it is a more predictable change that is usually just a function of the distance and not many other random factors.

A LOS is not the only path that an electromagnetic wave can take from a transmitter to a receiver. An electromagnetic wave may reflect when it meets an object that is much larger than the wavelength. Through reflection from many surfaces, the wave may find its path to the receiver. Of course, such paths go through longer distances resulting in power strengths and phases other than those of the LOS path. Another way that electromagnetic waves propagate is diffraction. Diffraction occurs when the electromagnetic wave hits a surface with irregularities like sharp edges.

Finally, scattering happens in the case where there are a large number of objects smaller than the wavelength between the transmitter and the receiver. Going through these objects, the wave scatters and many copies of the wave propagate in many different directions. There are also other phenomenon that affects the propagation of electromagnetic waves like absorption and refraction.

The effects of the above propagation mechanisms and their combination result in many properties of the received signal that is unique to wireless channels. These effects may reduce the power of the signal in different ways. There are two general aspects of such a power reduction that require separate treatments. One aspect is the large-scale effect which corresponds to the characterization of the signal power over large distances or the time-average behaviours of the signal. This is called attenuation or path loss and sometimes large-scale fading. The other aspect is the rapid change in the amplitude and power of the signal and this is called small-scale fading, or just fading. It relates to the characterization of the signal over short distances or short time intervals. Small-scale fading and its statistical models are explained in next section.

2.1.1 Fading

Fading, or equivalently small-scale fading, is caused by interference between two or more versions of the transmitted signal which arrive at the receiver at slightly different times. These signals, called multipath waves, combine at the receiver antenna and the corresponding matched filter and provide an effective combined signal. This resulting signal can vary widely in amplitude and phase. The rapid

fluctuation of the amplitude of a radio signal over a short period of time, equivalently a short travel distance, is such that the large-scale path loss effects may be ignored. The randomness of multipath effects and fading results in the use of different statistical arguments to model the wireless channel. To understand the behaviour and reasoning behind different models, the cause and properties of fading are studied and described.

First, the effects of mobility on these channel models are described. Let us assume that the objects in the environment between the transmitter and the receiver are static and only the receiver is moving. In this case, the fading is purely a spatial phenomenon and is described completely by the distance. On the other hand, as the receiver moves through the environment, the spatial variations of the resulting signal translate into temporal variations for the receiver. In other words, due to the mobility, there is a relationship between time and distance that creates a time varying fading channel. Therefore, we can use time and distance interchangeably and equivalently in such a scenario. The time-varying nature of the wireless channel is also applied to the case that the surrounding objects are moving. Similarly, the resulting fluctuations in the received signal are random.

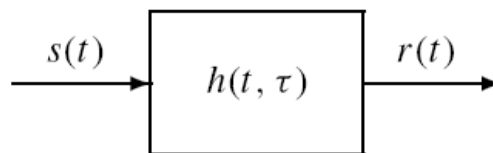


Figure 2.2: Modelling a Multipath Channel with a Linear time-varying Impulse Response

As it is clear from the name, multipath fading is caused by the multiple paths that exist between the transmitter and the receiver. As discussed before, reflection, diffraction, and scattering create several versions of the signal at the receiver. The effective combined signal is random in nature and its strength changes rapidly over a small period of time. A multipath channel can be modeled as a linear time-varying channel as depicted in Figure 2.2. The behaviour of the linear time-varying impulse response depends on different parameters of the channel. For example, the speed of the mobile and surrounding objects affect the characteristic of the model. The presence of reflecting objects and scatterers creates a constantly changing

environment. Multipath propagation increases the time required for the baseband portion of the signal to reach the receiver. The resulting dissipation of the signal energy in amplitude, phase, and time may cause intersymbol interference (ISI). If the channel has a constant gain and linear phase response over a bandwidth which is greater than the bandwidth of the transmitted signal, the impulse response $h(t, \tau)$ can be approximated by a delta function at $\tau = 0$ that may have a time varying amplitude. In other words, $h(t, \tau) = \alpha(t) \delta(\tau)$, where $\delta(\cdot)$ is the Dirac delta Function. This is a narrowband channel in which the spectral characteristics of the transmitted signal are preserved at the receiver. It is called flat fading or frequency non-selective fading. An example of the impulse response for a flat fading channel is depicted in Figure 2.3. As can be seen from the figure, the narrowband nature of the channel can be checked from the time and frequency properties of the channel. In the frequency domain, the bandwidth of the signal is smaller than the bandwidth of the channel. In the time domain, the width of the channel impulse response is smaller than the symbol period. As a result, a channel might be flat for a given transmission rate, or correspondingly for a given symbol period, while the same channel is not flat for a higher transmission rate. Therefore, it is not meaningful to say a channel is flat without having some information about the transmitted signal.

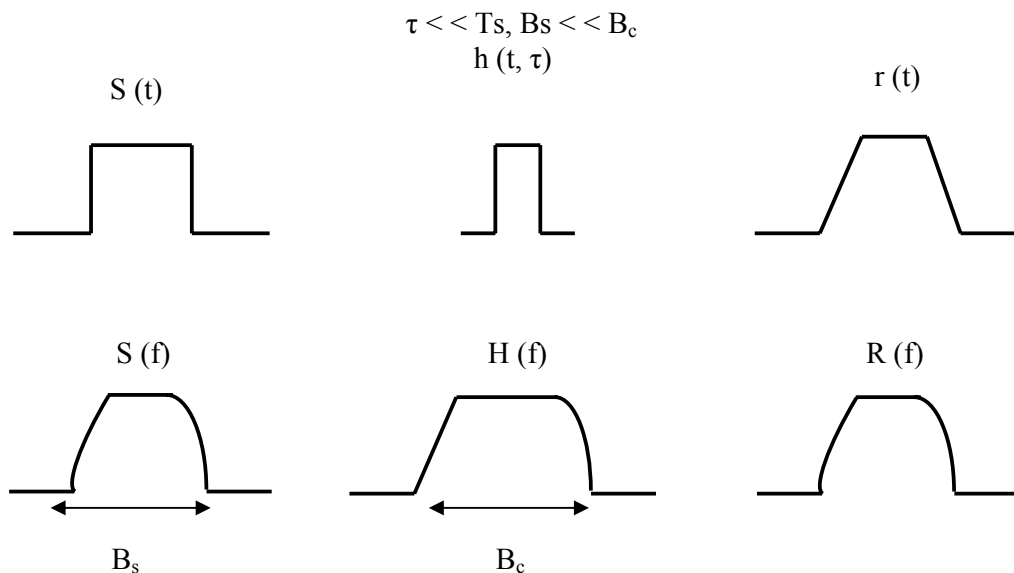


Figure 2.3: Flat Fading

Also, it is need to define the bandwidth of the channel to be able to compare it with the bandwidth of the signal. Usually the bandwidth of the channel is defined using its

delay spread. To define the delay spread, let us assume that the multipath channel includes I paths and the power and delay of the i^{th} path are p_i and τ_i , respectively. Then, the weighted average delay is

$$\bar{\tau} = \frac{\sum_{i=1}^I p_i \tau_i}{\sum_{i=1}^I p_i} \quad \dots (2.1)$$

The delay spread is defined as

$$\sigma_\tau = \sqrt{\overline{\tau^2} - \bar{\tau}^2} \quad \dots (2.2)$$

$$\overline{\tau^2} = \frac{\sum_{i=1}^I p_i \tau_i^2}{\sum_{i=1}^I p_i} \quad \dots (2.3)$$

Finally, the channel “coherence bandwidth” is approximated by

$$B_c = \frac{1}{5\sigma_\tau} \quad \dots (2.4)$$

As we defined earlier, in a flat fading channel, the channel coherence bandwidth B_c is much larger than the signal bandwidth B_s .

On the other hand, if the channel possesses a constant gain and linear phase over a bandwidth that is smaller than the signal bandwidth, ISI exists and the received signal is distorted. Such a wideband channel is called frequency selective fading. Figure 2.4 shows an example of the impulse response for a frequency selective fading channel. In this case, the impulse response $h(t, \tau)$ may be approximated by a number of delta functions as shown in Figure 2.5. In other words,

$$h(t, \tau) = \sum_{j=1}^J \alpha_j(t) \delta(\tau - \tau_j) \quad \dots (2.5)$$

Each delta component fades independently, that is $\alpha_j(t)$ are independent. To be more specific, for frequency selective fading, the bandwidth of the signal is larger than the coherence bandwidth of the channel. Equivalently, in the time domain, the width of the channel impulse response is larger than the symbol period. Again, the frequency selective nature of the channel depends on the transmission rate as well as the channel characteristics. In summary, based on multipath time delay, the fading channel is categorized into two types: flat and frequency selective.

Another independent phenomenon caused by mobility is the Doppler shift in frequency. Let us assume a signal with a wavelength of λ and a mobile receiver with a velocity of v . Also, we define θ as the angle between the direction of the motion of the mobile and the direction of the arrival of the wave. In this case, the frequency change of the wave, known as Doppler shift and denoted by f_d , is given by

$$f_d = \frac{v}{\lambda} \cos \theta \quad \dots (2.6)$$

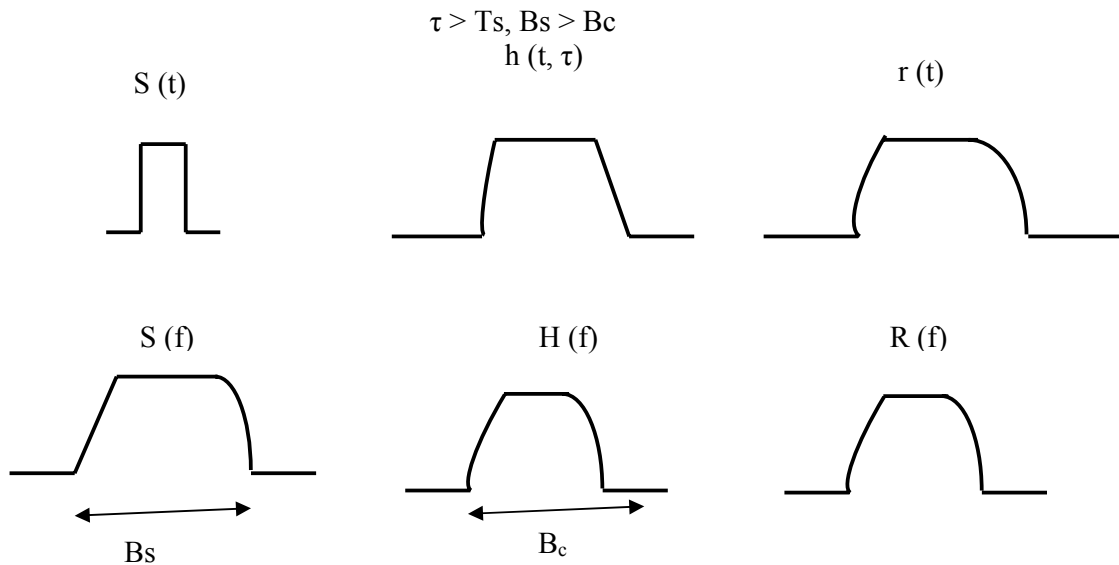


Figure 2.4: Frequency Selective Fading

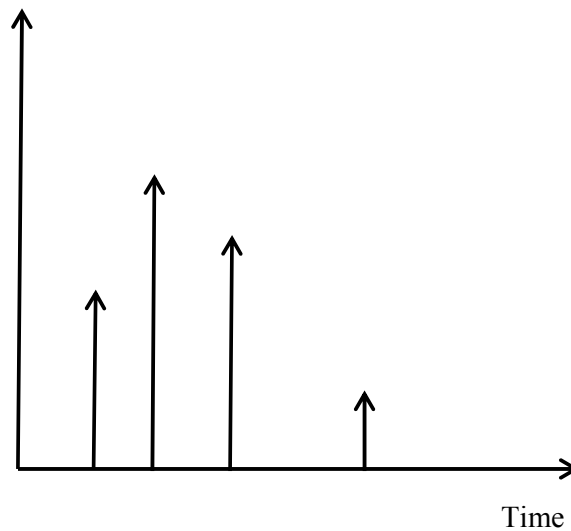


Figure 2.5: An Approximated Impulse Response for a Frequency Selective Fading

Since different paths have different angles, a variety of Doppler shifts corresponding to different multipath signals are observed at the receiver. In fact, the frequency change is random as the angle θ is random. The relative motion between the transmitter and the receiver results in random frequency modulation due to different Doppler shifts on each of the multipath components. Also, if the surrounding objects are moving, they create a time-varying Doppler shift on different multipath components. Such a time-varying frequency shift can be ignored if the mobile speed is much higher than that of the surrounding objects. Since the receiver observes a range of different Doppler shifts, any transmitted frequency results in a range of received frequencies. This results in a spectral broadening at the receiver. Doppler spread is a measure of such a spectral widening and is defined as the range of frequencies over which the received Doppler spectrum is not zero. If the maximum Doppler shift is f_s , the transmitted frequency, f_c , is received with components in the range $f_c - f_s$ to $f_c + f_s$. If the baseband signal bandwidth is much greater than the Doppler spread, the fading is called slow fading. In this case, the effects of Doppler spread are negligible. The channel impulse response changes at a rate much slower than the transmitted baseband signal and the channel is assumed to be static over one or several reciprocal bandwidth intervals. On the other hand,

If the effects of the Doppler spread are not negligible, it is a fast-fading channel. The channel impulse response changes rapidly within the symbol duration in a fast-fading channel. In summary, based on Doppler spread, the fading channel is categorized into two types: slow and fast.

Defining the slow versus fast nature of a fading channel in terms of the signal bandwidth and Doppler spread may sound a little bit strange. Equivalently, slow and fast-fading channels can be defined based on time domain properties. Towards this goal, first, it is need to define the coherence time of a channel denoted by T_c . Two samples of a fading channel that are separated in time by less than the coherence time are highly correlated. This is a statistical measure since the definition depends on how much “correlation” is considered highly correlated. Practically, the coherence time is the duration of time in which the channel impulse response is effectively invariant. If a correlation threshold of 0.5 is chosen, the coherence time is approximated by

$$T_c = \frac{9}{16\pi f_s} \quad \dots (2.7)$$

Where f_s is the maximum Doppler shift. If the signal duration is smaller than the coherence time, the whole signal is affected similarly by the channel and the channel is a slow fading channel. On the other hand, if the signal duration is larger than the coherence time, the channel changes are fast enough such that in practice different parts of the transmitted signal experience different channels. This is called fast fading since its main cause is the fast motion of the receiver or transmitter.

- Flat Slow Fading or Frequency Non-Selective Slow Fading: When the bandwidth of the signal is smaller than the coherence bandwidth of the channel and the signal duration is smaller than the coherence time of the channel.
- Flat Fast Fading or Frequency Non-Selective Fast Fading: When the bandwidth of the Signal is smaller than the coherence bandwidth of the channel and the signal duration is larger than the coherence time of the channel.

- Frequency Selective Slow Fading: When the bandwidth of the signal is larger than the Coherence bandwidth of the channel and the signal duration is smaller than the coherence time of the channel.
- Frequency Selective Fast Fading: When the bandwidth of the signal is larger than the Coherence bandwidth of the channel and the signal duration is larger than the coherence time of the channel.

2.1.1.1 Statistical Models for Fading Channels

So far, the fading channel by a linear time-varying impulse response has been modelled. The impulse response was approximated by one delta function in the case of flat fading and multiple delta functions in the case of frequency selective fading. As discussed before, the nature of the multipath channel is such that the amplitude of these delta functions is random. This randomness mainly originates from the multipath and the random location of objects in the environment. Therefore, statistical models are needed to investigate the behaviour of the amplitude and power of the received signal. In this section, study of some important models has been carried out.

2.1.1.2 Rayleigh Fading Model

First, let us concentrate on the case of flat fading. The results for frequency selective channels are very similar since the amplitudes of different delta functions fade independently. It is assumed that there is no LOS path between the transmitter and the receiver. Later, the case where such a LOS path exists can be considered. In a multipath channel with I multiple paths, transmitting a signal over the carrier frequency f_c results in receiving the sum of I components from different paths plus a Gaussian noise as follows:

$$r(t) = \sum_{i=1}^I a_i \cos(2\pi f_c t + \phi_i) + \eta(t) \quad \dots (2.8)$$

Where a_i and ϕ_i are the amplitude and phase of the i^{th} component, respectively, and $\eta(t)$ is the Gaussian noise. Expanding the $\cos(\cdot)$ terms.

$$r(t) = \cos(2\pi f_c t) \sum_{i=1}^I a_i \cos(\phi_i) - \sin(2\pi f_c t) \sum_{i=1}^I a_i \sin(\phi_i) + \eta(t) \quad \dots (2.9)$$

It is customary in digital communications to call the first and second summations “in phase” and “quadrature” terms, respectively. The terms $A = \sum_{i=1}^I a_i \cos(\phi_i)$ and $B = \sum_{i=1}^I a_i \sin(\phi_i)$ are the summation of I random variables since the objects in the environment are randomly located. For a large value of I , as is usually the case, using the central limit theorem, the random variables A and B are independent identically distributed (i.i.d.) Gaussian random variables. The envelope of the received signal is $R = \sqrt{A^2 + B^2}$ since A and B are i.i.d. zero-mean Gaussian random variables, the envelope follows a Rayleigh distribution. The probability density function (pdf) of a Rayleigh random variable is

$$f_R(r) = \frac{r}{\sigma^2} \exp\left(\frac{-r^2}{2\sigma^2}\right), r \geq 0 \quad \dots (2.10)$$

Where σ^2 is the variance of the random variables A and B . The received power is an exponential random variable with a pdf:

$$f(x) = \frac{1}{2\sigma^2} \exp\left(\frac{-x^2}{2\sigma^2}\right), x \geq 0 \quad \dots (2.11)$$

Note that the average power, the average of the above exponential random variable, is $E[R^2] = 2\sigma^2$ which is the sum of the variances of A and B .

The received signals in (2.8) or (2.9) represent the analog signal at the first stage of the receiver. We usually deal with the baseband digital signal after the matched filter and the sample and hold block. It is denoted such a baseband discrete-time signal by r_t . In fact, r_t is the output of the matched filter after demodulation when the input of the receiver is $r(t)$. Similarly, s_t and η_t are the discrete-time versions of $s(t)$ and $\eta(t)$, the transmitted signal and the noise, respectively. Note that in the above analysis the transmitted signal was implicit. Then, using the above arguments, one can show that the relationship between the baseband signals is

$$r_t = \alpha s_t + \eta_t \quad \dots (2.12)$$

Where α is a complex Gaussian random variable. In other words, the real and imaginary parts of the fade coefficient α are zero-mean Gaussian random variables. The amplitude of the fade coefficient, $|\alpha|$, is a Rayleigh random variable. The input output relationship in (2.12) is called a fading channel model. The coefficient α is called the path gain and the additive noise component η_t is usually a Gaussian noise.

2.1.1.3 Rician Fading Model

In a flat fading channel, if in addition to random multiple paths, a dominant stationary component exists, the Gaussian random variables A and B are not zero mean anymore. This, for example, happens when a LOS path exists between the transmitter and the receiver. In this case, the distribution of the envelope random variable, R , is a Rician distribution with the following pdf

$$f_R(r) = \frac{r}{\sigma^2} \exp\left(\frac{-(r^2 + D^2)}{2\sigma^2}\right) I_0\left(\frac{Dr}{\sigma^2}\right), r \geq 0, D \geq 0 \quad \dots (2.13)$$

Where D denotes the peak amplitude of the dominant signal and $I_0(\cdot)$ is the modified Bessel function of the first kind and of zero-order. As expected, the Rician distribution converges to a Rayleigh distribution when the dominant signal disappears, that is $D \rightarrow 0$. Similarly to the case of Rayleigh fading model, the discrete-time input–output relationship in the case of a Rician fading model is also governed by (2.20). The main difference is that the real and imaginary parts of the path gain α are Gaussian random variables with non-zero means. As a result, the distribution of the amplitude $|\alpha|$ is Rician instead of Rayleigh.

2.1.1.4 Frequency Selective Fading Models

In general, as discussed before, frequency selective fading is modeled by intersymbol interference. Therefore, the channel can be modeled by the sum of a few

delta functions. In this case, the corresponding discrete-time input–output relationship is

$$r_t = \sum_{j=0}^{j-1} \alpha^j s_{t-j} + \eta_t \quad \dots (2.14)$$

The path gains α^j are independent complex Gaussian distributions and η_t represents the noise. In the case of Rayleigh fading, they are zero-mean i.i.d. complex Gaussian random variables. A special case that has been extensively utilized in the literature is the case of a two-ray Rayleigh fading model. For a two-ray Rayleigh fading model, we have

$$r_t = \alpha^0 s_t + \alpha^1 s_{t-1} + \eta_t \quad \dots (2.15)$$

Where the real and imaginary parts of α_0 and α_1 are i.i.d. zero-mean Gaussian random variables.

2.2 MIMO BACKGROUND

Normally the standard and conventional Wi-Fi system uses one antenna to receive and one to transmit data. MIMO overcomes the bottlenecks in the conventionally used Single Input Single Output (SISO) system in the last decade and has evolved as a prime and promising area of research in the field of wireless communication. The possibilities to increase the channel capacity in the SISO wireless system is quite limited, provided the bandwidth is increased allowing the corresponding increase in the bits per second or to increase the transmit power, allowing a higher level modulation scheme to be utilized for a given Bit Error Rate, effectively increasing the bits per second within the same bandwidth. The problem with both of these techniques is that any increase in power or bandwidth can negatively impact other communications systems operating in adjacent spectral channels or within a given geographic area. As such, bandwidth and power for a given communications system are generally well regulated, limiting the ability of the system to support any increase in the capacity or performance [2]-[4].

MIMO uses two or more antennas at each end of a connection to send and receive data, enabling transmitter and receiver to accept signals more efficiently than with a single antenna and thus overcomes the problems and restrictions compared to the conventional system. The multiple antennas at the transmitter and receiver can achieve a data rate, which is very much higher than that of the SISO system. In order to support the larger data rate coupled with high quality and to fight against effects of multipath fading and additive noise in the channel multiple copies of signal over various paths to multiple receivers is used.

The success of MIMO lies in its ability to utilize the multipath reception, which was considered to be an unavoidable by product of radio communications, and convert it into a distinct advantage that actually multiplies transmission speed and improves throughput. The multiple antennas improve the performance of the system through various diversity techniques like time, frequency, space and polarization. It basically uses the principle of spatial diversity to distinguish among different signals on the same frequency.

The Data are transmitted over N transmit antennas through a specifically designed MIMO channel to M receive antennas. Moreover, the transmission can be encoded so that information on each can be used to help reconstruct the information on the others. Just like error detection/correction codes, space-time block coding here allows us to increase reliability in addition to throughput. Space-time diversity has the advantage of using the same bandwidth as that of SISO system with high data rate transfer and quality [2]. To be precise, MIMO utilizes a multiple antenna system to take advantage of the multi-path affect in RF technology, rather than fight against it as conventional 802.11 Access Points do, as a result the improvement in both range and capacity provides substantially more reliable signal quality and greater bandwidth. The multipath radio reception is one of the driving forces behind the usage and outcome of MIMO based system. The signal being send to the receiver contains not only a direct line-of-sight radio signal, but also a large number of reflected radio waves.

MIMO concepts have been under development for many years for both wireless and wire-line systems. The usage of multiple antennas is not a newly discovered method. It is been used in few of the radio transmission many years back and in early 80's Bell labs came out with few of MIMO based wireless applications.

MIMO systems use spatial multiplexing to distinguish among different signals on the same frequency and yield an impressive increase in spectral efficiency. It has been proposed that using multiple transmitting and receiving antennas, and associated coding techniques could increase the performance of wireless communication systems [5]. The main reason for the possibility and the reality of MIMO based system in the current trend is the advent of inexpensive, high-speed chips with millions of transistors.

2.3 THE MIMO CHANNEL

Multiple-Input Multiple-Output (MIMO) systems yield vast capacity increases when the rich scattering environment is properly exploited [1]. When examining the performance of MIMO systems, the MIMO channel must be modeled properly. The primary MIMO channel model under consideration is the quasi-static, frequency non-selective, Rayleigh fading channel model. Figure 2.6 shows a block diagram of a MIMO system with N_t transmit antennas and N_r receive antennas. The channel for a MIMO system can be represented by

$$H = \begin{bmatrix} h_{11} & \cdots & h_{1N_t} \\ h_{21} & \cdots & h_{2N_t} \\ \vdots & \ddots & \vdots \\ h_{N_r1} & \cdots & h_{N_rN_t} \end{bmatrix} \quad \dots (2.16)$$

Where h_{ij} is the complex channel gain between transmitter j and receiver i . Each channel gain h_{ij} is assumed to be independently identically distributed (i.i.d) zero mean complex Gaussian random variables with unit variance [1].

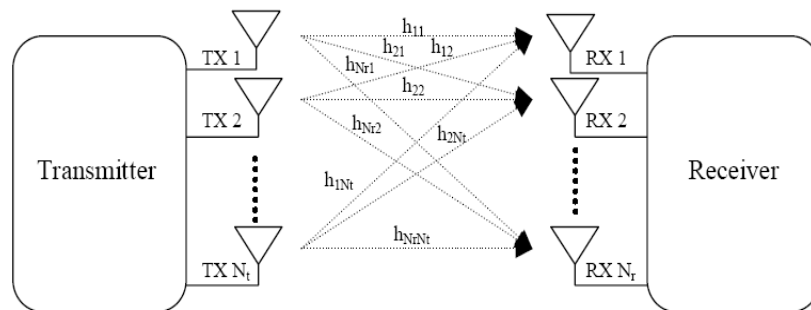


Figure 2.6: MIMO Channel

Under the quasi-static assumption, the channel remains constant over the length of a frame, changing independently between consecutive frames. When the antenna elements are spaced sufficiently apart (at least half a wavelength, for indoor applications) and there are enough scatterers present that the received signal at any receive antenna is the sum of several multipath components, the channel paths are modeled as independent and uncorrelated. The channel undergoes frequency non-selective fading when the coherence bandwidth of the channel is large compared to the bandwidth of the transmitted signal [3]

2.4 DEFINITION OF MIMO SYSTEMS

2.4.1 Single Input Single Output Channel

To explain MIMO, we begin with the simpler SISO (Single Input Single Output) system. Figure 2.7 shows a SISO channel, with one transmit and one receive antenna. Correspondingly, there is only one channel vector $h(t)$

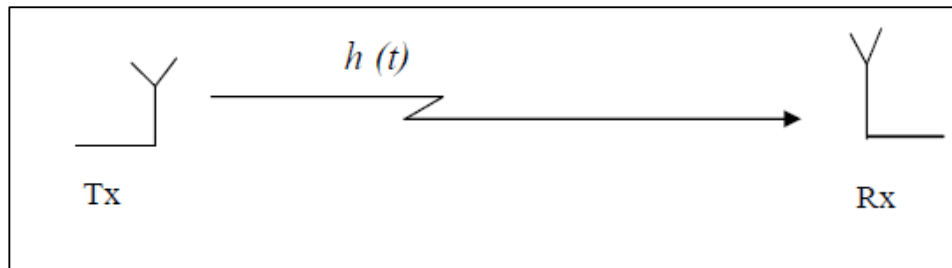


Figure 2.7: Single Input Single Output (SISO) Channel

MIMO is part of the category of smart antenna systems. Traditional smart antenna systems employ multiple antennas at the receiver, whereas in a general MIMO system, multiple antennas are employed, both at transmit and at the receive sides. The addition of multiple antennas at transmit combined with advanced signal processing algorithms at transmit and receive results in a significant advantage over traditional smart antenna systems - both in terms of capacity and diversity. This is the conventional system that is used everywhere. Assume that for a given channel, whose bandwidth is B , and a given transmitter power of P the signal at the receiver has an

average signal-to noise ratio of SNR_0 . Then, an estimate for the Shannon limit on channel capacity, C , is

$$C \approx B \log_2 (1 + SNR_0) \quad \dots (2.17)$$

2.4.2 Single Input Multiple Output (SIMO) System

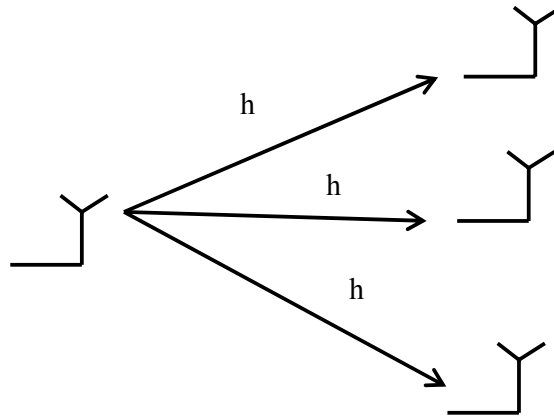


Figure 2.8: Single Input Multiple Output (SIMO) System

For the SIMO system (Figure: 2.8), we have N antennas at the receiver. If the signals received on these antennas have on average the same amplitude, then they can be added coherently to produce an N^2 increase in the signal power. On the other hand, there are N sets of noise that are added incoherently and result in an N -fold increase in the noise power. Hence, there is an overall increase in the SNR

$$SNR \approx \frac{N^2(\text{Signalpower})}{N(\text{noise})} = N(SNR_0) \quad \dots (2.18)$$

Thus, the **channel capacity** for this channel is approximately equal to

$$C \approx B \log_2 (1 + N(SNR_0)) \quad \dots (2.19)$$

2.4.3 Multiple Input Single Output (MISO) System

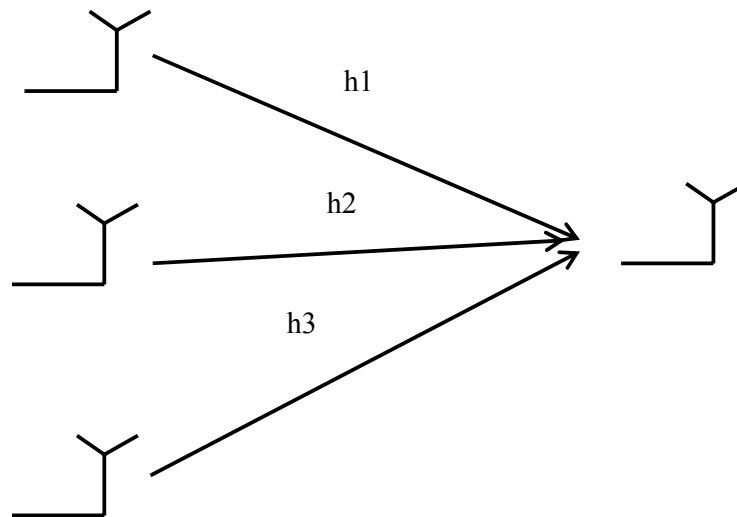


Figure 2.9: Multiple Input Single Output (MISO) System

In the MISO system (Figure 2.9), we have M transmitting antennas. The total transmitted power is divided up into the M transmitter branches. Following a similar argument as for the SIMO case, if the signals add coherently at the receiving antenna we get approximately an M -fold increase in the SNR as compared to the SISO case. Note here, that because there is only one receiving antenna the noise level is the same as in the SISO case. Thus, the overall increase in SNR is approximately

$$SNR \approx \frac{M^2(\text{signalpower} / M)}{\text{noise}} = M(SNR_0) \quad \dots (2.20)$$

Thus, the **channel capacity** for this channel is approximately equal to

$$C \approx B \log_2(1 + M(SNR_0)) \quad \dots (2.21)$$

2.4.4 Multiple-Input, Multiple-Output (MIMO)

Figure 2.10 gives an example of a 2 by 2 MIMO channel. There are two transmitting and two receiving antennas. Therefore, the 2 by 2 MIMO channel has

four channel vectors: h_{11} , h_{12} , h_{21} and h_{22} which form a channel matrix: the difference between the SISO channel and the MIMO channel is that the parameter of the SISO channel is a single transfer function, while that of the MIMO channel is a matrix of transfer functions.

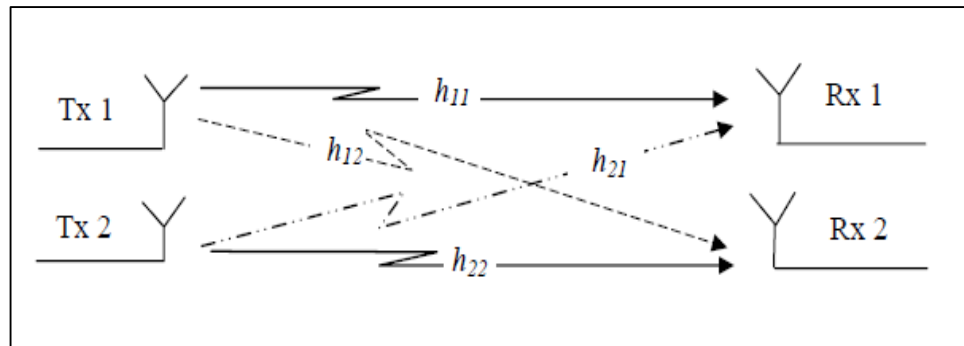


Figure 2.10: 2 x 2 Multi Input Multi Output Channel

So MIMO system can be defined in the following way: “If a wireless communication system has multiple antenna elements at both transmit and receive ends, it is called a MIMO system”. By using some proper signal processing schemes, one can improve transmission quality and/or throughput in a MIMO system. Due to modulators append in a MIMO system, two different kinds of MIMO systems are distinguished, which will be described next.

In this case, it is possible to get approximately an MN -fold increase in the SNR yielding a **channel capacity** equal to

$$C \approx B \log_2(1 + MN(SNR_0)) \quad \dots (2.22)$$

Thus, we can see that the channel capacity for the MIMO system is higher than that of MISO or SIMO. However, we should note here that in all four cases the relationship between the channel capacity and the SNR is logarithmic. This means that trying to increase the data rate by simply transmitting more power is extremely costly.

2.4.5 MIMO Systems with One Modulator/Demodulator

A schematic representation of a MIMO system with one modulator is given in Figure 2.11. The system has n transmitting antennas and m receiving antennas. The channel impulse response is given by matrix \mathbf{H} . The signals to (and from) all the antennas are all from (and to) one modulator (demodulator).

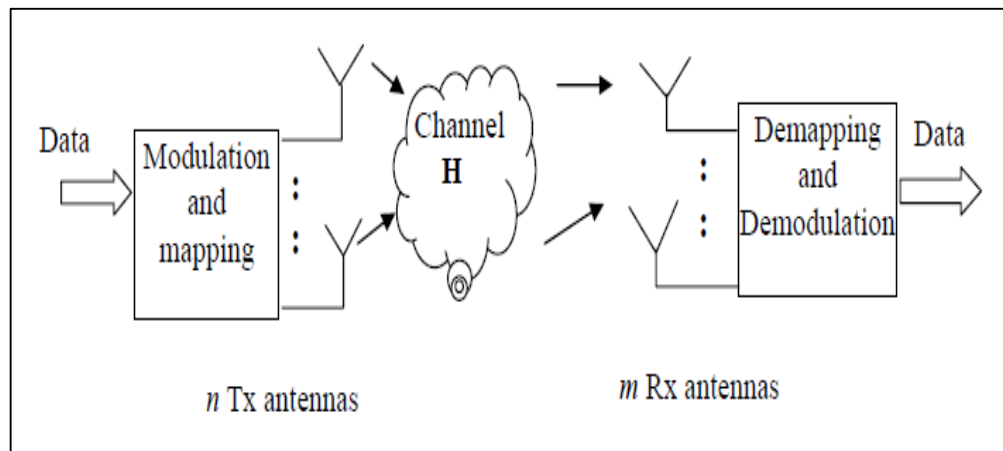


Figure 2.11: One-Modulator/Demodulator MIMO System with n Transmit and m Receive Antennas

2.4.6 MIMO Systems with Multiple Modulators/Demodulators

Figure 2.12 gives another type of MIMO system with multiple modulators/demodulators. Each modulator/demodulator is connected with one antenna. At the transmit side, the data stream is converted from serial to parallel and fed to different modulators. After independent modulation, each group of data is transmitted simultaneously via its own antenna. In the receiver, each group of data received from different antennas is fed to a different demodulator. After parallel to serial conversion, the demodulated data becomes one data stream.

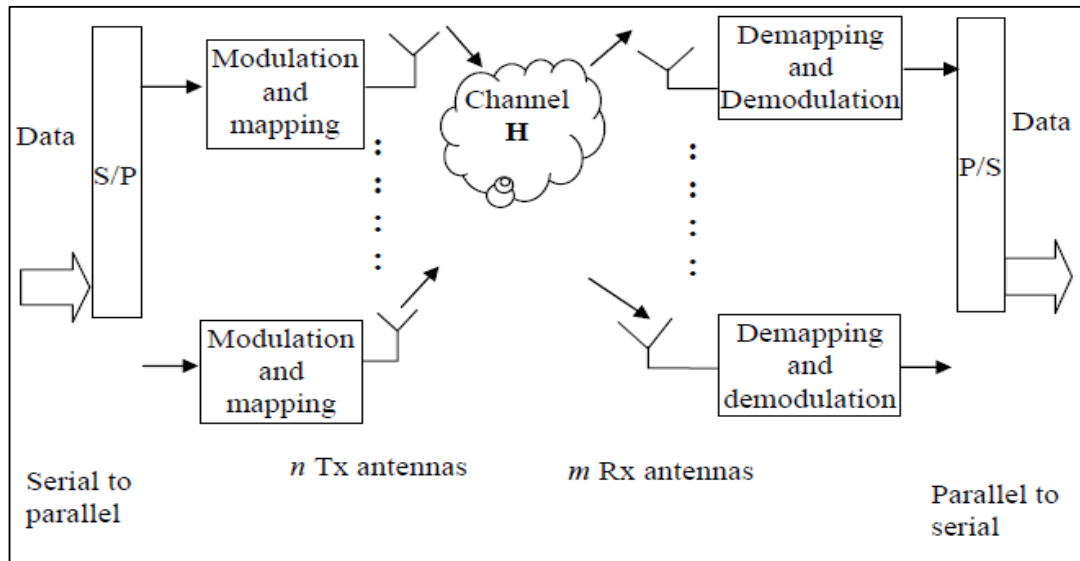


Figure 2.12: Multiple-Modulator/Demodulator MIMO System with n Transmit and m Receive antennas

2.5 SPACE TIME BLOCK CODING

A MIMO communication system uses multiple antennas at the transmitter and receiver to achieve various advantages. Traditionally, antenna arrays have been used at the transmitter and the receiver to achieve array gain, which increases the output SNR of the system. In the mid-1990s, adaptive antennas and smart antennas were introduced to describe antenna arrays that are made adaptive in a manner that it changes its transmission and reception characteristics when the radio environment changes. Array antennas have been implemented in GSM networks, fixed Broadband Wireless Access (BWA) networks, and third Generation (3G) CDMA networks. More recently, a way of using multiple antennas has been discovered to achieve diversity and multiplexing gain by exploiting the once negative effect of multipath. Under suitable conditions, i.e. a scatter rich environment, the channel paths between the different transmit and receive antennas can be treated as independent channels due to the multipath effects caused by the scatterers. Initial works in this research area, suggests that MIMO effectively takes advantage of the random fading and multipath delay spread to increase the transfer rate of the system. The exploitation of this

additional ‘spatial’ degree of freedom can increase the throughput and improve the performance of the system

These variations are referred to as fading and cause deterioration of the system quality. Furthermore, wireless channels suffer from co channel interference (CCI) from other cells that share the same frequency channel, leading to distortion of the desired signal and also low system performance. Therefore, wireless systems must be designed to mitigate fading and interference to guarantee a reliable communication. A successful method to improve reliable communication over a wireless link is to use multiple antennas.

2.5.1 Array Gain

Array gain is achieved by coherently combining the signals from the multiple antennas to increase the average output to SNR, which will improve the range and coverage of the system. Figure (2.13) illustrates a simple case of a system consisting of one transmit antenna and a set of receive antenna array. Assume the distance between the transmitter and the receiver is significantly larger than the antenna separation of the array at the receiver and then the received signal at each antenna will differ in phase due to the relative delay caused by the antenna separation. To maximize the received signal energy, an optimum receiver will be beamforming techniques to adjust for different delays of the multiple antennas so that the received signal can be constructively combined.

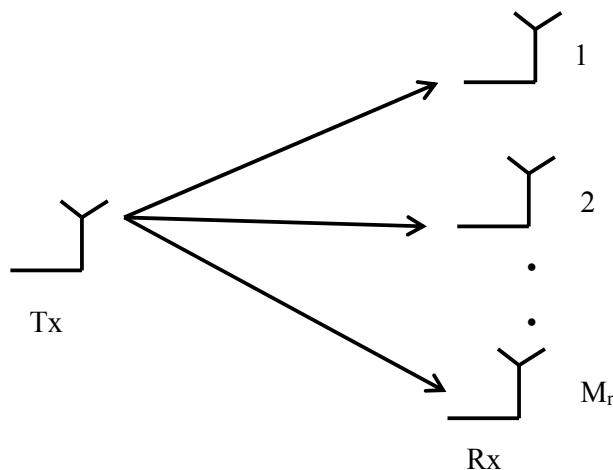


Figure 2.13: Single Transmit and Multiple Receive Antenna System

This will yield N_r -fold power gain, where N_r is the number of receiver's antennas. In a MIMO case where antenna arrays are used at the transmitter and receiver, then an $N_t N_r$ -fold power gain is available; where N_t is the number of transmit antennas.

2.5.2 Interference Reduction

Co-channel interference contributes to the overall noise of the system and deteriorates performance. By using multiple antennas it is possible to suppress interfering signals what leads to an improvement of *system capacity*. Interference reduction requires knowledge of the channel of the desired signal, but exact knowledge of channel may not be necessary.

2.5.3.1.1 Spatial Multiplexing Gain

Multiplexing gain is achieved through transmitting different signals on independent channels in a MIMO system. The multiplexing gain order is the number of parallel independent spatial data pipes in the same frequency band between the transmitter and receiver. As shown in Figure (2.14), a signal is split into two parts and transmitted on two separate antennas. At each receive antenna it will detect a signal from a specific transmit antenna and the signals from other antennas will be seen as interference. Combining techniques are required at the receiver to eliminate the interference and to multiplex the signal back together. As demonstrated, capacity gain is achieved by reducing the transmission time without using additional bandwidth [3].

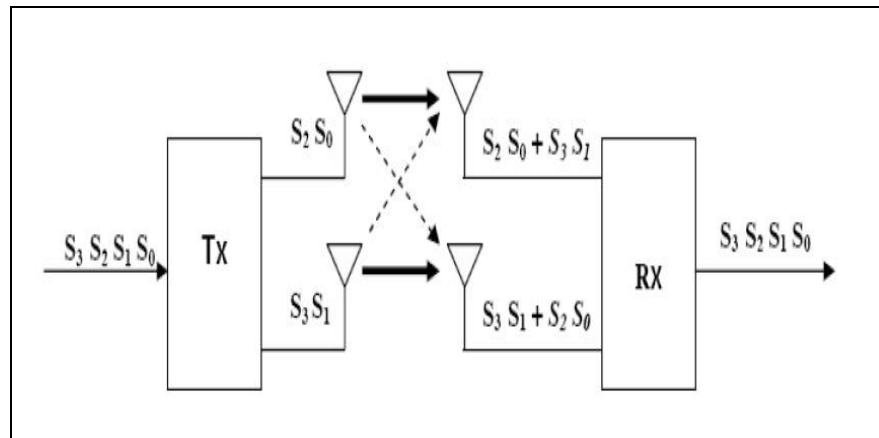


Figure 2.14: Multiplexing Gain 2X2 MIMO System

In summary, the use of MIMO has many benefits. However, it is not possible to achieve all the above benefits of MIMO techniques in one system as some of them are mutually conflicting goals.

2.5.4 Diversity Gain

Diversity is a technique to mitigate fading in wireless links by transmitting a signal over multiple independently fading paths. The main idea behind diversity is that by transmitting multiple copies of the signal increases the probability that at least one copy is recovered correctly at the receiver. Diversity can be obtained through time, frequency, or space. Time diversity assumes that a signal will experience independent fading at different times due to changes in the channel. The benefit of time diversity is that it does not require additional hardware. However it requires memory storage of the repeated signals for processing. Frequency diversity is achieved when the carrier frequencies are sufficiently separated such that each carrier frequency will experience independent fading. In frequency diversity, the same signal is transmitted on various independent carrier frequencies. Multiple receivers are used to detect the multiple signals at different frequencies, and the one with the highest energy will be selected. Alternatively, a multiantenna system can exploit the independent multipath channels to achieve spatial diversity. The diversity order is the total number of the independent fading signal paths between the transmitter and the receiver, and depends on the spatial separation of the antennas and the scatterers of the environment. The maximum spatial diversity gain of a MIMO system is $M_t M_r$. Joint diversity schemes such as space-time and space-frequency coding at the transmitter and the receiver has been developed to increase the diversity order of the system. In 1998, independent pioneer work by Alamouti and Tarokh et al. developed a breakthrough space-time diversity system that provides the diversity gain without sacrificing the bandwidth.

An effective method to combat fading is diversity. According to the domain where diversity is introduced, diversity techniques are classified into time, frequency and space diversity. *Space* or *antenna* diversity has been popular in wireless microwave communications and can be classified into two categories: *receive*

diversity and *transmit diversity* depending on whether multiple antennas are used for reception or transmission.

➤ Receive Diversity

It can be used in channels with multiple antennas at the receive side. The receive signals are assumed to fade independently and are combined at the receiver so that the resulting signal shows significantly reduced fading. Receive diversity is characterized by the number of independent fading branches and it is at most equal to the number of receive antennas.

➤ Transmit Diversity

Transmit diversity is applicable to channels with multiple transmit antennas and it is at most equal to the number of the transmit antennas, especially if the transmit antennas are placed sufficiently apart from each other. Information is processed at the transmitter and then spread across the multiple antennas.

In case of multiple antennas at both link ends, utilization of diversity requires a combination of the receive and transmit diversity explained above. The diversity order is bounded by the product of the number of transmit and receive antennas, if the channel between each transmit-receive antenna pair fades independently.

The key feature of all diversity methods is a low probability of simultaneous deep fades in the various diversity channels. In general the system performance with diversity techniques depends on how many signal replicas are combined at the receiver to increase the overall SNR. There exist four main types of signal combining methods at the receiver: selection combining, switched combining, equal-gain combining and maximum ratio combining (MRC). More information about combining methods can be found in.

Wireless systems consisting of a transmitter, a radio channel and a receiver are categorized by their number of inputs and outputs. The simplest configuration is a single antenna at both sides of the wireless link, denoted as Single Input Single Output (SISO) system. Using multiple antennas on one or both sides of the communication links are denoted as Multiple Input Multiple Output (MIMO) systems.

The difference between a SISO system and a MIMO system with N_t transmit antennas and N_r receive antennas is the way of mapping the single stream of data symbols to N_t streams of symbols and the corresponding inverse operation at the receiver side.

Systems with multiple antennas on the receive side only are called Single Input Multiple Output (SIMO) systems and systems with multiple antennas at the transmitter side and a single antenna at the receiver side are called multiple input/single output (MISO) systems. The MIMO system is the most general and includes SISO, MISO, and SIMO systems as special cases. Therefore, the term MIMO will be used in general for multiple antenna systems. The fundamental problem of MIMO systems is the mapping operation at the transmitter and the corresponding inversion at the receiver to optimize the overall performance of the wireless system. Mostly, researchers concentrate on the following system parameters: **bit rate**, **reliability** and **complexity**. The goal is to design a robust and low complex wireless system that provides the highest possible bit rate per unit bandwidth.

In summary, the use of MIMO has many benefits. However, it is not possible to achieve all the above benefits of MIMO techniques in one system as some of them are mutually conflicting goals. In general, a MIMO system improves

- Spectral efficiency: multiplexing gain
- Link reliability: diversity gain
- Coverage: Diversity gain and array gain
- Capacity: Multiplexing gain

2.6 ALAMOUTI SCHEME

The encoder for Alamouti schemes can be seen in figure-(2.15). This scheme with two transmit antennas and two receive antenna is interpreted here. In general case, we may use N receive antennas. In Alamouti encoding scheme, during any given transmission period two signals are transmitted simultaneously from two transmit antennas [1].

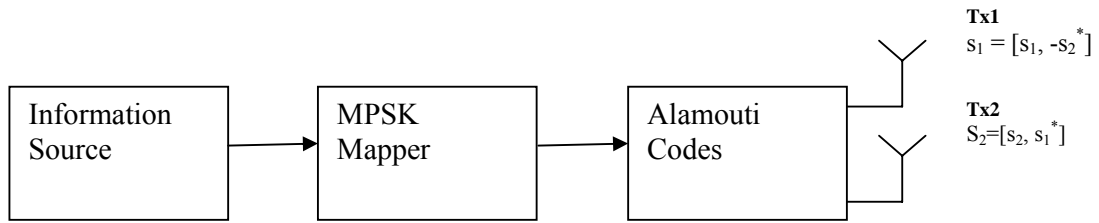


Figure 2.15: Alamouti Transmitter

The encoder takes two modulated symbols s_1 and s_2 at a time. The transmit matrix S is given by Equation (2.23).

$$S = \begin{pmatrix} s_1 & -s_2^* \\ s_2 & s_1^* \end{pmatrix} \quad \dots (2.23)$$

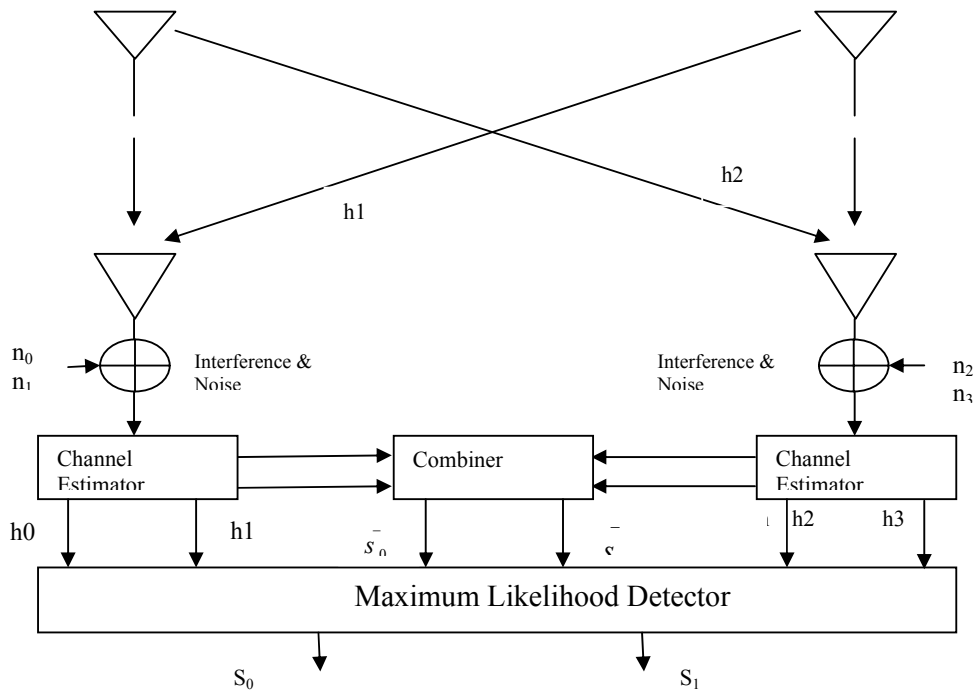


Figure 2.16: Receivers for Alamouti Scheme

Where s^* is complex conjugate of s . During the first transmission period, two signals s_1 and s_2 are transmitted simultaneously from antenna one and antenna two,

respectively. In the second transmission period, signal $-s_2^*$ is transmitted from transmit antenna one and signal s_1^* from transmit antenna two. It is clear that the encoding is done in both space and time domain. The transmit sequence from antennas one and two is showed by s^1 and s^2 , respectively.

$$s^1 = [s_1, -s_2^*] \quad \dots (2.24)$$

$$s^2 = [s_2, s_1^*] \quad \dots (2.25)$$

The key feature of the Alamouti scheme is given in Equation (2.26).

$$s.s^H = (|s_1|^2 + |s_2|^2)I_2 \quad \dots (2.26)$$

I_2 is the 2×2 identity matrix.

The block diagram of the receiver for the Alamouti scheme is shown in Figure (2.16). The fading channel coefficients from the first and second transmit antennas to the receive antenna one is denoted by $h_0(t)$ and $h_1(t)$ while to the receive antenna two is denoted by $h_2(t)$ and $h_3(t)$ respectively. Assuming that the fading coefficients are constant across two consecutive symbol transmission periods, means that channel is quasi static within transmission block. Hence following equation (2.27), (2.28), (2.29) and (2.30) for every single channel coefficients at time interval T can be written.

$$h_0(t) = h_0(t+T) = h_0 = |h_0|e^{j\theta_0} \quad \dots (2.27)$$

$$h_1(t) = h_1(t+T) = h_1 = |h_1|e^{j\theta_1} \quad \dots (2.28)$$

$$h_2(t) = h_2(t+T) = h_2 = |h_2|e^{j\theta_2} \quad \dots (2.29)$$

$$h_3(t) = h_3(t+T) = h_3 = |h_3|e^{j\theta_3} \quad \dots (2.30)$$

Where $|h_i|$ and θ_i , are the amplitude gain and phase shift for the path, and T is the symbol duration. At the receive antenna one, the received signals over two consecutive symbol periods, denoted by r_0 and r_1 , at time t and $t + T$, respectively, while received signal for received antenna two, denoted by r_2 and r_3 . Received signal by antenna one and two can be expressed by equation (2.31), (2.32), (2.33) and (2.34).

$$r_0 = h_0 s_0 + h_1 s_1 + n_0 \quad \dots (2.31)$$

$$r_1 = h_0 s_1^* + h_1 s_0^* + n_1 \quad \dots (2.32)$$

$$r_2 = h_2 s_0 + h_3 s_1 + n_2 \quad \dots (2.33)$$

$$r_3 = -h_2 s_1^* + h_3 s_0^* + n_3 \quad \dots (2.34)$$

n_0, n_1, n_2 , and n_3 are independent complex variables representing additive white Gaussian noise with zero mean and one-sided power spectral density N_0

2.6.1 Maximum Ratio Combining and Decoding

If the channel fading attenuations h_i can be perfectly recovered at the receiver, the receiver will use them as the channel state information (CSI) in the decoder. A combiner forms the following combined signals represented in equation (2.35) and (2.36).

$$\tilde{s}_1 = h_1^* r_0 - h_0 r_1^* + h_3^* r_2 - h_2 r_3^* \quad \dots (2.35)$$

$$\tilde{s}_0 = h_0^* r_0 + h_1 r_1^* + h_2^* r_2 + h_3 r_3^* \quad \dots (2.36)$$

Substituting r_i from (2.31)-(2.33), in equation (2.35) and (2.36) the combined signals can be written as equation (2.37) and (2.38).

$$\tilde{s}_0 = \left(|h1|^2 + |h2|^2 + |h3|^2 + |h4|^2 \right) s_0 + h_0^* n_0 + h_1 n_1^* + h_2^* n_2 + h_3 n_3^* \quad \dots (2.37)$$

$$\tilde{s}_1 = \left(|h0|^2 + |h1|^2 + |h2|^2 + |h3|^2 \right) s_1 - h_0 n_1^* + h_1^* n_0 - h_2 n_2^* + h_3^* n_2 \quad \dots (2.38)$$

As the signal \tilde{s}_0 depends only on s_0 and \tilde{s}_1 only on s_1 we can decide on s_1 and s_2 by applying the maximum likelihood rule on \tilde{s}_0 and \tilde{s}_1 separately. These combined signals are sent to a maximum likelihood decoder which for each transmitted symbol s_i , $i = 1, 2$, selects a symbol \hat{s}_i from the ary signal set such that $d^2(\tilde{s}_i, \hat{s}_i)$ is minimum, where $d^2(\tilde{s}_i, \hat{s}_i)$ is the Euclidean distance between the two symbols. \hat{s}_i is the estimate of the transmitted symbol s_i . The complexity of the decoder is linearly proportional to the number of antennas and the transmission rate.

The code with two antennas was generalized to an arbitrary number of transmit antennas by applying the theory of orthogonal designs and is referred to as orthogonal space-time block codes (OSTBC). The distinguishing feature of this type of OSTBC over other space-time codes is to have a simple maximum likelihood decoding algorithm based only on linear processing at the receiver.

2.6.2 Alamouti Schemes for 2×N Structure

Alamouti schemes can be written in simple matrix form. For instance for 2 by 2 system, received signal at time interval t_1 and t_2 can be expressed in equation (2.39).

$$\begin{pmatrix} r_0 & r_1 \\ r_2 & r_3 \end{pmatrix} = \begin{pmatrix} h_0 & h_1 \\ h_2 & h_3 \end{pmatrix} \times \begin{pmatrix} s_0 & -s_1^* \\ s_1 & s_0^* \end{pmatrix} + \begin{pmatrix} n_0 & n_1 \\ n_2 & n_3 \end{pmatrix} \quad \dots (2.39)$$

For the combiner following simple matrix form represented by equation (2.40) can be written.

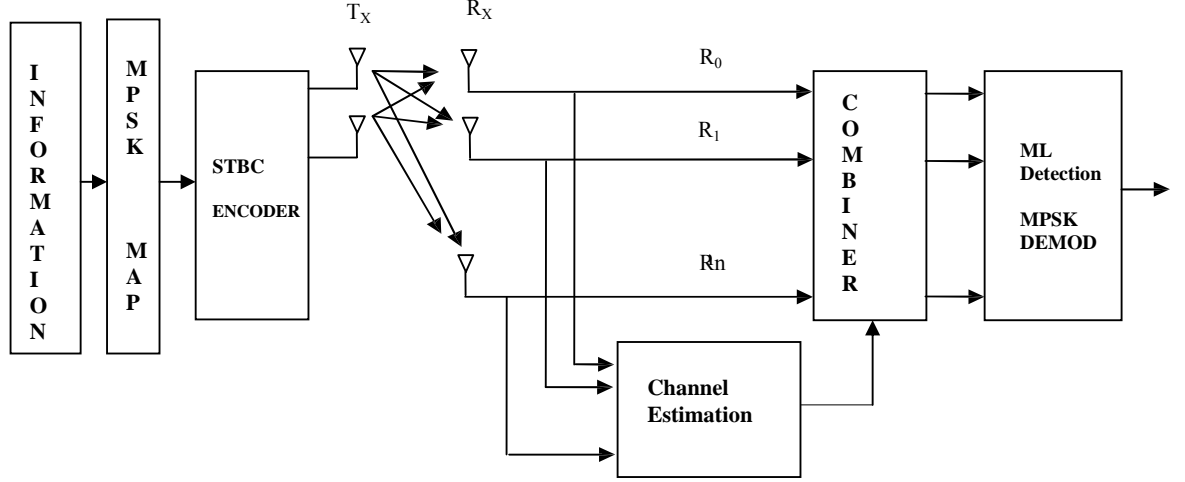


Figure 2.17: 2×N MIMO System Using Combiner

$$\begin{pmatrix} - \\ s_0 \\ - \\ s_1 \end{pmatrix} = \begin{pmatrix} h_0^* & h_1 & h_2^* & h_3 \\ h_1^* & -h_0 & h_3^* & -h_2 \end{pmatrix} \times \begin{pmatrix} r_0 \\ r_1^* \\ r_2 \\ r_3^* \end{pmatrix} \quad \dots (2.40)$$

Then by applying maximum likelihood detector s_0 and s_1 can be estimated. In the similar way for 2 by 4 systems following matrix form in equation (2.41) for the received signal in time interval t_1 and t_2 can be written.

$$\begin{pmatrix} r_0 & r_1 \\ r_2 & r_3 \\ r_4 & r_5 \\ r_6 & r_7 \end{pmatrix} = \begin{pmatrix} h_0 & h_1 \\ h_2 & h_3 \\ h_4 & h_5 \\ h_6 & h_7 \end{pmatrix} \times \begin{pmatrix} s_0 & -s_1^* \\ s_1 & s_0^* \end{pmatrix} + \begin{pmatrix} n_0 & n_1 \\ n_2 & n_3 \\ n_4 & n_5 \\ n_6 & n_7 \end{pmatrix} \quad \dots (2.41)$$

For the combiner, following simple matrix form in equation (2.42) can be defined.

$$\begin{pmatrix} - \\ s_0 \\ - \\ s_1 \end{pmatrix} = \begin{pmatrix} h_0^* & h_1 & h_2^* & h_3 & h_4^* & h_5 & h_6^* & h_7 \\ h_1^* & -h_0 & h_3^* & -h_2 & h_5^* & -h_4 & h_7^* & -h_6 \end{pmatrix} \times \begin{pmatrix} r_0 \\ r_1^* \\ r_2 \\ r_3^* \\ r_4 \\ r_5^* \\ r_6 \\ r_7 \end{pmatrix} \quad \dots (2.42)$$

Then by applying maximum likelihood detector, s_0 and s_1 can be estimated. In the similar way for 2 by N system following matrix form in equation (2.43) for the received signal in time interval t_1 and t_2 can be written.

$$\begin{pmatrix} r_0 & r_1 \\ r_2 & r_3 \\ \cdot & \cdot \\ \cdot & \cdot \\ r_{(2n-2)} & r_{(2n-1)} \end{pmatrix} = \begin{pmatrix} h_0 & h_1 \\ h_2 & h_3 \\ \cdot & \cdot \\ \cdot & \cdot \\ h_{(2n-2)} & h_{(2n-1)} \end{pmatrix} \times \begin{pmatrix} s_0 & -s_1^* \\ s_1 & s_0^* \end{pmatrix} + \begin{pmatrix} n_0 & n_1 \\ n_2 & n_3 \\ \cdot & \cdot \\ \cdot & \cdot \\ n_{(2n-2)} & n_{(2n-1)} \end{pmatrix} \dots (2.43)$$

For the combiner for 2 by N antenna configuration, shown in equation (2.44)

$$\begin{pmatrix} - \\ s_0 \\ - \\ s_1 \end{pmatrix} = \begin{pmatrix} h_0^* & h_1 & h_2^* & h_3 & \cdot & \cdot & h_{(2n-2)}^* & h_{(2n-1)} \\ h_1^* & -h_0 & h_3^* & -h_2 & \cdot & \cdot & h_{(2n-1)}^* & -h_{(2n-2)} \end{pmatrix} \times \begin{pmatrix} r_0 \\ r_1^* \\ r_2 \\ r_3^* \\ r_4 \\ r_5^* \\ \vdots \\ r_{(2n-2)} \\ r_{(2n-1)} \end{pmatrix} (2.44)$$

And finally in the same way symbols s_0 and s_1 can be detected using maximum likelihood detector.

2.7 ADVANTAGE & DISADVANTAGE OF MIMO

2.7.1 Advantages of MIMO

In wireless communications, the objectives are to increase throughput and transmission quality. MIMO systems can take advantage of the shortcoming of a wireless channel – the multipath- and turn it into an advantage. In MIMO systems, random fading and multipath delay spread can be used to increase throughput. MIMO systems offer an increase in capacity without the need to increase bandwidth and/or power.

Spatial Multiplexing (SM) is a technology that exploits this feature of MIMO systems in order to achieve the theoretical capacity limit in practice. Spatial Multiplexing uses different transmit antennas which send different signals. The signals are multiplexed in the channel and in the receive antennas, and then demultiplexed in the receiver. A schematic representation of the SM scheme is given in Figure 2.18.

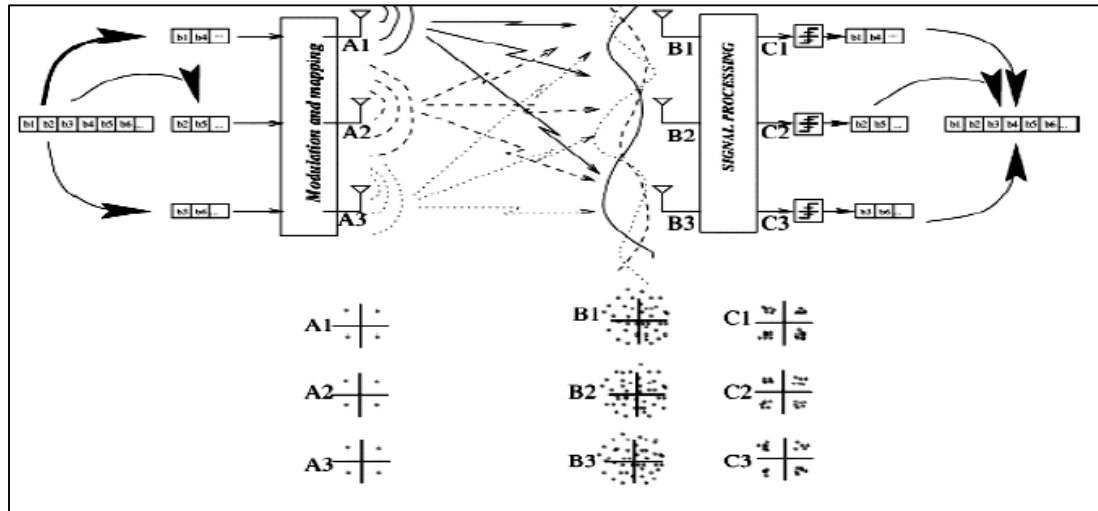


Figure 2.18: Schematic Representation of a Basic Spatial Multiplexing Scheme with 3 Transmit and 3 Receive Antennas

Apart from improving throughput, MIMO systems can also improve transmission quality. Diversity is a technology used in MIMO for this purpose. Multiple antennas can be used to minimize the effect of fading caused by multi-path propagation. When the antennas at the receive side are adequately spaced, then several copies of the transmitted signal are received through different channels and with different fading. The probabilities, that all received copies of the transmitted signal are in deep fading, can be regarded as small. We can thus deduce that diversity should improve the quality of the wireless link.

2.7.2 Disadvantages and Limitations of MIMO

One obvious disadvantage of MIMO is that they contain more antennas: MIMO increases complexity, volume, and hardware costs of the system compared to

SISO. MIMO systems are not always beneficial knowing that channel conditions depend on the radio environment. When there is Line of Sight (LOS), a higher LOS strength at receive will result in better performance and capacity in SISO system, while in MIMO systems capacity is reduced with higher LOS strength. This is because strong contributions from LOS lead to higher correlation among antennas, which reduces the advantage of using a MIMO system.

2.8 SUMMARY

This chapter mainly discussed properties of wireless channel by focusing various fading channel models, MIMO background, MIMO channel model, SISO, SIMO, MISO and MIMO systems with its channel capacity, space time block coding technique by exploiting Alamouti Scheme. Lastly advantages and disadvantages of MIMO systems have been described.

CHAPTER-3

CHANNEL ESTIMATION

3.1 INTRODUCTION

A Multiple-Input Multiple-Output (MIMO) communication technology has attracted attention in wireless communications, because it offers significant increases in data throughput and link range without additional bandwidth or increased transmit power. It achieves this goal by spreading the same total transmit power over the antennas to achieve an array gain that improves the spectral efficiency (more bits per second per hertz of bandwidth) or to achieve a diversity gain that improves the link reliability (reduced fading). In wireless communications, channel state information (CSI) refers to known channel properties of a communication link. This information describes how a signal propagates from the transmitter to the receiver. The CSI makes it possible to adapt transmissions to current channel conditions, which is crucial for achieving reliable communication with high data rates in MIMO systems.

Many channel estimation algorithms have been developed in recent years. In the literature [6]-[18], MIMO channel estimation methods can be classified into three classes: training based, blind and semi-blind. For pure training based scheme, a long training is necessary in order to obtain a reliable channel estimate, which considerably reduces system bandwidth efficiency. In Blind methods, no training symbols are used and channel state information is acquired by relying on the received signal statistics [19]-[25], which achieves high system throughput requiring high computational complexity. Semi-blind channel estimation approaches as a combination of the two aforementioned procedures [31]-[37], with few training symbols along with blind statistical information. Such techniques can solve the convergence problems and high complexity associated with blind estimators.

3.2 SYSTEM MODEL

In the following, we discuss a MIMO communication system that consists on M transmitter and N receiver antennas (denoted as $M \times N$ system). At the receiver we assume sampling with the period $T = 1/B$, where B is the signal bandwidth, thus preserving the sufficient statistics. The received signal is a spatial vector $y(k)$ given as

$$y(k) = H(k)X(k) + n(k), \quad y(k) \in \mathbb{C}^N, X(k) \in \mathbb{C}^M, n(k) \in \mathbb{C}^N, H(k) \in \mathbb{C}^{N \times M} \quad \dots (3.1)$$

Where $X(k) = [x_1(k) \dots x_M(k)]^T$ is the transmitted vector, $n(k) = [n_1(k) \dots n_N(k)]^T$ is the AWGN vector with $(E[n(k)n(k)^H]) = \sigma_n^2 I_{N \times N}$, and $H(k)$ is the MIMO channel response matrix, all corresponding to the time instance k . We assign index $m = 1, \dots, M$ to denote the transmit antennas, and index $n = 1, \dots, N$ to denote the receive antennas. Thus, $h_{nm}(k)$ is the n -th row and m -th column element of the matrix $H(k)$. Note that it corresponds to a SISO channel response between the transmit antenna m and the receive antenna n . $x_m(k)$ is the transmitted signal from the m -th transmit antenna. The n -th component of the received spatial vector $y(k) = [y_1(k) \dots y_N(k)]^T$ (i.e., signal at the receive antenna n) is

$$y_n(k) = \sum_{m=1}^M h_{nm}(k)x_m(k) + n_n(k) \quad \dots (3.2)$$

To perform estimation of the channel response $H(k)$, the receiver uses a pilot (training) signal that is a part of the transmitted data. The pilot is sent periodically. We consider the transmitted signal to be comprised of two parts: one is the data bearing signal and the other is the pilot signal. Within the total transmitted K symbols, first L symbols (i.e., signal dimensions) are allocated as pilot (training) symbols per transmit antenna and remaining $K-LM$ symbols are data bearing symbols. As a common practical solution, it is assumed that the pilot signals assigned to the different transmit antennas, are mutually orthogonal. This assumption requires that $K \geq LM$.

Consequently we define a K -dimensional temporal vector $x_m = [x_m(1) \dots x_m(K)]^T$ whose k -th component is $x_m(k)$ as

$$x_m = \underbrace{\sum_{i=1}^{K-LM} a_{im}^d d_{im}^d S_i^d}_{Data} + \underbrace{\sum_{j=1}^L a_{jm}^p d_{jm}^p S_{jm}^p}_{Pilot} \quad \dots (3.3)$$

In the above the first sum is the information, i.e., data bearing signal and the second corresponds to the pilot signal, corresponding to the transmit antennas. Superscripts "d" and "p" denote values assigned to the data and pilot, respectively. d_{im}^d is the unit-variance circularly symmetric complex data symbol. The pilot symbols $d_{jm}^p, j=1, \dots, L$ are predefined and known at the receiver. We also assume that the amplitudes are $a_{im}^d = A$, and $a_{jm}^p = A_p$, and they are known at the receiver. Note that the amplitudes are identical across the transmit antennas (because we assumed that the transmit power is equally distributed across them). Furthermore, $S_i^d = [S_i^d(1) \dots S_i^d(k)]^T, (i=1, \dots, (K-LM))$ and $S_{jm}^p = [S_{jm}^p(1) \dots S_{jm}^p(K)]^T, (j=1, \dots, L, \text{ and } m=1, \dots, M)$ are waveforms, denoted as temporal signatures. The temporal signatures are mutually orthogonal.

As said earlier that the pilot signals are orthogonal between the transmit antennas. The indexing and summation limits in (3.3) conform to this assumption, i.e., temporal signatures $S_{jm}^p (j=1, \dots, L)$ are uniquely assigned to the transmit antennas. In other words, transmit antennas must not use the temporal signatures that are assigned as pilots to other antennas and assigned to data, which is consequently lowering the achievable data rates. Unlike the pilot temporal signatures, the data bearing temporal signatures $S_i^d (1, \dots, (K-LM))$ are reused across the transmit antennas, which is an inherent property of MIMO systems, potentially resulting in high achievable data rates. Received spatial vector can be described as

$$y(k) = H(k)(d(k) + p(k)) + n(k), \quad d(k) \in C^M, p(k) \in C^M \quad \dots (3.4)$$

Where $d(k)$ is the information, i.e., data bearing signal and $p(k)$ is the pilot portion of the transmitted spatial signal, at the time instance k . The m -th component of the data vector

$d(k) = [d_1(k) \dots d_M(k)]^T$ (i.e., data signal at the transmit antenna) is

$$d_m(k) = \sum_{i=1}^{K-LM} a_{im}^d d_{im}^d S_i^d(k) \quad \dots (3.5)$$

The m -th component of the pilot vector $p(k) = [p_1(k) \dots p_M(k)]^T$ (i.e., pilot signal at the transmit antenna) is

$$p_m(k) = \sum_{j=1}^L a_{jm}^p d_{jm}^p S_{jm}^p(k) \quad \dots (3.6)$$

Let us now describe the assumed properties of the MIMO channel $H(k)$. The channel coherence time is assumed to be greater or equal to KT . This assumption approximates the channel to be constant over at least K samples ($h_{nm}(k) \approx h_{nm}$, for $k = 1, \dots, K$, for all m and n), i.e., approximately constant during the pilot period. In the literature, channels with the above property are known as block-fading channels. Furthermore, the elements of H are independent identically distributed (i.i.d.) random variables, corresponding to highly scattering channels. In general, the MIMO propagation measurements and modeling have shown that the elements of H are correlated (i.e., not independent). Based on that, the received temporal vector at the receiver n , whose k -th component is $y_n(k)$, which shown in the equation (3.2), is

$$r_n = [y_n(1) \dots y_n(K)]^T = \sum_{m=1}^M h_{nm} x_m + n_n, \quad r_n \in C^K \quad \dots (3.7)$$

Where $n_n = [n_n(1) \dots n_n(K)]^T$ and $E[n_n n_n^H] = \sigma_n^2 I_{K \times K}$

3.2.1 Simplified Form for System Model

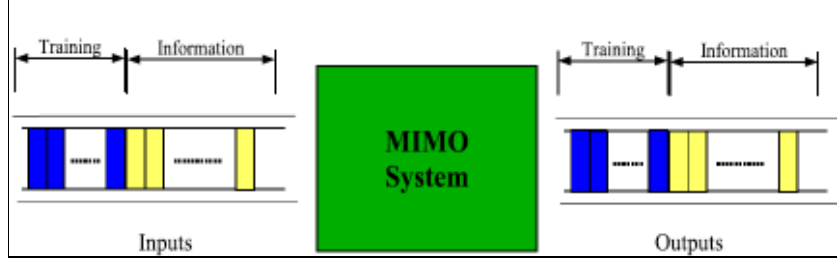


Figure 3.1: Schematic Representation of a MIMO Frame

The MIMO wireless system can be represented as a matrix wireless channel. Let $X_d(k) \in C^{M \times 1}$ be the k^{th} transmitted MIMO symbol vector. This vector $X_d(k)$ is given as,

$$X_d(k) = \begin{bmatrix} X_{d,1}(k) \\ X_{d,2}(k) \\ \vdots \\ X_{d,M}(k) \end{bmatrix} \quad \dots (3.8)$$

Where $X_{d,j}(k)$, $1 \leq j \leq M$ is the symbol transmitted from the j^{th} transmit antenna.

Similarly, the receive symbol vector $y_d(k)$ is given as,

$$y_d(k) = \begin{bmatrix} y_{d,1}(k) \\ y_{d,2}(k) \\ \vdots \\ y_{d,N}(k) \end{bmatrix} \quad \dots (3.9)$$

Where $y_{d,i}(k)$, $1 \leq i \leq N$ is the received signal at the i^{th} receive antenna. In a flat-fading MIMO system (where symbol duration is much greater than the multipath delay spread of the channel), the input-output system model at each receive antenna can be expressed as

$$y_{d,i}(k) = \sum_{j=1}^M h_{i,j} X_{d,j}(k) + \eta_i(k) \quad \dots (3.10)$$

Here $\eta_i(k)$ is the noise added at the i^{th} receiver. This can be represented in matrix form as

$$y_d(k) = HX_d(k) + \eta(k) \quad \dots (3.11)$$

Where the matrix $H \in C^{N \times M}$ represents the MIMO channel. This matrix H is given as,

$$H = \begin{bmatrix} h_{11} & h_{12} & \dots & h_{1M} \\ h_{21} & h_{22} & \dots & h_{2M} \\ \vdots & \vdots & \ddots & \vdots \\ h_{N1} & h_{N2} & \dots & h_{NM} \end{bmatrix} \quad \dots (3.12)$$

The coefficients $h_{i,j}$ represents the flat fading channel between i^{th} receiver and j^{th} transmitter. Knowledge of this channel matrix is necessary for detection of the transmitted symbols $X_d(k)$. Hence, it is necessary to estimate the channel matrix H . This procedure of estimating H is known as channel estimation. This channel estimate can either be employed at the receiver for detection or feedback to the transmitter for transmit precoding and beam forming.

3.3 ESTIMATION PHILOSOPHIES

3.3.1 Pilot based Estimation

The most commonly employed channel estimation scheme is pilot (training) based channel estimation. In this scheme, pilot symbols are used with information symbols in the transmission frame shown in figure 3.1. These pilots are fixed set of symbols which are known at the receiver and from the received output of pilot symbols, estimation of MIMO channel can be performed which further employed for detection of the information symbols transmitted subsequently. This scheme has

benefit of robust estimate and low computational complexity, however drawback of this scheme is pilot symbols themselves carry no information hence overhead on communication system and results in wastage of bandwidth hence this scheme is “bandwidth inefficient”. Various pilot based channel estimation techniques like Least Square (LS), Minimum Mean Square Error (MMSE), Maximum Likelihood (ML), and Maximum a-Posteriori (MAP) etc. can be employed for channel estimation.

3.3.2 Blind Estimation

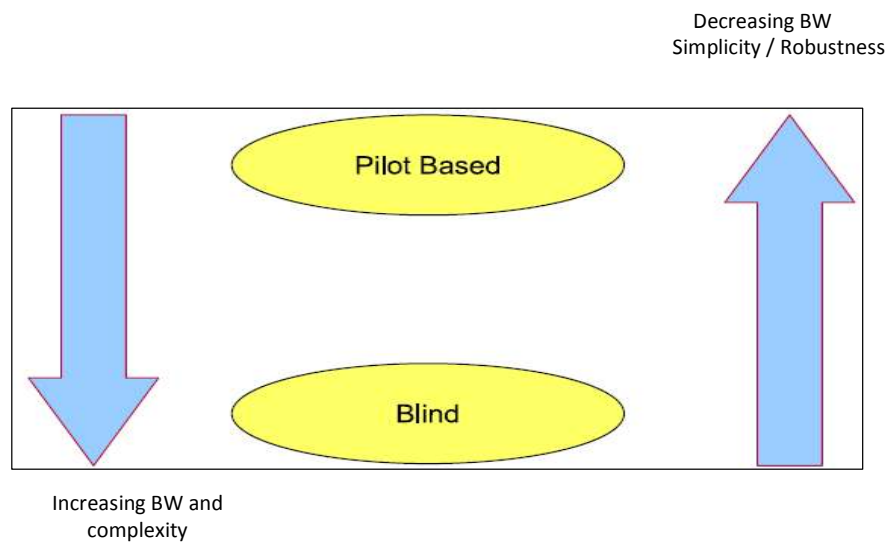


Figure 3.2: Pictorial Representation of Pilot Vs Blind Tradeoff

Blind channel estimation does not require pilot symbols to estimate a channel hence this scheme is “bandwidth efficient”. In this scheme channel can be estimated using statistical knowledge of received output symbols. For the case, if the transmitter employs a symmetric transmit constellation with equal priori probabilities (as is the case frequently), then the received symbol stream has a statistical mean of zero. Further, with knowledge of the covariance of the input information symbols, the computed covariance of the output information symbols can be employed to estimate at least part of the channel. Thus, statistical information provides a viable means to estimate the channel. This scheme is computationally complex and having some convergence problems. Thus blind schemes while being extremely bandwidth efficient are unattractive to implement in wireless systems where robustness of the

estimate and computational complexity are critical. A widely studied blind estimation technique is the subspace method using second order statistics (SOS) [25],[27]. In the subspace method, the autocorrelation matrix of the received signal is decomposed into the signal and noise subspaces. Due to the orthogonality of the noise and signal subspace, the channel estimates can be calculated based on the noise subspace. More importantly, the decomposition of the autocorrelation function via eigenvalue decomposition (EVD) or singular value decomposition (SVD) is used. Further other matrix decomposition techniques can be preferred like QR decomposition which restricts direct matrix inversions and convert full rank channel matrix in to simpler form hence it's having low complexity.

3.3.3 Semi-Blind Philosophy

This scheme employs combination of both pilot channel estimation and blind channel estimation to take the advantage of low complexity with robustness by using limited number of pilot symbols and bandwidth efficiency by using statistical blind information. Thus, as seen above, there is an inherent complexity and robustness vs. bandwidth efficiency tradeoff in pilot and blind estimation schemes as shown in fig (3.2). The development of such a scheme is motivated for the following reason. Given a certain amount of pilot information, the quality of the channel estimate is enhanced by employing statistical information to aid the estimation process, or in other words, minimize the number of pilot symbols transmitted by employing statistical information to improve the nature of the channel estimate, thereby increasing the bandwidth efficiency.

3.4 CHANNEL ESTIMATION TECHNIQUES

The performance boost brought by MIMO systems mainly attributes to the space-time techniques which aimed to compensate the channel effects at both transmission and detection phase. Channel state information generated by the channel estimation module, is either sent into the detection block or fed back to the transmitter

side to construct beam forming weight vector. Methods of channel estimation in MIMO systems are discussed here briefly.

Basically, methods of channel estimation can be classified as follows:

- From the view of estimation theory, there are
 - Least Square (LS) Estimation
 - Minimum Mean Square Error (MMSE) Estimation
 - Maximum a-Posteriori (MAP) Estimation
- Due to the different pilot-symbol arrangements, there are
 - Estimator with Block-Type Pilot (Training Based)
 - Estimator with Comb-Type Pilot (Pilot Symbol Aided Modulation)

3.4.1 LS and MMSE

Estimation theory is a branch of statistical signal processing. It deals with a problem of estimating parameters based on the measured data. The purpose of the estimation theory is to develop an estimator, preferably an implementable one that can be used in practice. The estimator takes the measurement data as inputs and produces estimated values of the parameters.

Thus the system equation from equation (3.11) can be written as

$$Y = XH + \eta \quad \dots (3.13)$$

Now considering channel matrix h , we can rewrite following equation as

$$Y = Xh + \eta \quad \dots (3.14)$$

By examining (3.13) and (3.14), both of them are linear equations. H and h are unknown vectors. X is the known matrix. Y is the measurement matrix for both. There

are two estimators mainly used for the problem of channel estimation, namely Least Squares (LS) and Minimum Mean Square Error (MMSE) channel estimators.

3.4.1.1 Least-Squares (LS) Channel Estimation

With reference to equation (3.14), the channel estimation is to find a solution \hat{h} for the equation $X\hat{h} \approx Y$. In Least Square, minimization of the Euclidean norm squared of the residual $X\hat{h} - Y$, is to be performed

$$\begin{aligned} \arg_h \min \|X\hat{h} - Y\|^2 \\ \|X\hat{h} - Y\|^2 &= (X\hat{h} - Y)^H (X\hat{h} - Y) \\ &= (X\hat{h})^H (X\hat{h}) - Y^H X\hat{h} - (X\hat{h})^H Y + Y^H Y \end{aligned}$$

The minimum is found at the zero of the derivative with respect to \hat{h} , then

$$2X^H X\hat{h} - 2X^H Y = 0 \quad \Rightarrow X^H X\hat{h} = X^H Y$$

Therefore, \hat{h} will be given by

$$\hat{h} = (X^H X)^{-1} X^H Y = X^\dagger Y \quad \dots (3.15)$$

Under the condition that the X has full column rank. The term $(X^H X)^{-1} X^H$ is called pseudo-inverse of matrix X , sometimes denoted by X^\dagger .

3.4.1.2 Minimum Mean Square Error (MMSE) Channel Estimation

MMSE estimator aims to approach optimal result by exploiting the statistical dependence between the measured data and the estimated parameters. (3.14) is chosen to be an example, where h is to be estimated.

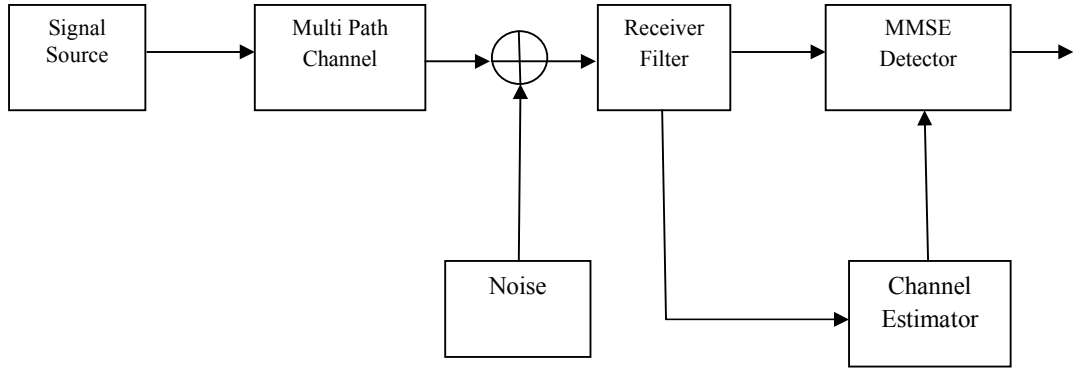


Figure 3.3: Block Diagram of a Noise-Corrupted System with MMSE Estimation

On purpose of minimizing the Mean Square Error (MSE) $E[(h - \hat{h}_{MMSE})^2]$, the estimated channel impulse response can be given as

$$\hat{h} = R_{hY} R_{YY}^{-1} Y \quad \dots (3.16)$$

Where R_{hY} , R_{YY} are the cross covariance matrices between h and Y and the auto-covariance matrix of Y .

$$R_{hY} = E[hY^H] = E[h(Xh + \eta)^H] = R_{hh} X^H \quad \dots (3.17)$$

$$\begin{aligned} R_{YY} &= E[YY^H] = E[(Xh + \eta)(Xh + \eta)^H] \\ &= E[Xh(Xh)^H + Xh\eta^H + \eta(Xh)^H + \eta\eta^H] \\ &= XR_{hh}X^H + \sigma_n^2 I \quad \dots (3.18) \end{aligned}$$

$R_{hh} = E[hh^H]$ is the auto-covariance matrix of h and σ_n^2 denotes the noise variance $E[\eta\eta^H]$. These two quantities are assumed to be known at the estimator.

Then 3.18 can be rewritten as

$$\hat{h} = R_{hh}^{-1} X^H (X R_{hh}^{-1} X^H + \sigma_n^2 I)^{-1} Y \quad \dots (3.19)$$

3.4.1.3 Maximum A Posteriori (MAP) Channel Estimation

MAP channel estimation requires knowledge of the training sequence, the channel covariance, and the noise covariance at the receiver. The same system model described for LS estimation applies to MAP estimation. The MAP estimate for the channel matrix maximizes the a posteriori probability density function $p(H|Y,X)$ with respect to H . The MAP estimate for H satisfy

$$\frac{\partial}{\partial H} \ln(p(H|Y, X)) \Big|_{H = \hat{H}_{MAP}} = 0 \quad \dots (3.20)$$

By using Bayes' identity solving equation yields

$$p(H|Y, X) = \frac{p(Y|H, X)p(H, X)}{p(Y|X)}$$

$$\hat{H}_{MAP} = (X^H C_n^{-1} X + C_H)^{-1} X^H C_n^{-1} Y \quad \dots (3.21)$$

Where noise covariance $C_n = R_{\eta\eta} = E[\eta\eta^H]$ and channel covariance $C_H = R_{HH} = E[HH^H]$

For independent Rayleigh Fading channels, C_H can be approximated as an identity matrix.

3.4.2 Block-Type Pilot vs. Comb-Type Pilot

One of the crucial parts of channel estimation is how to design the pilot symbols which will be agreed to both sides of the transmission. Basically, pilot tones can be inserted either into all of the sub-carriers of blocks periodically or a subset of sub-carriers of each block.

The first one, channel estimation with block-type pilot, sometimes also mentioned as training based, has been developed under the assumption of slow fading channel. The second, comb-type pilot channel estimation is introduced to satisfy the need for equalizing when the channel changes even from one block to the subsequent one.

3.4.2.1 Estimation with Block-Type Pilot

Figure 3.4 illustrate the block-type pilot that a continuous pilot blocks to obtain channel impulse response on all sub-carriers. The length of the training block is fixed to the number of sub-carriers in the block. Estimation is fulfilled over each period of channel coherence time T_c , which is a statistical measure of the time duration over the channel impulse response is essentially invariant. It is assumed that the channel is flat block-fading when block-type pilot is employed.

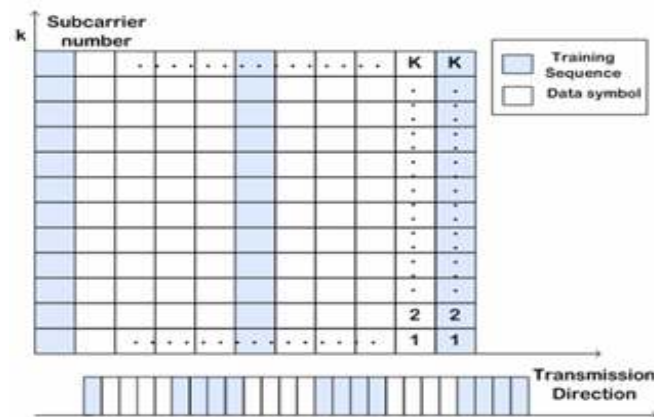


Figure 3.4: Block-type Pilot

3.4.2.2 Estimation with Comb-Type Pilot

Comb-type pilot channel estimation is introduced to handle the situation that the channel changes even from one block to the subsequent one. It is performed by inserting pilot symbols into a subset of the sub-carriers of each block as in Figure 3.5 or some of the blocks periodically (Figure 3.6).

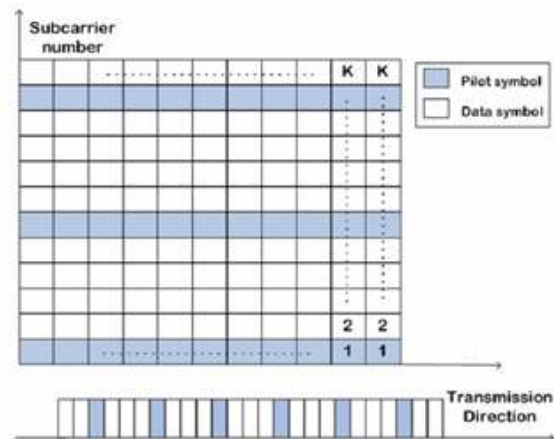


Figure 3.5: Comb Type Pilot

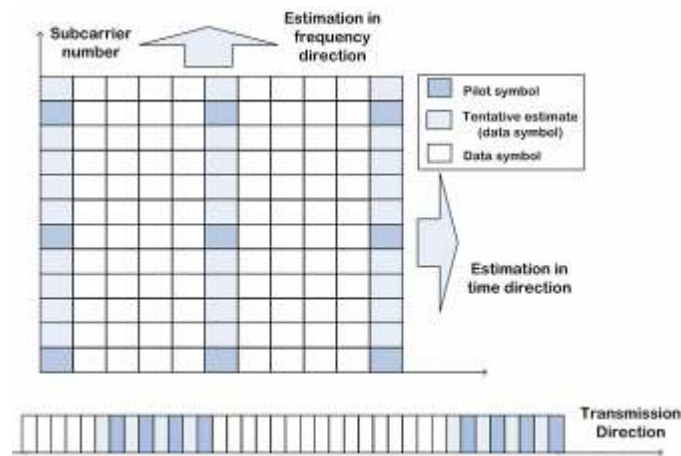


Figure 3.6: Pilot Tones in Two Dimensions

Estimation is done upon these known sub-carriers. The other tones are handled by interpolation. Such a scheme that multiplexing pilot symbols with data is referred to as Pilot-Symbol-Aided-Modulation (PSAM), giving the corresponding channel estimator named as Pilot-Symbol-Aided (PSA) estimator. By periodically inserting pilots in the time-frequency grid such that sampling theorem is satisfied, the channel response can be reconstructed by exploiting the correlation of the received signal in frequency and time. In wireless communication, small-scale channel fading can be characterized in both dimensions of frequency and time. Let τ_{\max} and f_{\max} be the maximum delay spread and Doppler frequency, and D_f and D_t be the pilot spacing in

frequency and time domain, they must satisfy $\frac{D_f \tau_{\max}}{T} \leq 1$ and $f_{\max} T_{\text{sym}} D_T \leq 1/2$. T and T_{sym} are the symbol duration without and with the guard interval. Two times oversampling has a good compromise between pilot overhead and performance.

3.5 SUMMARY

This chapter mainly focused on basic MIMO system model, different channel estimation philosophies like training based channel estimation, blind channel estimation and semi-blind channel estimation techniques. Further basic training (pilot) based channel estimation techniques like Least Square (LS), Minimum Mean Square Error (MMSE) channel estimation and Maximum a-Posteriori (MAP) channel estimation were discussed.

CHAPTER-4

PROPOSED SEMI-BLIND CHANNEL ESTIMATION TECHNIQUES

4.1 INTRODCUTION

MIMO and smart antenna systems are widely being studied for employment in current and upcoming wireless communication systems. Smart antenna systems, which are built with multiple antennas on receive or transmit side, offer a variety of gains such as improved SNR due to diversity of reception or transmission and also enhanced signal quality from interference suppression. In addition to these, MIMO systems also provide the additional advantage of increased data communication rates for the same SNR by using the multiple spatial multiplexing modes available for communication.

As the number of data channels increases in MIMO systems, the number of associated training streams for the estimation of the channel coefficients increases proportionately hence reduction in spectral efficiency. Moreover, such pilot based techniques tend not to use the statistical information available in unknown data symbols to improve channel estimates. The MIMO channel estimation problem is further complicated because, as the diversity of the MIMO system increases, the SNR (per bit) required to achieve the same system performance (in terms of BER) decreases [1]. There is requirement of robust channel estimation techniques which use both training and blind data completely. Semi-blind techniques can potentially enhance the quality of such estimates by making a more complete use of available data. Overhead costs can be reduced by achieving training based estimation quality for smaller training symbol pay loads. With a few known training symbols along with blind statistical information, such techniques can avoid the convergence problems associated with completely blind techniques.

4.2 SYSTEM MODEL

Consider a flat fading MIMO channel matrix $H \in C^{N \times M}$ where M is the number of transmit antennas and N is the number of receive antennas in the system, and each h_{ij} represents the flat-fading channel coefficient between the i^{th} receiver and j^{th} transmitter. Denoting the complex received data by $Y \in C^{N \times 1}$, the equivalent base-band system can be modeled as

$$Y(k) = HX(k) + \eta(k) \quad \dots (4.1)$$

$$\text{Where } H = \begin{bmatrix} h_{11} & h_{12} & \dots & h_{1M} \\ h_{21} & h_{22} & \dots & h_{2M} \\ \vdots & \vdots & \ddots & \vdots \\ h_{N1} & h_{N2} & \dots & h_{NM} \end{bmatrix} \quad \dots (4.2)$$

k Represents the time instant, $X \in C^{M \times 1}$ is the complex transmitted symbol vector. η is additive white Gaussian noise such that $E\{\eta(k)\eta(l)^H\} = \delta(k,l)\sigma_n^2 I$ where $\delta(k,l) = 1$ if $k=l$ and 0 otherwise. Also, the sources are assumed to be spatially and temporally independent with identical source power σ_s^2 i.e. $E\{X(k)X(l)^H\} = \delta(k,l)\sigma_s^2 I$. The signal to noise ratio (SNR) of operation is defined as $\frac{\sigma_s^2}{\sigma_n^2}$. Assume that the channel has been used for a total of K symbol transmissions. Out of these K transmissions, the first L symbols are known training symbols X_p , stacking symbols we have $X_p = [X_1, X_2, \dots, X_L]$ where $X_p \in C^{M \times L}$ and its corresponding output $Y_p \in C^{N \times L}$ is received training output. Further remaining $K - L$ are blind data symbols X_b and their corresponding output Y_b , where $X_b \in C^{M \times (K-L)}$ and $Y_b \in C^{N \times (K-L)}$.

H can be exclusively estimated using only training symbols as a

$$\hat{H}_T = Y_p (X_p^H X_p)^{-1} X_p^H \quad \dots (4.3)$$

It is very easy to implement but results in poor usages of available bandwidth since training symbols contains no information. In the alternative, H may be estimated using blind data without any training symbols, means $L = 0$ and only Y_b is available. This is very efficient usages of bandwidth but blind methods which uses second order statics and higher order statistics having poor convergence speed and high computational complexity. Hence semi-blind channel estimation techniques, which require few amounts of training symbols and blind data symbols, could be very attractive solution for it.

First matrix decomposition based SVD-OPML semi-blind channel estimation technique is discussed [38],[40],[44]. In that semi-blind technique, blind estimation is performed using second order statistics (SOS) of received output data by decomposing autocorrelation matrix of output data using Singular Value Decomposition (SVD) and training (pilot) based estimation is performed using Orthogonal Pilot Maximum Likelihood (OPML) algorithm. Then after SVD-ROML semi-blind channel estimation technique is discussed [44]. In that semi-blind technique, blind channel estimation is performed same as above technique and for training based estimation, Rotation Optimization Maximal Likelihood (ROML) based estimator is used. Both techniques are discussed below.

4.3 SVD-OPML BASED SEMI-BLIND CHANNEL ESTIMATION

Now consider a MIMO channel $H \in C^{N \times M}$ which has at least as many receive antennas as transmit antennas i.e. $N \geq M$. Then, the channel matrix H can be decomposed as $H = WQ^H$ where $W \in C^{N \times M}$ is also known as the whitening matrix and $Q \in C^{M \times M}$, termed as the rotation matrix, that is unitary i.e. $Q^H Q = Q Q^H = I$ as shown in [44], the matrix W can be estimated from the autocorrelation matrix of received data alone. The pilot information can be employed to exclusively estimate the rotation matrix Q .

This semi-blind estimation procedure is also termed as a Whitening-Rotation (WR) scheme. Output autocorrelation matrix can be described as

$$R_{YY} = E[Y_b Y_b^H] = H X_b (H X_b)^H + \sigma_n^2 I \quad \dots (4.4)$$

The auto covariance matrix of blind symbols denoted as

$$E\{X_b(k) X_b(l)^H\} = \delta(k, l) \sigma_s^2 I \quad \dots (4.5)$$

And normalized source power is given by

$$\sigma_s^2 = 1 \quad \dots (4.6)$$

So equation further simplified as

$$R_{YY} = H H^H + \sigma_n^2 I \quad \dots (4.7)$$

$$\text{Further } H H^H = R_{YY} - \sigma_n^2 I = \tilde{R}_{YY} \quad \dots (4.8)$$

Consider identical Gaussian noise power is know to us and Let the Singular Value Decomposition (SVD) of \tilde{R}_{YY} be given as $U \Sigma^2 U^H$, where U and U^H are unitary matrices (rotation matrices) and Σ is diagonal matrix (scaling matrix). A possible choice for W is given by $W = U \Sigma$ and we assume this specific choice in the rest of the work. Now list of potential assumptions are employed as appropriate in subsequent parts of the work.

Assumption A. $W \in C^{N \times M}$ is perfectly known at the output.

Assumption B. $X_p \in C^{M \times L}$ is orthogonal i.e. $X_p X_p^H = \sigma_s^2 L I_{M \times M}$

Assumption A is reasonable if we assume the transmission of a long data

stream ($K \rightarrow \infty$) from which W can be estimated with considerable accuracy and Assumption B can be easily achieved by using an integer orthogonal structure such as the Hadamard matrix.

Hence blind channel estimation can be found as

$$W = U \Sigma \quad \dots (4.9)$$

Now training based channel estimation can be found using orthogonal pilot maximum likelihood algorithm, as an optimal estimation

Orthogonal Pilot Maximum Likelihood (OPML) estimator

$\hat{Q}: C^{N \times L} \rightarrow S$, where \hat{Q} the constrained ML estimator of is Q and S is the manifold of $M \times M$ unitary matrices, which is obtained by minimizing the likelihood function

$$\|Y_p - WQ^H X_p\|_F^2 \text{ Such that } QQ^H = I \quad \dots (4.10)$$

Further

$$\|Y_p - WQ^H X_p\|_F^2 = tr(Y_p Y_p^H) + tr(WW^H) - 2tr((Q^H X_p)^H W^H Y_p) \quad \dots (4.11)$$

Where $QQ^H = X_p X_p^H = I$, so the above equation is to maximize the trace of

$$2tr((Q^H X_p)^H W^H Y_p) \quad \dots (4.12)$$

Such as $(Q^H X_p)^H Q^H X_p = I$ is assumed to simplify above equation.

If $X_p X_p^H = I$, then cost minimizing function \hat{Q} in above equation is given as SVD of M_s , where $M_s = W^H Y_p X_p^H$. SVD of M_s is shown below [36].

$$\hat{Q} = V_{M_s} U_{M_s}^H \text{ Where } U_{M_s} \sum_{M_s} V_{M_s}^H = SVD(W^H Y_p X_p^H) = SVD(M_s) \quad \dots (4.13)$$

This procedure employs assumption B. (orthogonal pilot), which termed as the OPML estimator. The above expression yields a closed form expression for the computation of \hat{Q} , the ML estimate of Q . The channel matrix H is then estimated using blind and training based technique as

$$\hat{H} = W \hat{Q}^H \quad \dots (4.14)$$

4.4 SVD-ROML BASED SEMI-BLIND CHANNEL ESTIMATION

In this method, blind estimation of channel is performed using same way as performed in above technique. So W is calculated using SVD decomposition of autocorrelation matrix of received output data. Now training based estimating of channel is performed using Rotation Optimization Maximum Likelihood (ROML) based suboptimal technique, which is shown below.

Rotation Optimization Maximum Likelihood (ROML) based Semi-Blind Channel Estimation:

Here proposed a simplistic ROML procedure for the sub-optimal estimation of Q . The first step is to construct modified cost function as

$$\min_Q \left\| \tilde{W} Y_p - Q^H X_p \right\|^2 \quad \text{Where } Q Q^H = I$$

$\tilde{Y} = \tilde{W} Y_p$ Is the whitening pre-equalized data. Several choices can then be considered for the pre-equalization filter \tilde{W} . A robust MMSE pre-filter is given as

$$\tilde{W}_{MMSE} = \sigma_s^2 W^H (\sigma_s^2 W W^H + \sigma_n^2 I)^{-1} \quad \dots (4.15)$$

And Zero Forcing (ZF) equalizer is given as

$$\tilde{W}_{ZF} = W^\dagger \text{ Where } W^\dagger = (W^H W)^{-1} W^H \quad \dots (4.16)$$

However ZF is suitable for noise enhancement so it's better to use MMSE pre-filter

Further

$$\left\| \tilde{W} Y_p - Q^H X_p \right\|_F^2 = \text{tr}((\tilde{W} Y_p)(\tilde{W} Y_p)^H) + \text{tr}((Q^H X_p)(Q^H X_p)^H) - 2\text{tr}((Q^H X_p)^H \tilde{W} Y_p) \quad \dots (4.17)$$

Where $Q Q^H = X_p X_p^H = I$.

So the above equation is to maximize the trace of $2\text{tr}((Q^H X_p)^H \tilde{W} Y_p)$ such as

$Q^H X_p (Q^H X_p)^H = I$ is assumed to simplify above equation.

If $X_p X_p^H = I$, then cost minimizing function \hat{Q} in above equation is given as SVD of M_q , where is given as below

$$M_q = \tilde{W} Y_p X_p^H \quad \dots (4.18)$$

SVD of M_q is shown below.

$$\hat{Q} = V_{M_q} U_{M_q}^H \text{ Where } U_{M_q} \sum_{M_q} V_{M_q}^H = \text{SVD}(\tilde{W} Y_p X_p^H) = \text{SVD}(M_q) \quad \dots (4.19)$$

The channel matrix H is then estimated as

$$\hat{H} = W \hat{Q}^H \quad \dots (4.20)$$

Now semi-blind techniques explained above demonstrate good performance compare to training based channel estimation techniques and they are less computationally complex because they don't require direct matrix inversion operations. Still some complexity is due to SVD decomposition of matrix so there is

requirement to propose matrix decomposition based novel semi-blind channel estimation technique(s) which are less complex and outperform others by giving near optimal performance.

4.5 PROPOSED NOVEL SEMI-BLIND CHANNEL ESTIMATION TECHNIQUES

4.5.1 Joint Channel Estimation and Data Detection QR-NEW (Proposed Technique-I)

This novel technique based on joint channel and data estimation using QR-decomposition algorithm. Let X_p is pilot (training) and their corresponding output is Y_p , so initial channel estimation is calculated using pilot (training) data only using QR decomposition. Minimizing the norm square error function of equation (4.1)

$$\varepsilon = Y_p - \hat{H}X_p \quad \dots (4.21)$$

To avoid matrix inversion, directly apply QR decomposition to the error function and estimate initial channel using following steps.

1. $\varepsilon = Y_p - \hat{H}X_p$ and if $\varepsilon = 0 \Rightarrow Y_p = \hat{H}X_p$... (4.22)
2. Decompose X_p into, hermitian matrix Q_p and upper triangular matrix R_p using QR decomposition algorithm.

$$Y_p = \hat{H}X_p = \hat{H}Q_p \begin{bmatrix} R_p \\ 0 \end{bmatrix} \quad \dots (4.23)$$

Where $Q_p Q_p^H = I$ due to hermitian property multiply both sides by Q_p^H therefore,

$$\hat{H} \begin{bmatrix} R_p \\ 0 \end{bmatrix} = Y_p Q_p^H \quad \dots (4.24)$$

Then \hat{H} is estimated by solving above equation using back substitution method and that is channel estimation using pilot symbols X_p , so that $\hat{H}_{TS} = \hat{H}$

From that \hat{H}_{TS} , estimated blind data can be found as

$$X_{best} = (\hat{H}_{TS}^H \hat{H}_{TS})^{-1} \hat{H}_{TS}^H Y_b \quad \dots (4.25)$$

Where Y_b is received output data. Now perform same procedure to minimize norm square error function.

$$\varepsilon = Y_b - \hat{H}_F X_{best}, \text{ so } \varepsilon = 0 \Rightarrow Y_b = \hat{H}_F X_{best} \quad \dots (4.26)$$

Decompose X_{best} into, hermitian matrix Q_b and upper triangular matrix R_b using QR decomposition algorithm.

$$Y_b = \hat{H}_F Q_b \begin{bmatrix} R_b \\ 0 \end{bmatrix} \quad \dots (4.27)$$

Now $Q_b Q_b^H = I$, multiplying both side, therefore

$$\hat{H}_F \begin{bmatrix} R_b \\ 0 \end{bmatrix} = Y_b Q_b^H \quad \dots (4.28)$$

Final channel estimation \hat{H}_F is estimated form above equation using back substitution method.

4.5.2 Householder QR-OPML (Proposed Technique-II)

A novel algorithm is proposed and studied for QR decomposition-based scheme in the context of semi-blind Multi-Input Multi-Output (MIMO) channel estimation. Specifically, the flat-fading MIMO channel matrix H can be decomposed as an upper triangular matrix R and a unitary rotation matrix Q . The matrix R is estimated blindly from only received data by using orthogonal matrix triangularization based Householder QR decomposition while the optimum rotation matrix Q is estimated exclusively from training symbols based OPML (Orthogonal Pilot ML Estimator) technique.

Blind Estimation of R

Output autocorrelation matrix can be described as

$$R_{YY} = E[Y_b Y_b^H] = H X_b (H X_b)^H + \sigma_n^2 I \quad \dots (4.29)$$

We know that covariance matrix of blind symbols denoted as

$$E\{X_b(k) X_b(l)^H\} = \delta(k, l) \sigma_s^2 I \quad \dots (4.30)$$

And normalized source power is given by

$$\sigma_s^2 = 1 \quad \dots (4.31)$$

So equation further simplified as

$$R_{YY} = H H^H + \sigma_n^2 I \quad \dots (4.32)$$

Further

$$H H^H = R_{YY} - \sigma_n^2 I = \tilde{R}_{YY} \quad \dots (4.33)$$

Now apply Householder transformation to received output autocorrelation matrix \tilde{R}_{YY} . In the Householder approach, series of reflection matrix is applied to matrix \tilde{R}_{YY} column by column to annihilate the lower triangular elements.

The reflection transformations are ortho-normal matrices that can be written as

$$A = (I + \beta VV^H) \quad \dots (4.34)$$

Where V is the Householder vector and $\beta = -2\|V\|_2^2$

For the matrix \tilde{R}_{YY} to annihilate the lower elements of the k -th column the A_k is

Constructed as follows:

1. Let V equal the k -th column of \tilde{R}_{YY}
2. Update V by $V = \tilde{R}_{YY} + \|\tilde{R}_{YY}\|_2 \varphi$ where $\varphi = [1, 0, 0, 0, 0]^T$
3. Determine β equal to $\beta = -2\|V\|_2^2$
4. A_k is calculated as $A = (I + \beta VV^H)$

The from the above steps are pre-multiplied by \tilde{R}_{YY} sequentially as follows

$$A_n, \dots, A_1 \tilde{R}_{YY} = \begin{bmatrix} R \\ 0 \end{bmatrix} \quad \dots (4.35)$$

Where, R is an $n \times n$ upper triangular matrix, 0 is a null matrix, and the sequences of reflection matrices form the complex transpose of the orthogonal matrix Q^H where $Q^H = A_n \dots A_1$. Further unitary rotation matrix Q will be estimated exclusively using training sequence based on OPML algorithm which is given below

Orthogonal Pilot ML (OPML) estimator

As it is known that, channel matrix H can be decomposed using QR decomposition as shown below

$$H = RQ^H \quad \dots (4.36)$$

Here R is estimated blindly using Householder transformation of output autocorrelation matrix. Now estimation of unitary rotation matrix Q using training input X_p and its output Y_p is performed using OPML algorithm.

$\hat{Q}: C^{N \times L} \rightarrow S$, where \hat{Q} the constrained ML estimator of Q and S is the manifold of $M \times M$ unitary matrices, which is obtained by minimizing the likelihood function

$$\|Y_p - RQ^H X_p\|_F^2 \text{ Such that } QQ^H = I \quad \dots (4.37)$$

Further

$$\|Y_p - RQ^H X_p\|_F^2 = tr(Y_p Y_p^H) + tr(RR^H) - 2tr((Q^H X_p)^H R^H Y_p) \quad \dots (4.38)$$

Where $QQ^H = X_p X_p^H = I$.

so the above equation is to maximize the trace of $2tr((Q^H X_p)^H R^H Y_p)$

Such as $(Q^H X_p)^H Q^H X_p = I$ is assumed to simplify above equation where I is identity matrix.

If $X_p X_p^H = I$, then cost minimizing function \hat{Q} in above equation is given as SVD of M_Q , where $M_Q = R^H Y_p X_p^H$.

SVD of M_Q is shown below.

$$\hat{Q} = V_{MQ} U_{MQ}^H \quad \dots (4.39)$$

$$\text{Where } U_{MQ} \Sigma_{MQ} V_{MQ}^H = \text{SVD}(R^H Y_p X_p^H) = \text{SVD}(M_Q) \quad \dots (4.40)$$

The above expression thus yields a closed form expression for the computation of \hat{Q} . The channel matrix H is then estimated as

$$\hat{H} = R \hat{Q}^H \quad \dots (4.41)$$

Above technique uses Householder QR decomposition which having low computational complexity compare to others.

4.5.3 Householder QR-OPML-NEW (Proposed Technique-III)

The main steps of this novel joint semi-blind channel and data estimation technique as follows;

Step 1: First phase of semi-blind channel estimation is performed using proposed technique-II.

Step 2: Given channel knowledge (estimate), find error covariance matrix of estimated channel.

Step 3: In second phase of channel estimation, new pilot symbols are generated using error covariance matrix of estimated channel and conventional orthogonal pilots, further that apply to OPML algorithm and re-estimate channel as final channel estimation.

This technique is extended version of proposed technique II. We find the semi-blind channel estimation as per above technique

$$\hat{H}_{est} = R\hat{Q}^H \quad \dots (4.42)$$

Now estimation error is related to error caused by the estimated \hat{Q} . This error is due to noise embedded in M_Q (refer 4.40), as shown by

$$M_Q = R^H Y_p X_p^H \quad \dots (4.43)$$

$$= R^H (H X_p + \eta) X_p^H \quad \dots (4.44)$$

$$= R^H H X_p X_p^H + R^H \eta X_p^H \quad \dots (4.45)$$

We know that $X_p X_p^H = I$ and $H = RQ^H$, hence

$$M_Q = R^H H + R^H \eta X_p^H \quad \dots (4.46)$$

$$= R^H RQ^H + R^H \eta X_p^H \quad \dots (4.47)$$

$$= \underbrace{R^H RQ^H}_{\hat{M}_Q} + \underbrace{R^H \eta X_p^H}_{\text{Noise}} \quad \dots (4.48)$$

Now first factor $R^H RQ^H$ is \hat{M}_Q , error can be calculated as $e = \hat{M}_Q - M_Q$ hence error covariance is given as

$$\Re e = E(ee^H) \quad \dots (4.49)$$

$$= E(R^H \eta X_p^H (R^H \eta X_p^H)^H) \quad \dots (4.50)$$

$$= E(R^H R X_p^H X_p \eta \eta^H) \quad \dots (4.51)$$

$$\Re e = \sigma_n^2 E(R^H R) \quad \dots (4.52)$$

Further we know that $H = RQ^H$, hence

$$E(H^H H) = E(R^H Q^H R Q) = E(R^H R Q^H Q) = E(R^H R) \text{ Since } Q^H Q = I$$

$$\Re e = \sigma_n^2 E(H^H H) \quad \dots (4.53)$$

Now from above analysis, error covariance factor of estimated channel that minimizes given cost function $\arg \min E \|H - \hat{H}_{est}\|^2$ can be described as

$$\Re e_h = \sigma_n^2 E(H^H \hat{H}_{est}) \quad \dots (4.54)$$

Further using error covariance factor, new pilot symbols are derived as

$$X_{pnew} = (\Re e_h X_P) \quad \dots (4.55)$$

Where X_P are conventional orthogonal pilot (training) symbols and X_{pnew} are newly generated pilot symbols from error covariance factor and conventional orthogonal pilot symbols.

As we know that Y_P is received training output and again perform OPML algorithm to minimize given cost function represented as

$$\|Y_P - R Q_b^H X_{pnew}\|_F^2 \text{ Such that } Q_b Q_b^H = I \quad \dots (4.56)$$

Further

$$\|Y_P - R Q_b^H X_{pnew}\|_F^2 = \text{tr}(Y_P Y_P^H) + \text{tr}(R R^H) - 2 \text{tr}((Q_b^H X_{pnew})^H R^H Y_P) \quad \dots (4.57)$$

So the above equation is to maximize the trace of

$$2 \text{tr}((Q_b^H X_{pnew})^H R^H Y_P) \quad \dots (4.58)$$

Such as $(Q_b^H X_{pnew})^H Q_b^H X_{pnew} = I$ is assumed to simplify above equation.

Further cost minimizing function Q_b in above equation is given as SVD of $M_{Q_{new}}$, where $M_{Q_{new}} = R^H Y_p X_{p_{new}}^H$. SVD of $M_{Q_{new}}$ is shown below.

$$\hat{Q}_b = V_{M_{Q_{new}}} U_{M_{Q_{new}}}^H \text{ Where } U_{M_{Q_{new}}} \Sigma_{M_{Q_{new}}} V_{M_{Q_{new}}}^H = SVD(R^H Y_p X_{p_{new}}^H) = SVD(M_{Q_{new}}) \dots \quad (4.59)$$

The above expression thus yields a closed form expression for the computation of. The final channel matrix H is then estimated as

$$\hat{H} = R \hat{Q}_b^H \quad \dots (4.60)$$

4.5.4 Householder QR-OPML- Joint Semi-Blind Channel Estimation and Data Detection (JSBCDE) (Proposed Technique-IV)

The main steps of this novel joint semi-blind channel and data estimation technique as follows;

Step 1: First phase of semi-blind channel estimation is performed using proposed technique-II.

Step 2: Given channel knowledge (estimate) and received output, perform data detection.

Step 3: In second phase of channel estimation, new pilot symbols are generated using error covariance matrix of estimated data and conventional orthogonal pilots, further that apply to OPML algorithm and re-estimate channel as final channel estimation.

This technique is further extended version of proposed technique II. In that joint semi-blind channel and data estimation is performed. First the semi-blind channel estimation is found as per proposed technique II

$$\hat{H}_{est} = R\hat{Q}^H \quad \dots (4.61)$$

From that channel estimation and received output, estimated data is found as

$$X_{besti} = \hat{H}_{est}^\dagger Y_b = (\hat{H}_{est}^H \hat{H}_{est})^{-1} \hat{H}_{est}^H Y_b \quad \dots (4.62)$$

Further from that estimated data, new channel estimation using error covariance matrix of estimated data is performed. Now the error covariance factor of estimated data \mathfrak{R}_{e_i} is derived from the cost function

$$\arg \min E \|X_b - X_{besti}\|^2 \quad \dots (4.63)$$

$$= \arg \min E \|H^\dagger Y_b - \hat{H}_{est}^\dagger Y_b\|^2 \quad \dots (4.64)$$

So from error analysis presented in above section, error covariance factor of estimated data can be described as

$$\mathfrak{R}_{e_i} = \sigma_n^2 E(X_b X_{besti}^H) \quad \dots (4.65)$$

Further using error covariance factor, new pilot symbols are derived as

$$X_{pnewi} = (\mathfrak{R}_{e_i} X_P) \quad \dots (4.66)$$

Where X_P are conventional orthogonal pilot (training) symbols and X_{pnewi} are newly generated pilot symbols, which are derived from error covariance factor of estimated data and conventional orthogonal pilot sequences.

As we know that Y_P is received training output and again perform OPML algorithm to minimize given cost function represented as

$$\|Y_p - RQ_{bi}^H X_{pnewi}\|_F^2 \quad \text{Such that } Q_{bi}Q_{bi}^H = I \quad \dots (4.67)$$

Further

$$\|Y_p - RQ_{bi}^H X_{pnewi}\|_F^2 = tr(Y_p Y_p^H) + tr(RR^H) - 2tr((Q_{bi}^H X_{pnewi})^H R^H Y_p) \quad \dots (4.68)$$

So the above equation is to maximize the trace of

$$2tr((Q_{bi}^H X_{pnewi})^H R^H Y_p) \quad \dots (4.69)$$

Such as $(Q_{bi}^H X_{pnewi})^H Q_{bi}^H X_{pnewi} = I$ is assumed to simplify above equation.

Further cost minimizing function \hat{Q}_{bi} in above equation is given as SVD of M_{Qnewi} ,

Where $M_{Qnewi} = R^H Y_p X_{pnewi}^H$. SVD of M_{Qnewi} is shown below.

$$\hat{Q}_{bi} = V_{M_{Qnewi}} U_{M_{Qnewi}}^H \quad \dots (4.70)$$

$$\text{Where } U_{M_{Qnewi}} \Sigma_{M_{Qnewi}} V_{M_{Qnewi}}^H = SVD(R^H Y_p X_{pnewi}^H) = SVD(M_{Qnewi}) \quad \dots (4.71)$$

The above expression thus yields a closed form expression for the computation of \hat{Q}_{bi} .

The final channel matrix H is then estimated as

$$\hat{H} = R\hat{Q}_{bi}^H \quad \dots (4.72)$$

4.5.5 Modified Whitening Rotation (SVD-OPML) based Joint Semi-Blind Channel Estimation and Data Detection (Proposed Technique -V)

The main steps of this novel joint semi-blind channel and data estimation technique as follows;

Step 1: First phase of channel estimation is performed using Whitening Rotation (WR) based Semi blind channel estimation technique where whitening matrix W can be estimated blindly from received autocorrelation matrix of output data and rotation matrix Q can be estimated using Orthogonal Pilot Maximum Likelihood (OPML) algorithm with the help of training symbols.

Step 2: Given channel knowledge (estimate) and received output, perform data detection.

Step 3: In second phase of channel estimation, new pilot symbols are generated using error covariance matrix of estimated data and conventional orthogonal pilots, further these are applied to OPML algorithm and re-estimate channel as final channel estimation.

So first we find semi-blind channel estimation using SVD-OPML based technique and calculate channel estimate as

$$\hat{H} = W\hat{Q}^H \quad \dots (4.73)$$

From that channel estimation and received output, estimated data can be found as

$$X_{bestj} = \hat{H}_{est}^\dagger Y_b = (\hat{H}_{est}^H \hat{H}_{est})^{-1} \hat{H}_{est}^H Y_b \quad \dots (4.74)$$

Further from that estimated data, new channel estimation is performed using error covariance matrix of estimated data. Now the error covariance factor of estimated data \mathfrak{R}_{ej} is to be derived to minimizes the given cost function

$$\arg \min E \|X_b - X_{bestj}\|^2 \quad \dots (4.75)$$

So from error analysis presented in above section, error covariance factor of estimated data can be described as

$$\mathfrak{R}e_j = \sigma_n^2 E(X_b X_{bestj}^H) \quad \dots (4.76)$$

Further using error covariance factor, new pilot symbols are derived as

$$X_{pnewj} = (\mathfrak{R}e_j X_p) \quad \dots (4.77)$$

Where X_p is conventional orthogonal pilot (training) sequences and X_{pnewj} newly generated pilot sequence from error covariance factor of estimated data and conventional orthogonal pilot sequences.

As we know that Y_p is received training output and again perform OPML algorithm to minimize given cost function represented as

$$\|Y_p - W Q_{bj}^H X_{pnewj}\|_F^2 \quad \text{Such that } Q_{bj} Q_{bj}^H = I \quad \dots (4.78)$$

Further

$$\|Y_p - W Q_{bj}^H X_{pnewj}\|_F^2 = tr(Y_p Y_p^H) + tr(W W^H) - 2tr((Q_{bj}^H X_{pnewj})^H W^H Y_p) \quad \dots (4.79)$$

So the above equation is to maximize the trace of

$$2tr((Q_{bj}^H X_{pnewj})^H W^H Y_p) \quad \dots (4.80)$$

Such as $(Q_{bj}^H X_{pnewj})^H Q_{bj}^H X_{pnewj} = I$ is assumed to simplify above equation.

Further cost minimizing function \hat{Q}_{bj} in above equation is given

For $M_{Q_{newj}} = W^H Y_p X_{p_{newj}}^H$ as a SVD of $M_{Q_{newj}}$ that is shown below.

$$\hat{Q}_{bj} = V_{M_{Q_{newj}}} U_{M_{Q_{newj}}}^H \quad \dots (4.81)$$

$$\text{Where } U_{M_{Q_{newj}}} \Sigma_{M_{Q_{newj}}} V_{M_{Q_{newj}}}^H = SVD(W^H Y_p X_{p_{newj}}^H) = SVD(M_{Q_{newj}}) \quad \dots (4.82)$$

The above expression thus yields a closed form expression for the computation of \hat{Q}_{bj} , the ML estimate of Q_{bj} . The final channel matrix H is then estimated as

$$\hat{H} = W \hat{Q}_{bj}^H \quad \dots (4.83)$$

Proposed techniques III, IV and V exploits more statistical information of unitary matrix Q by using new pilot symbols, which are generated using error covariance matrix of estimated data (or channel) and conventional orthogonal pilot symbols. New pilot symbols are further applied to OPML estimator for final semi-blind channel estimate, which achieves near optimal performance with respect to perfect CSI (Channel state information). Further matrix decomposition based QR-decomposition techniques having advantage of reduced complexity compare to other channel estimation techniques because its avoid explicit matrix inversions and it reduces full rank matrix into simpler form to reduce complexity in estimation.

4.6 SUMMARY

In this chapter, Singular Value Decomposition based Orthogonal Pilot Maximum Likelihood (OPML) and Rotation Optimization Maximum likelihood (ROML) semi-blind channel estimation techniques with its mathematical modeling were described.

Further five novel semi-blind channel estimation and data detection techniques were proposed and studied with its mathematical modeling for performance improvements compared to conventional channel estimation techniques.

CHAPTER 5

SIMULATION RESULTS

5.1 SIMULATIONS OVERVIEW

In this chapter, different simulation setups have been carried out for $2 \times N$ (i.e. 2 transmitter antennas and N receiver antennas ($N=2, 4, 6, 8$)) Alamouti coded MIMO-STBC systems using quasi static, flat fading Rayleigh and Rician channel models with additive white Gaussian noise of zero mean and variance one. Channel matrix H was generated as matrix of complex Gaussian random entries. Transmission frame consist of orthogonal training (pilot) symbols, which are derived from Hadamard structure and information symbols, which are derived from m-PSK modulation constellations (where $m=2,4,8$).

Proposed novel semi-blind channel estimation and data detection techniques were compared with conventional LS, MAP based training channel estimation techniques and SVD-OPML, SVD-ROML based semi-blind channel estimation techniques. Final results show that proposed Technique-I and II show nearby performances compare to conventional SVD-OPML (WR) semi-blind channel estimation technique, while proposed Technique –III, IV and V outperform others and show near optimal performance by comparing with perfect channel state information (CSI). Finally same performance analyses of proposed techniques have been carried out under 4-PSK modulation scheme using flat fading Rician MIMO channel and different Rice factors.

Simulations parameters and basic steps are given as below

Table 5.0

Simulation Parameters for MIMO-STBC System

System	Multiple input multiple output (MIMO) - STBC
Space time block code	Alamouti scheme
No. of transmitter antennas (M)	2
No. of receiver antennas (N)	2,4,6,8
Channel models	Rayleigh flat fading, Quasi static Rician flat fading, Quasi static (with Rice factors $K=0$ (Rayleigh fading case), 5, 10, 15)
Noise	AWGN
Modulation schemes	m-PSK (2-PSK, 4-PSK, 8-PSK)
Transmission block	Complex with Alamouti format
Pilot symbols (training symbols)	Orthogonal pilots (4 pilots, 8 pilots, 16 pilots)
Maximum SNR value	6 dB

5.2 SIMULATION STEPS

- Step 1 Specify various simulation parameters like receiver antennas, m-PSK mapping value ($m = 2, 4, 8$), maximum SNR value and information symbols being transmitted.
- Step 2 Generate m-PSK modulated symbols using m-PSK mapper.
- Step 3 Generate Alamouti coded space time code matrix structure for m-PSK transmitted symbols which consider as MIMO-STBC coding.
- Step 4 Generate random channel matrix H coefficients using Rayleigh fading or Rician fading model.
- Step 5 Generate random AWGN noise matrix.
- Step 6 Generate orthogonal training (pilot) symbols.
- Step 7 Calculate Training data output and blind information data output using orthogonal training symbols, blind information symbols, channel coefficients matrix and noise coefficients matrix.
- Step 8 Apply channel estimation algorithm. Perform training based channel estimation using received training output and training symbols. Perform blind channel estimation using only received output statistics of blind information symbols.
- Step 9 Arrange the estimated channel matrix for space time decoding part.
- Step 10 Apply ML detection using received output and estimated channel matrix space time decoding structure. Further apply m-PSK demodulation to calculate received information symbols.
- Step 11 Calculate Bit Error Rate (BER) using transmitted symbols and received symbols. Plot SNR Vs BER as a performance analysis

criterion, which uses to investigate performance of various channel estimation techniques.

5.3 SIMULATIONS RESULTS

➤ **Estimation for 2x6 MIMO-STBC using 4PSK (4 pilots, 100 Blind)**

Table 5.1

Channel Estimation for 2x6 MIMO-STBC using 4-PSK (4pilots, 100 blind)

CE Algorithms	BER					
QR-NEW (Proposed Tech.-I):	0.0403	0.0243	0.0116	0.0049	0.0018	0.0007
ROML W-MMSE	0.0500	0.0303	0.0153	0.0071	0.0034	0.0012
WR	0.0364	0.0207	0.0097	0.0039	0.0017	0.0004
HQR-OPML (Proposed Tech.-II)	0.0437	0.0247	0.0111	0.0045	0.0019	0.0005
HQR-OPML-NEW (Proposed Tech.-III)	0.0155	0.0083	0.0034	0.0008	0.0004	0.0001
HQR-OPML-JSBCDE (Proposed Tech.-IV)	0.0155	0.0083	0.0034	0.0008	0.0004	0.0001
TBCE – LS	0.0554	0.0320	0.0152	0.0061	0.0024	0.0007
TBCE - MAP	0.0554	0.0320	0.0152	0.0061	0.0024	0.0007
WR-NEW-JSBCDE (Proposed Tech.-V)	0.0118	0.0071	0.0024	0.0008	0.0003	0.0001
Perfect – CSI	0.0098	0.0057	0.0021	0.0005	0.0003	0.0000

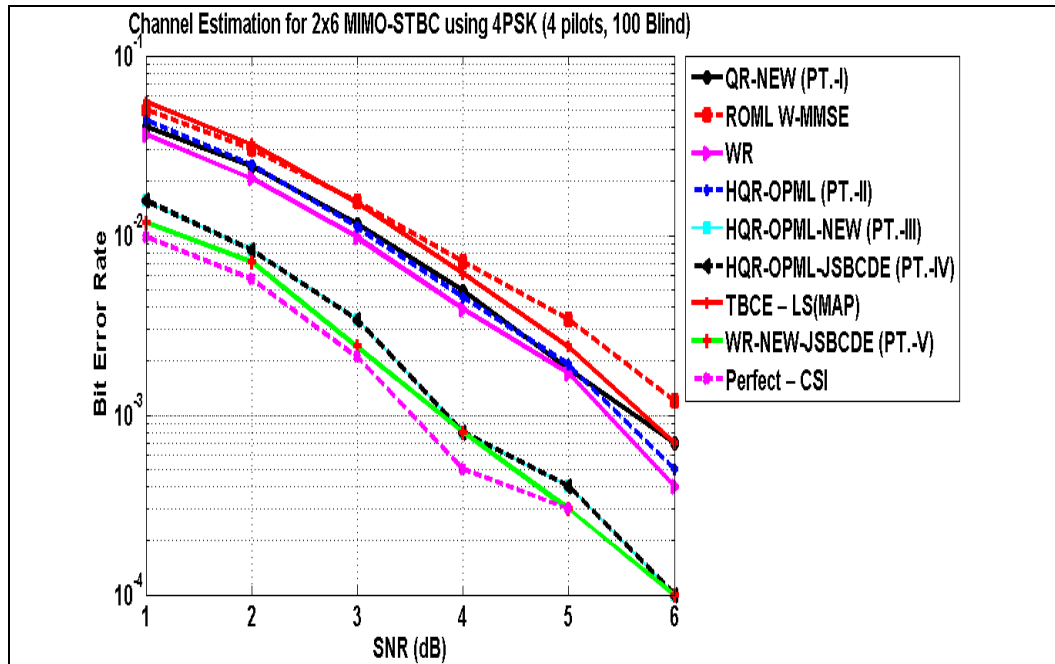


Figure 5.1: Channel Estimation for 2 Transmitter and 6 Receivers MIMO-STBC
Using 4PSK (4 Pilots, 100 Blind) for Rayleigh Fading Channel Model

➤ **Estimation for 2x8 MIMO-STBC using 4PSK (4 pilots, 100 Blind)**

Table 5.2

Channel Estimation for 2x8 MIMO-STBC using 4-PSK (4pilots, 100 blind)

CE Algorithms	BER					
QR-NEW (Proposed Tech.-I):	0.0182	0.0089	0.0036	0.0010	0.0003	0.0001
ROML W-MMSE	0.0204	0.0110	0.0046	0.0014	0.0006	0.0001
WR	0.0156	0.0079	0.0033	0.0008	0.0002	0
HQR-OPML (Proposed Tech.-II)	0.0190	0.0098	0.0039	0.0010	0.0003	0
HQR-OPML-NEW (Proposed Tech.-III)	0.0057	0.0026	0.0008	0.0002	0	0
HQR-OPML-JSBCDE (Proposed Tech.-IV)	0.0057	0.0026	0.0008	0.0002	0	0
TBCE – LS	0.0272	0.0131	0.0049	0.0014	0.0006	0.0001
TBCE - MAP	0.0272	0.0131	0.0049	0.0014	0.0006	0.0001
WR-NEW-JSBCDE (Proposed Tech.-V)	0.0045	0.0016	0.0005	0.0002	0	0
Perfect – CSI	0.0036	0.0013	0.0004	0.0001	0	0

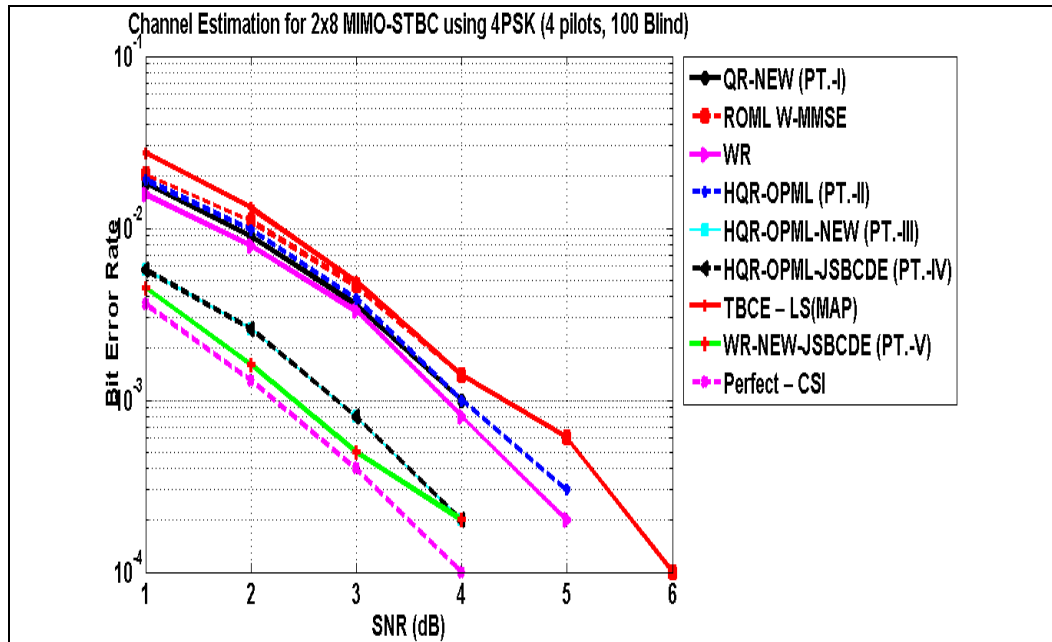


Figure 5.2: Channel Estimation for 2 Transmitter and 8 Receivers MIMO-STBC Using 4PSK (4 Pilots, 100 Blind) for Rayleigh Fading Channel Model

➤ **Estimation for 2x4 MIMO-STBC using 4PSK (4 pilots, 100 Blind)**

Table 5.3

Channel Estimation for 2x4 MIMO-STBC using 4-PSK (4pilots, 100 blind)

CE Algorithms	BER					
QR-NEW (Proposed Tech.-I):	0.1033	0.0661	0.0419	0.0239	0.0132	0.0056
ROML W-MMSE	0.1234	0.0853	0.0577	0.0385	0.0235	0.0124
WR	0.0948	0.0619	0.0369	0.0210	0.0111	0.0048
HQR-OPML (Proposed Tech.-II)	0.1053	0.0676	0.0415	0.0236	0.0123	0.0053
HQR-OPML-NEW (Proposed Tech.-III)	0.0509	0.0271	0.0156	0.0081	0.0037	0.0014
HQR-OPML-JSBCDE (Proposed Tech.-IV)	0.0509	0.0271	0.0156	0.0081	0.0037	0.0014
TBCE – LS	0.1213	0.0770	0.0478	0.0282	0.0140	0.0059
TBCE - MAP	0.1213	0.0770	0.0478	0.0282	0.0140	0.0059
WR-NEW-JSBCDE (Proposed Tech.-V)	0.0452	0.0244	0.0140	0.0070	0.0032	0.0018
Perfect – CSI	0.0395	0.0213	0.0119	0.0058	0.0026	0.0010

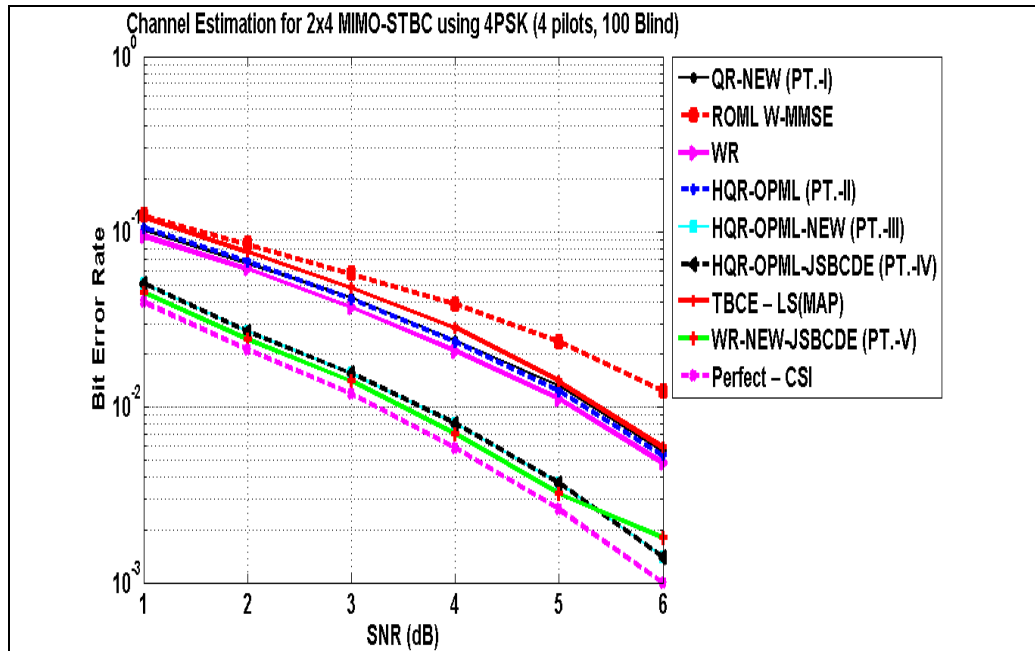


Figure 5.3: Channel Estimation for 2 Transmitter and 4 Receivers MIMO-STBC Using 4PSK (4 Pilots, 100 Blind) for Rayleigh Fading Channel Model

➤ **Estimation for 2x2 MIMO-STBC using 4PSK (4 pilots, 100 Blind)**

Table 5.4

Channel Estimation for 2x2 MIMO-STBC using 4-PSK (4pilots, 100 blind)

CE Algorithms	BER					
QR-NEW (Proposed Tech.-I):	0.2480	0.2064	0.1607	0.1142	0.0822	0.0561
ROML W-MMSE	0.3042	0.2622	0.2195	0.1802	0.1459	0.1169
WR	0.2541	0.2069	0.1592	0.1131	0.0802	0.0534
HQR-OPML (Proposed Tech.-II)	0.2541	0.2069	0.1592	0.1131	0.0802	0.0534
HQR-OPML-NEW (Proposed Tech.-III)	0.1551	0.1174	0.0859	0.0581	0.0372	0.0243
HQR-OPML-JSBCDE (Proposed Tech.-IV)	0.1551	0.1174	0.0859	0.0581	0.0372	0.0243
TBCE – LS	0.2611	0.2137	0.1658	0.1193	0.0830	0.0563
TBCE - MAP	0.2611	0.2137	0.1658	0.1193	0.0830	0.0563
WR-NEW-JSBCDE (Proposed Tech.-V)	0.1556	0.1177	0.0866	0.0575	0.0381	0.0261
Perfect – CSI	0.1451	0.1090	0.0811	0.0537	0.0350	0.0226

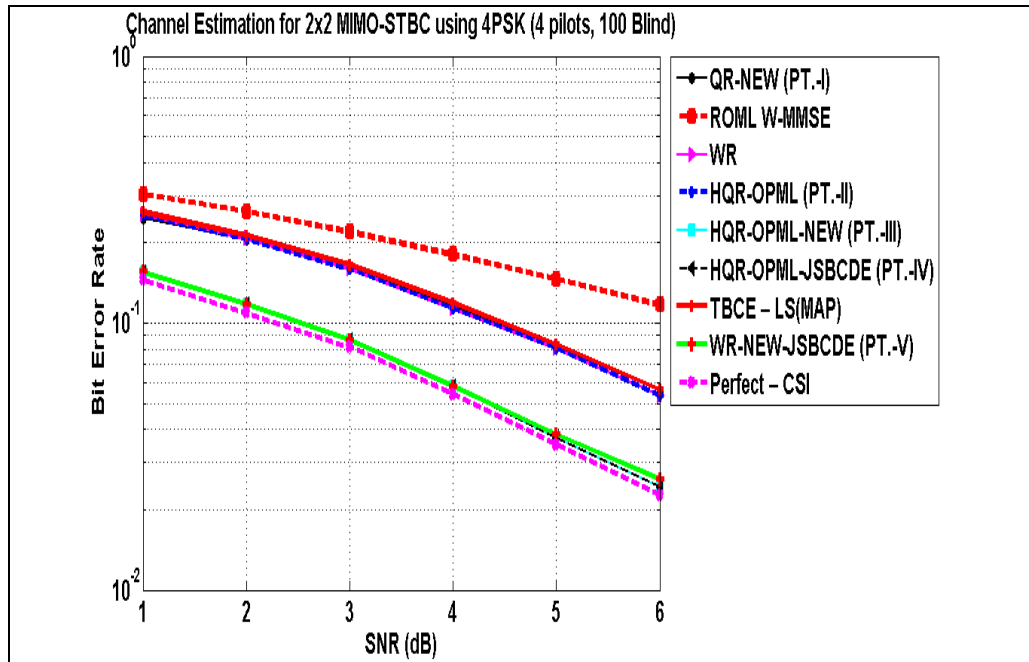


Figure 5.4: Channel Estimation for 2 Transmitter and 2 Receivers MIMO-STBC Using 4PSK (4 Pilots, 100 Blind) for Rayleigh Fading Channel Model

➤ **Estimation for 2x2 MIMO-STBC using BPSK (4 pilots, 100 Blind)**

Table 5.5

Channel Estimation for 2x2 MIMO-STBC using 2-PSK (4pilots, 100 blind)

CE Algorithms	BER					
QR-NEW (Proposed Tech.-I):	0.0645	0.0461	0.0314	0.0201	0.0116	0.0063
ROML W-MMSE	0.0887	0.0674	0.0499	0.0362	0.0255	0.0181
WR	0.0684	0.0468	0.0328	0.0205	0.0117	0.0063
HQR-OPML (Proposed Tech.-II)	0.0684	0.0468	0.0328	0.0205	0.0117	0.0063
HQR-OPML-NEW (Proposed Tech.-III)	0.0311	0.0201	0.0138	0.0080	0.0041	0.0024
HQR-OPML-JSBCDE (Proposed Tech.-IV)	0.0311	0.0201	0.0138	0.0080	0.0041	0.0024
TBCE – LS	0.0709	0.0503	0.0341	0.0220	0.0129	0.0071
TBCE - MAP	0.0709	0.0503	0.0341	0.0220	0.0129	0.0071
WR-NEW-JSBCDE (Proposed Tech.-V)	0.0311	0.0204	0.0138	0.0077	0.0045	0.0027
Perfect – CSI	0.0277	0.0174	0.0123	0.0072	0.0037	0.0021

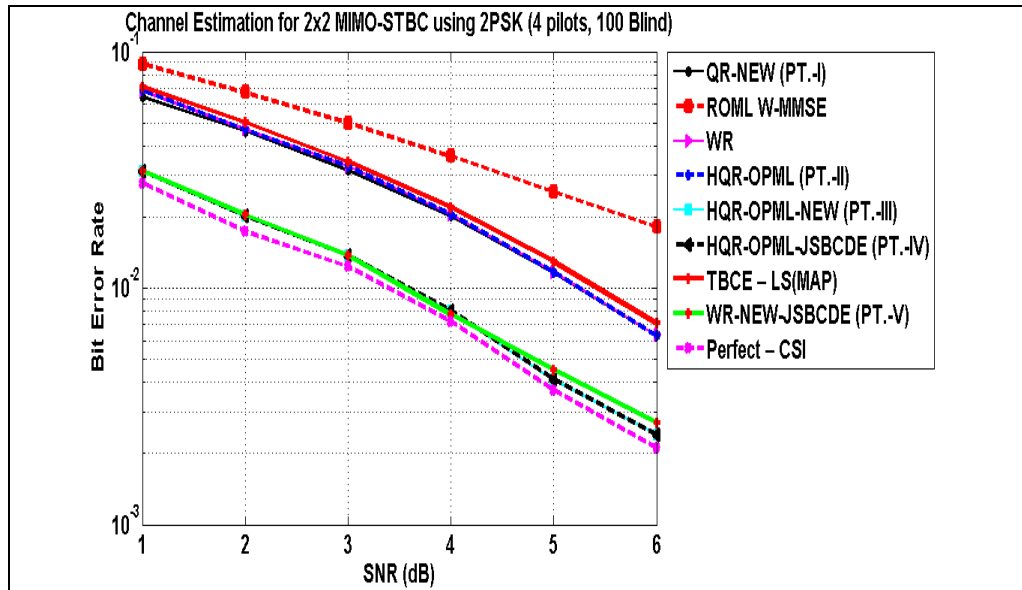


Figure 5.5: Channel Estimation for 2 Transmitters and 2 Receivers MIMO-STBC Using 2-PSK (4 Pilots, 100 Blind) for Rayleigh Fading Channel Model

➤ **Estimation for 2x4 MIMO-STBC using BPSK (4 pilots, 100 Blind)**

Table 5.6

Channel Estimation for 2x4 MIMO-STBC using 2-PSK (4pilots, 100 blind)

CE Algorithms	BER					
QR-NEW (Proposed Tech.-I):	0.0123	0.0058	0.0029	0.0010	0.0006	0.0001
ROML W-MMSE	0.0174	0.0093	0.0050	0.0023	0.0014	0.0004
WR	0.0112	0.0050	0.0022	0.0008	0.0004	0.0001
HQR-OPML (Proposed Tech.-II)	0.0139	0.0063	0.0029	0.0010	0.0006	0.0001
HQR-OPML-NEW (Proposed Tech.-III)	0.0046	0.0022	0.0009	0.0004	0.0001	0
HQR-OPML-JSBCDE (Proposed Tech.-IV)	0.0046	0.0022	0.0009	0.0004	0.0001	0
TBCE – LS	0.0172	0.0084	0.0037	0.0017	0.0009	0.0003
TBCE - MAP	0.0172	0.0084	0.0037	0.0017	0.0009	0.0003
WR-NEW-JSBCDE (Proposed Tech.-V)	0.0029	0.0015	0.0006	0.0003	0.0001	0.0000
Perfect – CSI	0.0023	0.0013	0.0004	0.0002	0.0001	0.0000

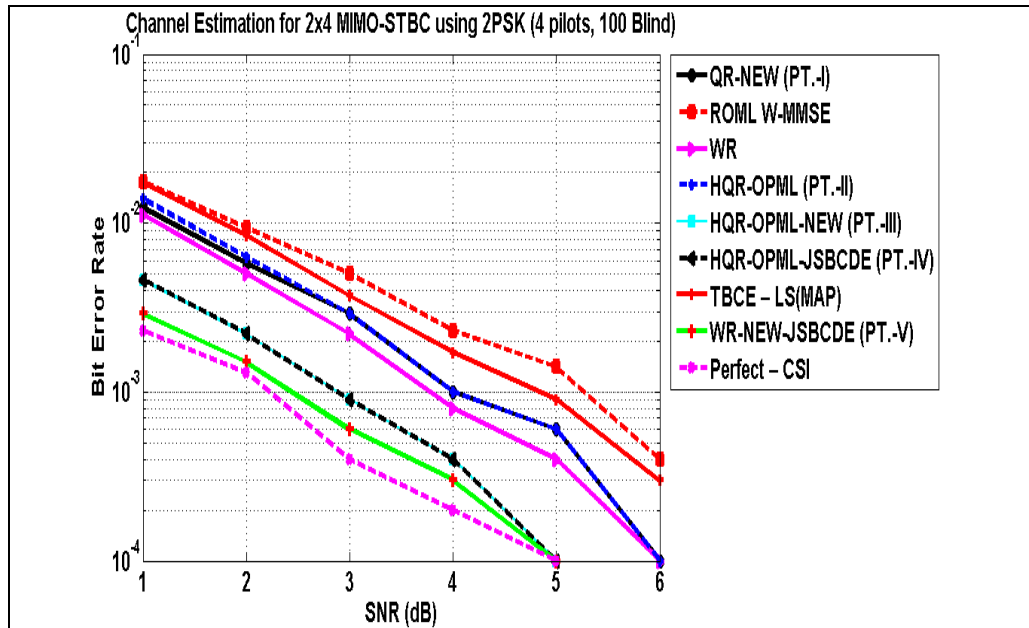


Figure 5.6: Channel Estimation for 2 Transmitters and 4 Receivers MIMO-STBC Using 2-PSK (4 Pilots, 100 Blind) for Rayleigh Fading Channel Model

➤ **Estimation for 2x6 MIMO-STBC using BPSK (4 pilots, 100 Blind)**

Table 5.7

Channel Estimation for 2x4 MIMO-STBC using 2-PSK (4pilots, 100 blind)

CE Algorithms	BER						
QR-NEW (Proposed Tech.-I):		0.0024	0.0010	0.0002	0.0002	0	0
ROML W-MMSE		0.0033	0.0015	0.0002	0.0001	0	0
WR		0.0021	0.0008	0.0001	0.0001	0	0
HQR-OPML (Proposed Tech.-II)		0.0031	0.0011	0.0002	0.0001	0	0
HQR-OPML-NEW (Proposed Tech.-III)	1.0e-003 *	0.5750	0.2750	0.0750	0.0250	0	0
HQR-OPML-JSBCDE (Proposed Tech.-IV)	1.0e-003 *	0.5750	0.2750	0.0750	0.0250	0	0
TBCE – LS		0.0044	0.0017	0.0005	0.0002	0	0
TBCE - MAP		0.0044	0.0017	0.0005	0.0002	0	0
WR-NEW-JSBCDE (Proposed Tech.-V)	1.0e-003 *	0.4000	0.1500	0.0500	0.0250	0	0
Perfect – CSI	1.0e-003 *	0.2750	0.1250	0.0250	0.0250	0	0

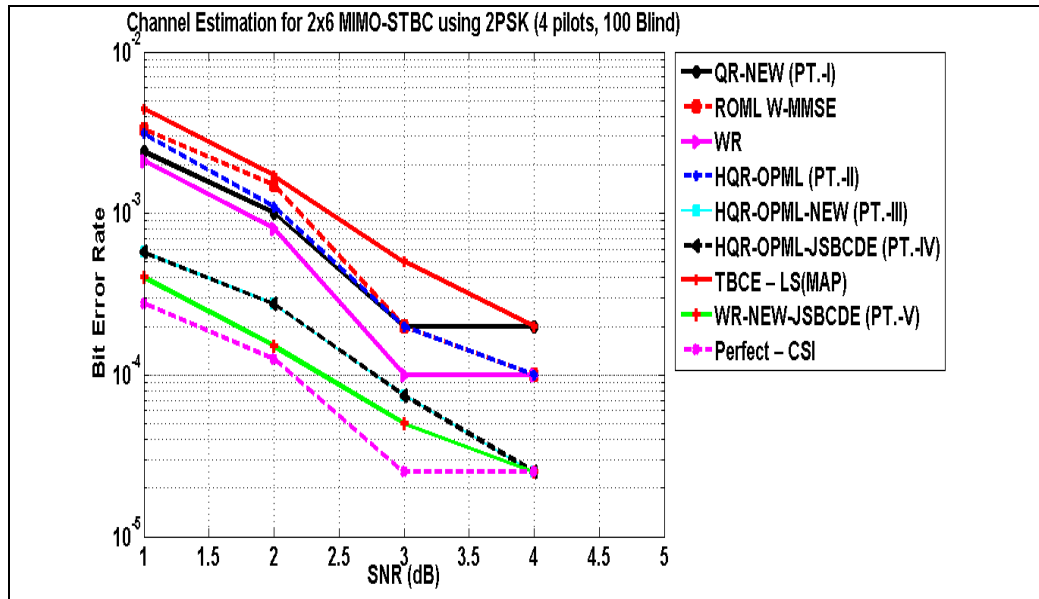


Figure 5.7: Channel Estimation for 2 Transmitters and 6 Receivers MIMO-STBC Using 2-PSK (4 Pilots, 100 Blind) for Rayleigh Fading Channel Model

➤ **Estimation for 2x8 MIMO-STBC using 8-PSK (4 pilots, 100 Blind)**

Table 5.8

Channel Estimation for 2x8 MIMO-STBC using 8-PSK (4pilots, 100 blind)

CE Algorithms	BER					
QR-NEW (Proposed Tech.-I):	0.1895	0.1469	0.1007	0.0654	0.0403	0.0236
ROML W-MMSE	0.1999	0.1545	0.1093	0.0709	0.0494	0.0294
WR	0.1798	0.1358	0.0922	0.0585	0.0361	0.0208
HQR-OPML (Proposed Tech.-II)	0.1921	0.1446	0.0970	0.0614	0.0377	0.0221
HQR-OPML-NEW (Proposed Tech.-III)	0.1155	0.0789	0.0457	0.0248	0.0138	0.0053
HQR-OPML-JSBCDE (Proposed Tech.-IV)	0.1155	0.0789	0.0457	0.0248	0.0138	0.0053
TBCE – LS	0.2189	0.1620	0.1118	0.0714	0.0424	0.0228
TBCE - MAP	0.2189	0.1620	0.1118	0.0714	0.0424	0.0228
WR-NEW-JSBCDE (Proposed Tech.-V)	0.1053	0.0724	0.0442	0.0221	0.0143	0.0073
Perfect – CSI	0.0969	0.0644	0.0377	0.0196	0.0109	0.0047

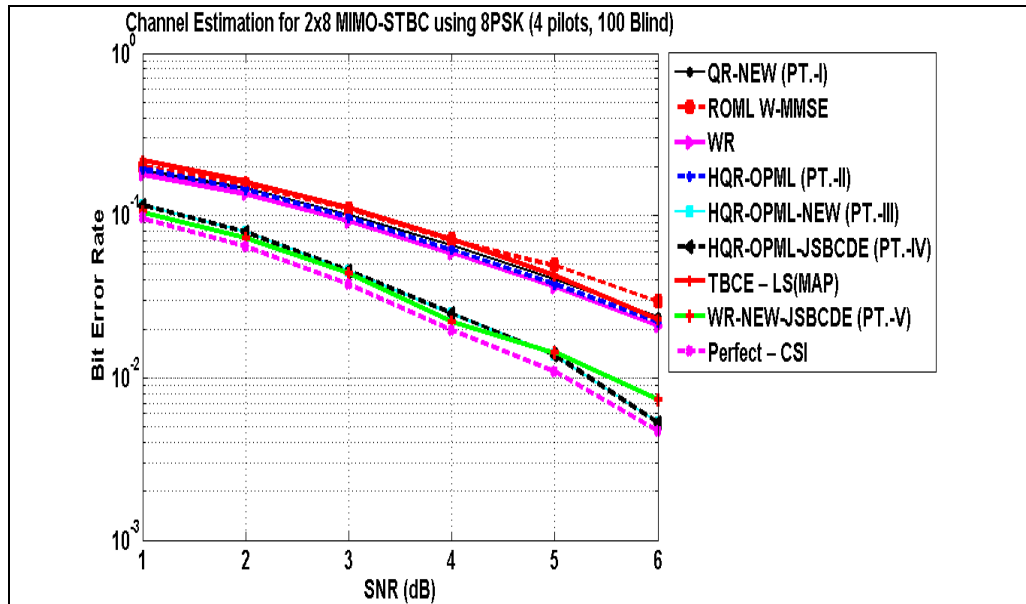


Figure 5.8: Channel Estimation for 2 Transmitters and 8 Receivers MIMO-STBC Using 8-PSK (4 Pilots, 100 Blind) for Rayleigh Fading Channel Model

➤ **Estimation for 2x6 MIMO-STBC using 8-PSK (4 pilots, 100 Blind)**

Table 5.9

Channel Estimation for 2x6 MIMO-STBC using 8-PSK (4pilots, 100 blind)

CE Algorithms	BER					
QR-NEW (Proposed Tech.-I):	0.2659	0.2105	0.1601	0.1124	0.0784	0.0516
ROML W-MMSE	0.2808	0.2256	0.1764	0.1288	0.0952	0.0662
WR	0.2511	0.1978	0.1480	0.1041	0.0699	0.0452
HQR-OPML (Proposed Tech.-II)	0.2637	0.2090	0.1555	0.1083	0.0735	0.0474
HQR-OPML-NEW (Proposed Tech.-III)	0.1729	0.1253	0.0884	0.0549	0.0330	0.0175
HQR-OPML-JSBCDE (Proposed Tech.-IV)	0.1729	0.1253	0.0884	0.0549	0.0330	0.0175
TBCE – LS	0.2886	0.2252	0.1734	0.1190	0.0790	0.0490
TBCE - MAP	0.2886	0.2252	0.1734	0.1190	0.0790	0.0490
WR-NEW-JSBCDE (Proposed Tech.-V)	0.1585	0.1178	0.0825	0.0508	0.0339	0.0193
Perfect – CSI	0.1480	0.1089	0.0749	0.0455	0.0266	0.0145

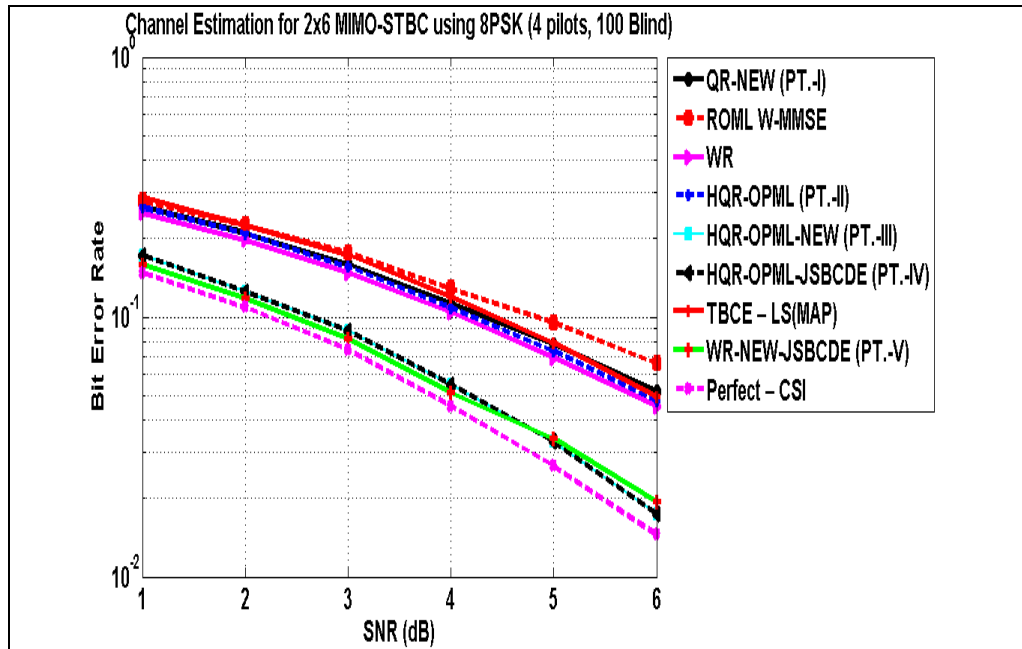


Figure 5.9: Channel Estimation for 2 Transmitters and 6 Receivers MIMO-STBC Using 8-PSK (4 Pilots, 100 Blind) for Rayleigh Fading Channel Model

➤ **Estimation for 2x6 MIMO-STBC using 4-PSK (8 pilots, 100 Blind)**

Table 5.10

Channel Estimation for 2x6 MIMO-STBC using 4-PSK (8 pilots, 100 blind)

CE Algorithms	BER					
QR-NEW (Proposed Tech.-I):	0.0271	0.0127	0.0062	0.0024	0.0011	0.0002
ROML W-MMSE	0.0288	0.0155	0.0065	0.0026	0.0012	0.0005
WR	0.0237	0.0115	0.0049	0.0018	0.0008	0.0002
HQR-OPML (Proposed Tech.-II)	0.0278	0.0138	0.0060	0.0021	0.0010	0.0004
HQR-OPML-NEW (Proposed Tech.-III)	0.0165	0.0073	0.0029	0.0010	0.0004	0.0001
HQR-OPML-JSBCDE (Proposed Tech.-IV)	0.0165	0.0073	0.0029	0.0010	0.0004	0.0001
TBCE – LS	0.0309	0.0154	0.0067	0.0024	0.0010	0.0003
TBCE - MAP	0.0309	0.0154	0.0067	0.0024	0.0010	0.0003
WR-NEW-JSBCDE (Proposed Tech.-V)	0.0143	0.0057	0.0029	0.0011	0.0004	0.0001
Perfect – CSI	0.0117	0.0044	0.0021	0.0009	0.0004	0.0001

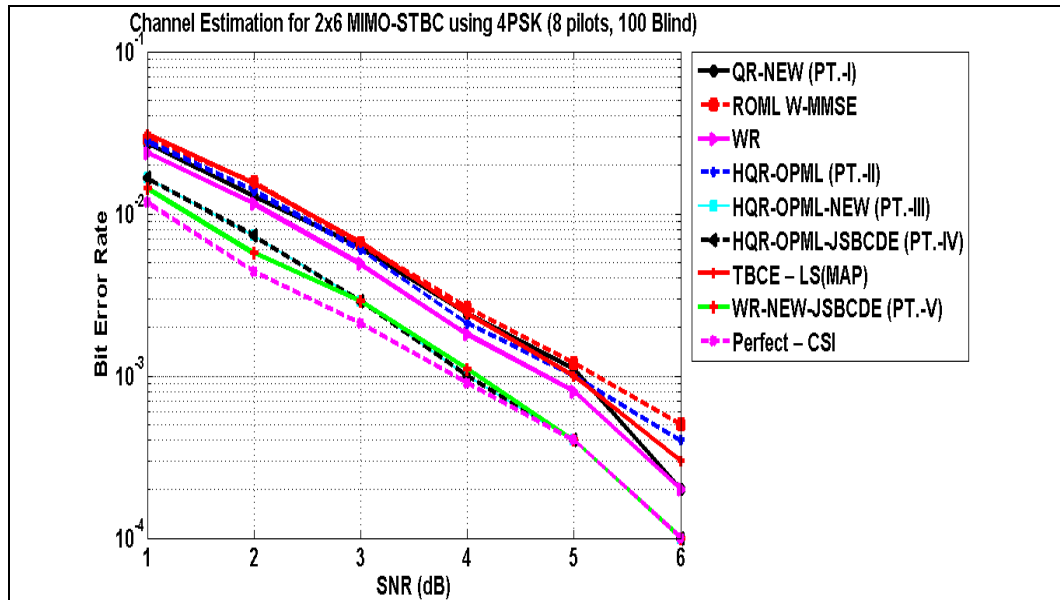


Figure 5.10: Channel Estimation for 2 Transmitters and 6 Receivers MIMO-STBC Using 4-PSK (8 Pilots, 100 Blind) for Rayleigh Fading Channel Model

➤ Estimation for 2x8 MIMO-STBC using 4-PSK (8 pilots, 100 Blind)

Table 5.11

Channel Estimation for 2x8 MIMO-STBC using 4-PSK (8 pilots, 100 blind)

CE Algorithms	BER					
	QR-NEW (Proposed Tech.-I):	0.0109	0.0045	0.0019	0.0006	0.0001
ROML W-MMSE	0.0111	0.0047	0.0014	0.0006	0.0002	0.0001
WR	0.0090	0.0037	0.0012	0.0004	0.0001	0.0001
HQR-OPML (Proposed Tech.-II)	0.0116	0.0046	0.0018	0.0006	0.0002	0.0001
HQR-OPML-NEW (Proposed Tech.-III)	0.0053	0.0022	0.0004	0.0001	0	0
HQR-OPML-JSBCDE (Proposed Tech.-IV)	0.0053	0.0022	0.0004	0.0001	0	0
TBCE – LS	0.0134	0.0047	0.0017	0.0006	0.0002	0.0000
TBCE - MAP	0.0134	0.0047	0.0017	0.0006	0.0002	0.0000
WR-NEW-JSBCDE (Proposed Tech.-V)	0.0041	0.0016	0.0005	0.0001	0.0000	0.0000
Perfect – CSI	0.0036	0.0013	0.0004	0.0001	0	0

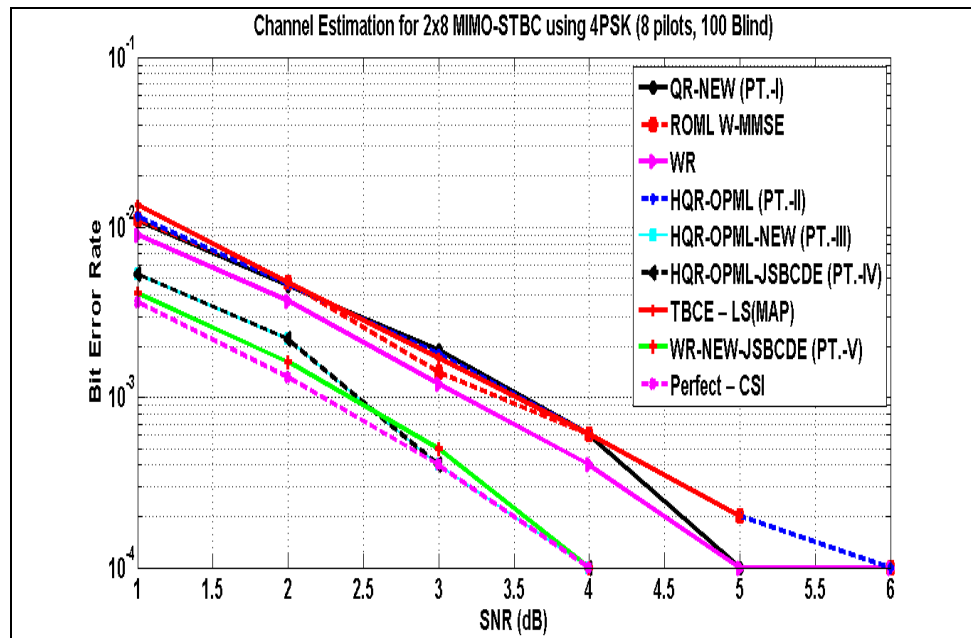


Figure 5.11: Channel Estimation for 2 Transmitters and 8 Receivers MIMO-STBC Using 4-PSK (8 Pilots, 100 Blind) for Rayleigh Fading Channel Model

➤ **Estimation for 2x4 MIMO-STBC using 4-PSK (8 pilots, 100 Blind)**

Table 5.12

Channel Estimation for 2x4 MIMO-STBC using 4-PSK (8 pilots, 100 blind)

CE Algorithms	BER					
QR-NEW (Proposed Tech.-I):	0.0716	0.0440	0.0260	0.0142	0.0081	0.0032
ROML W-MMSE	0.0827	0.0522	0.0328	0.0193	0.0118	0.0055
WR	0.0658	0.0398	0.0231	0.0123	0.0069	0.0028
HQR-OPML (Proposed Tech.-II)	0.0755	0.0451	0.0260	0.0136	0.0075	0.0031
HQR-OPML-NEW (Proposed Tech.-III)	0.0471	0.0287	0.0147	0.0078	0.0039	0.0014
HQR-OPML-JSBCDE (Proposed Tech.-IV)	0.0471	0.0287	0.0147	0.0078	0.0039	0.0014
TBCE – LS	0.0790	0.0480	0.0268	0.0154	0.0078	0.0032
TBCE - MAP	0.0790	0.0480	0.0268	0.0154	0.0078	0.0032
WR-NEW-JSBCDE (Proposed Tech.-V)	0.0428	0.0248	0.0127	0.0072	0.0036	0.0018
Perfect – CSI	0.0380	0.0217	0.0114	0.0060	0.0030	0.0012

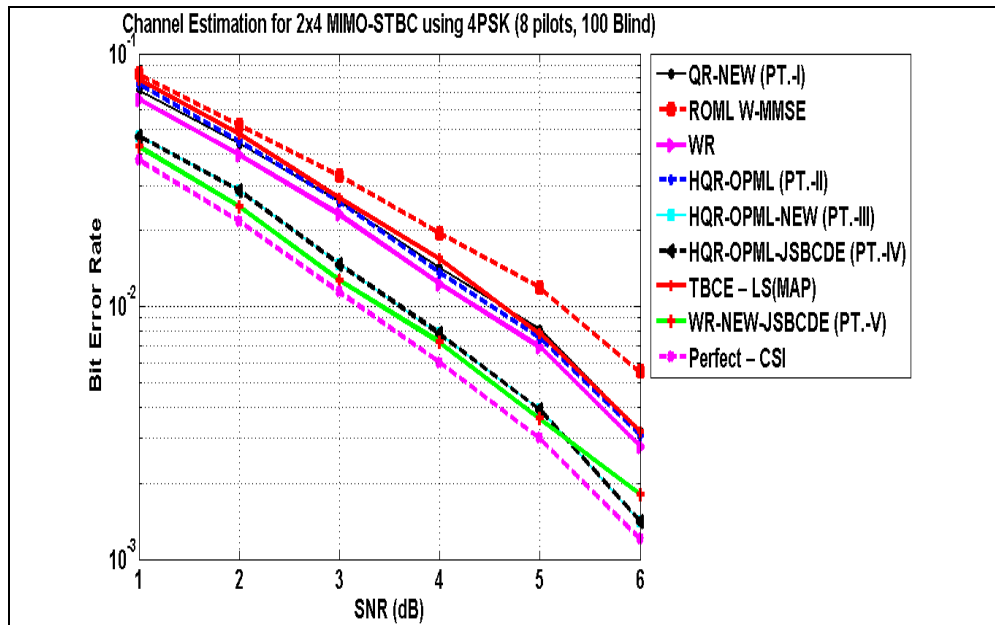


Figure 5.12: Channel Estimation for 2 Transmitters and 4 Receivers MIMO-STBC Using 4-PSK (8 Pilots, 100 Blind) for Rayleigh Fading Channel Model

➤ **Estimation for 2x2 MIMO-STBC using 4-PSK (8 pilots, 100 Blind)**

Table 5.13

Channel Estimation for 2x2 MIMO-STBC using 4-PSK (8 pilots, 100 blind)

CE Algorithms	BER					
QR-NEW (Proposed Tech.-I):	0.2039	0.1631	0.1205	0.0862	0.0579	0.0391
ROML W-MMSE	0.2449	0.2037	0.1615	0.1260	0.0982	0.0758
WR	0.2051	0.1622	0.1185	0.0842	0.0559	0.0371
HQR-OPML (Proposed Tech.-II)	0.2051	0.1622	0.1185	0.0842	0.0559	0.0371
HQR-OPML-NEW (Proposed Tech.-III)	0.1511	0.1152	0.0807	0.0563	0.0373	0.0233
HQR-OPML-JSBCDE (Proposed Tech.-IV)	0.1511	0.1152	0.0807	0.0563	0.0373	0.0233
TBCE – LS	0.2085	0.1653	0.1214	0.0861	0.0578	0.0375
TBCE - MAP	0.2085	0.1653	0.1214	0.0861	0.0578	0.0375
WR-NEW-JSBCDE (Proposed Tech.-V)	0.1525	0.1172	0.0815	0.0575	0.0393	0.0256
Perfect – CSI	0.1412	0.1086	0.0773	0.0542	0.0347	0.0225

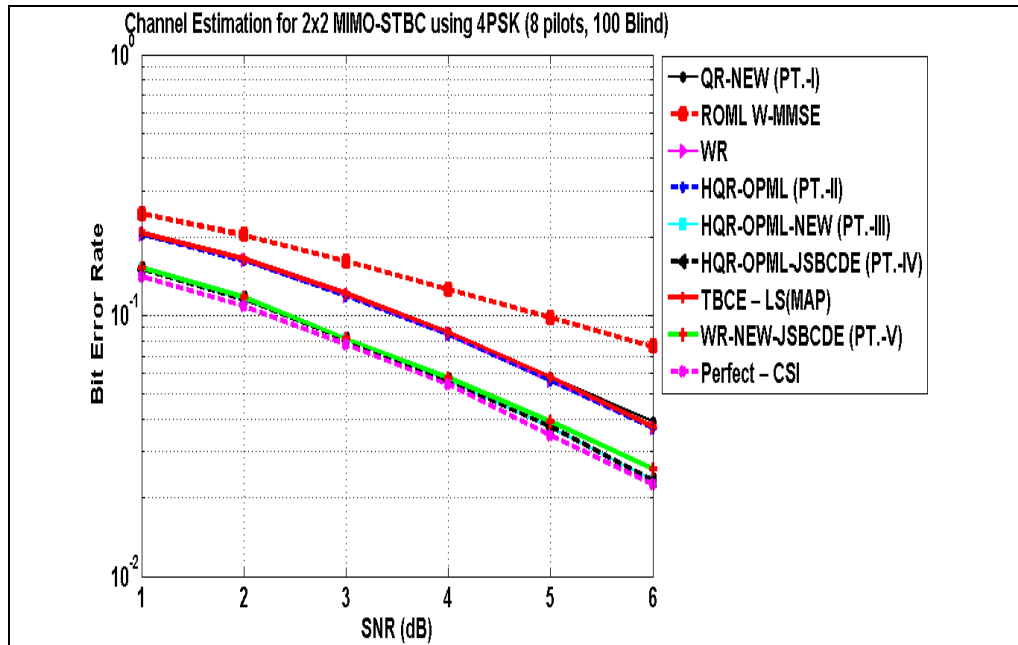


Figure 5.13: Channel Estimation for 2 Transmitters and 2 Receivers MIMO-STBC Using 4-PSK (8 Pilots, 100 Blind) for Rayleigh Fading Channel Model

➤ **Estimation for 2x6 MIMO-STBC using BPSK (8 pilots, 100 Blind)**

Table 5.14

Channel Estimation for 2x6 MIMO-STBC using 2-PSK (8 pilots, 100 blind)

CE Algorithms	BER						
QR-NEW (Proposed Tech.-I):		0.0016	0.0006	0.0001	0	0	0
ROML W-MMSE		0.0016	0.0003	0.0001	0.0001	0	0
WR		0.0012	0.0003	0.0001	0.0000	0	0
HQR-OPML (Proposed Tech.-II)		0.0020	0.0005	0.0001	0.0000	0	0
HQR-OPML-NEW (Proposed Tech.-III)	1.0e-003 *	1.0000	0.1500	0.1000	0	0	0
HQR-OPML-JSBCDE (Proposed Tech.-IV)	1.0e-003 *	1.0000	0.1500	0.1000	0	0	0
TBCE – LS		0.0018	0.0006	0.0001	0.0000	0	0
TBCE - MAP		0.0018	0.0006	0.0001	0.0000	0	0
WR-NEW-JSBCDE (Proposed Tech.-V)	1.0e-003 *	0.5750	0.1500	0.0500	0	0	0
Perfect – CSI	1.0e-003 *	0.4000	0.1000	0.0500	0	0	0

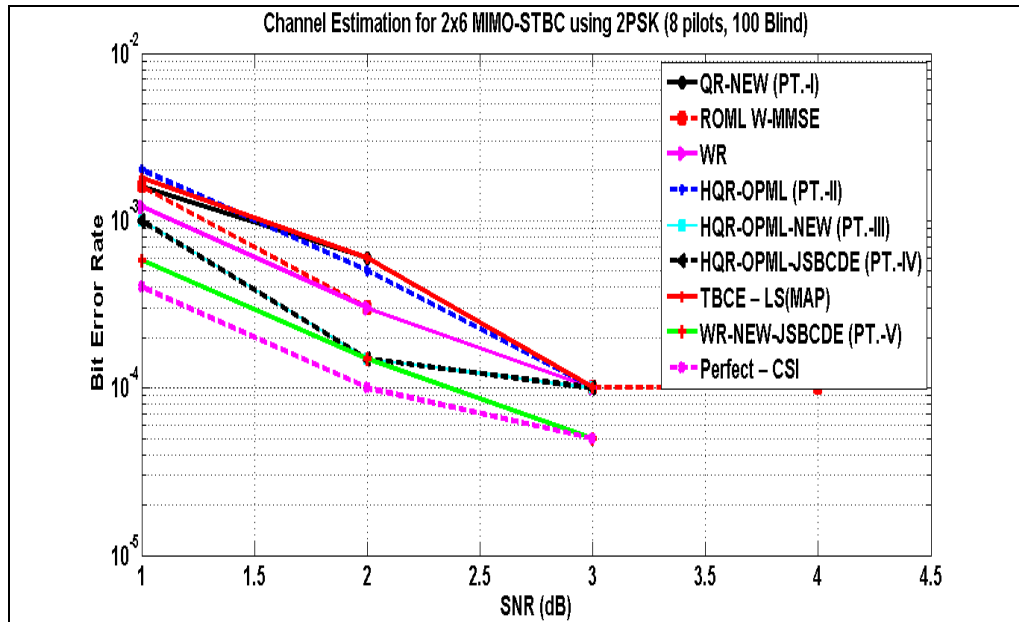


Figure 5.14: Channel Estimation for 2 Transmitters and 6 Receivers MIMO-STBC Using 2-PSK (8 Pilots, 100 Blind) for Rayleigh Fading Channel Model

➤ **Estimation for 2x4 MIMO-STBC using BPSK (8 pilots, 100 Blind)**

Table 5.15

Channel Estimation for 2x4 MIMO-STBC using 2-PSK (8 pilots, 100 blind)

CE Algorithms	BER					
QR-NEW (Proposed Tech.-I):	0.0077	0.0029	0.0016	0.0006	0.0004	0.0002
ROML W-MMSE	0.0083	0.0036	0.0022	0.0009	0.0005	0.0003
WR	0.0064	0.0026	0.0014	0.0005	0.0003	0.0001
HQR-OPML (Proposed Tech.-II)	0.0079	0.0033	0.0018	0.0007	0.0004	0.0001
HQR-OPML-NEW (Proposed Tech.-III)	0.0046	0.0019	0.0008	0.0003	0.0001	0.0001
HQR-OPML-JSBCDE (Proposed Tech.-IV)	0.0046	0.0019	0.0008	0.0003	0.0001	0.0001
TBCE – LS	0.0093	0.0037	0.0019	0.0006	0.0003	0.0001
TBCE - MAP	0.0093	0.0037	0.0019	0.0006	0.0003	0.0001
WR-NEW-JSBCDE (Proposed Tech.-V)	0.0029	0.0014	0.0008	0.0002	0.0001	0.0001
Perfect – CSI	0.0026	0.0010	0.0006	0.0001	0	0

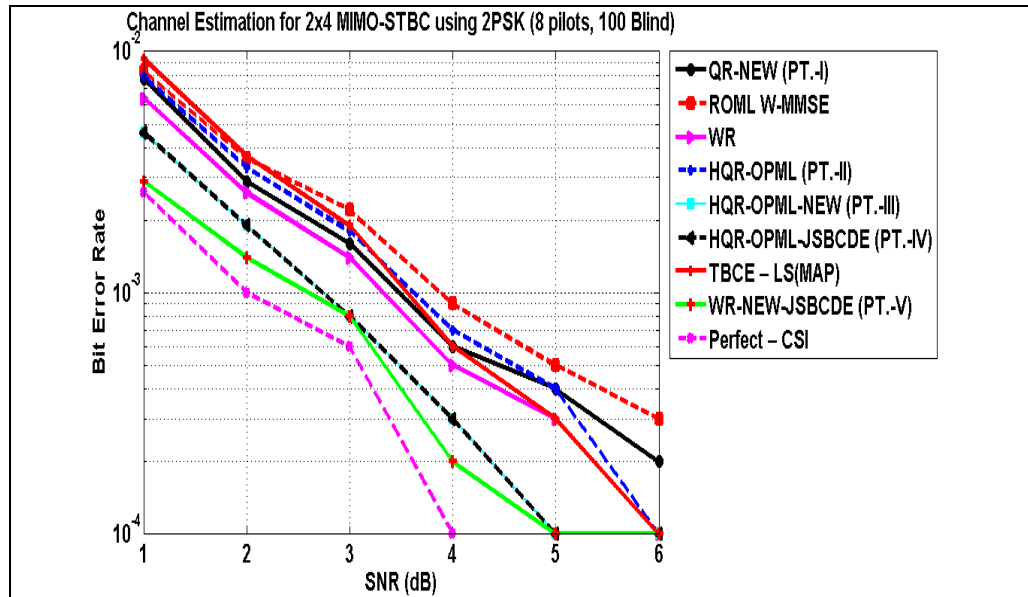


Figure 5.15: Channel Estimation for 2 Transmitters and 4 Receivers MIMO-STBC Using 2-PSK (8 Pilots, 100 Blind) for Rayleigh Fading Channel Model

➤ **Estimation for 2x2 MIMO-STBC using BPSK (8 pilots, 100 Blind)**

Table 5.16

Channel Estimation for 2x2 MIMO-STBC using 2-PSK (8 pilots, 100 blind)

CE Algorithms	BER					
QR-NEW (Proposed Tech.-I):	0.0473	0.0317	0.0216	0.0119	0.0063	0.0040
ROML W-MMSE	0.0607	0.0435	0.0304	0.0196	0.0130	0.0096
WR	0.0487	0.0321	0.0208	0.0117	0.0064	0.0041
HQR-OPML (Proposed Tech.-II)	0.0487	0.0321	0.0208	0.0117	0.0064	0.0041
HQR-OPML-NEW (Proposed Tech.-III)	0.0307	0.0201	0.0124	0.0065	0.0037	0.0023
HQR-OPML-JSBCDE (Proposed Tech.-IV)	0.0307	0.0201	0.0124	0.0065	0.0037	0.0023
TBCE – LS	0.0502	0.0340	0.0216	0.0117	0.0067	0.0041
TBCE - MAP	0.0502	0.0340	0.0216	0.0117	0.0067	0.0041
WR-NEW-JSBCDE (Proposed Tech.-V)	0.0323	0.0203	0.0130	0.0070	0.0039	0.0026
Perfect – CSI	0.0285	0.0181	0.0112	0.0057	0.0034	0.0020

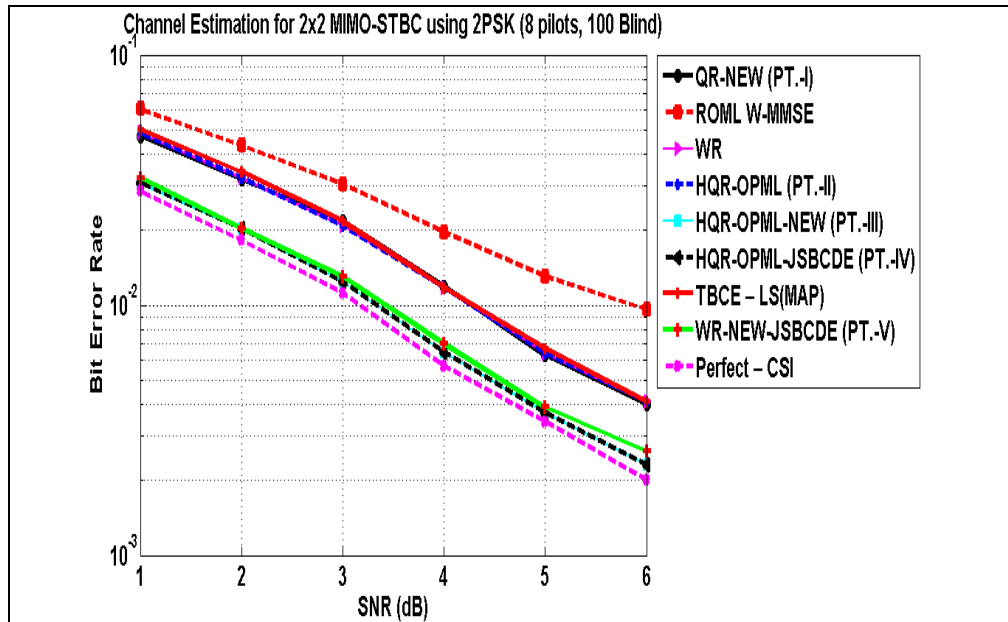


Figure 5.16: Channel Estimation for 2 Transmitters and 2 Receivers MIMO-STBC Using 2-PSK (8 Pilots, 100 Blind) for Rayleigh Fading Channel Model

➤ **Estimation for 2x2 MIMO-STBC using BPSK (16 pilots, 100 Blind)**

Table 5.17

Channel Estimation for 2x2 MIMO-STBC using 2-PSK (16 pilots, 100 blind)

CE Algorithms	BER					
	QR-NEW (Proposed Tech.-I):	0.0359	0.0259	0.0158	0.0088	0.0053
ROML W-MMSE	0.0462	0.0321	0.0205	0.0133	0.0095	0.0056
WR	0.0376	0.0259	0.0153	0.0095	0.0057	0.0028
HQR-OPML (Proposed Tech.-II)	0.0376	0.0259	0.0153	0.0095	0.0057	0.0028
HQR-OPML-NEW (Proposed Tech.-III)	0.0282	0.0200	0.0121	0.0070	0.0039	0.0019
HQR-OPML-JSBCDE (Proposed Tech.-IV)	0.0282	0.0200	0.0121	0.0070	0.0039	0.0019
TBCE – LS	0.0379	0.0265	0.0155	0.0092	0.0057	0.0029
TBCE - MAP	0.0379	0.0265	0.0155	0.0092	0.0057	0.0029
WR-NEW-JSBCDE (Proposed Tech.-V)	0.0294	0.0212	0.0129	0.0072	0.0046	0.0024
Perfect – CSI	0.0260	0.0185	0.0114	0.0064	0.0039	0.0020

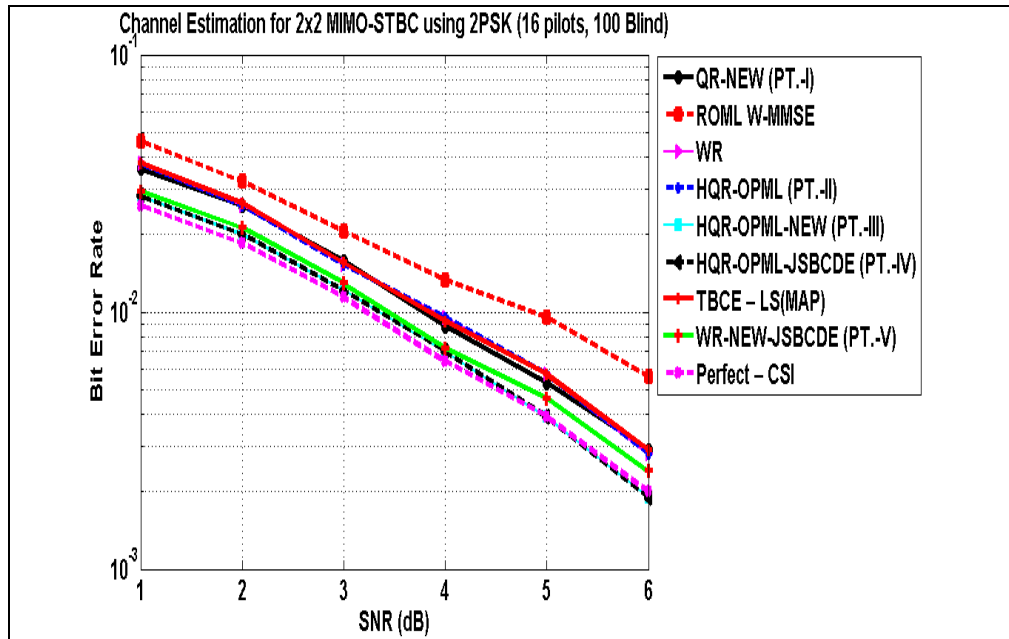


Figure 5.17: Channel Estimation for 2 Transmitters and 2 Receivers MIMO-STBC Using 2-PSK (16 Pilots, 100 Blind) for Rayleigh Fading Channel Model

➤ **Estimation for 2x4 MIMO-STBC using BPSK (16 pilots, 100 Blind)**

Table 5.18

Channel Estimation for 2x4 MIMO-STBC using 2-PSK (16 pilots, 100 blind)

CE Algorithms	BER					
	QR-NEW (Proposed Tech.-I):	0.0051	0.0023	0.0010	0.0004	0.0001
ROML W-MMSE	0.0061	0.0024	0.0012	0.0005	0.0002	0.0001
WR	0.0053	0.0020	0.0008	0.0003	0.0001	0.0001
HQR-OPML (Proposed Tech.-II)	0.0060	0.0028	0.0011	0.0004	0.0002	0.0001
HQR-OPML-NEW (Proposed Tech.-III)	0.0046	0.0022	0.0008	0.0002	0.0001	0.0001
HQR-OPML-JSBCDE (Proposed Tech.-IV)	0.0046	0.0022	0.0008	0.0002	0.0001	0.0001
TBCE – LS	0.0063	0.0028	0.0009	0.0003	0.0001	0.0001
TBCE - MAP	0.0063	0.0028	0.0009	0.0003	0.0001	0.0001
WR-NEW-JSBCDE (Proposed Tech.-V)	0.0040	0.0017	0.0006	0.0003	0.0001	0.0001
Perfect – CSI	0.0034	0.0014	0.0004	0.0002	0.0001	0

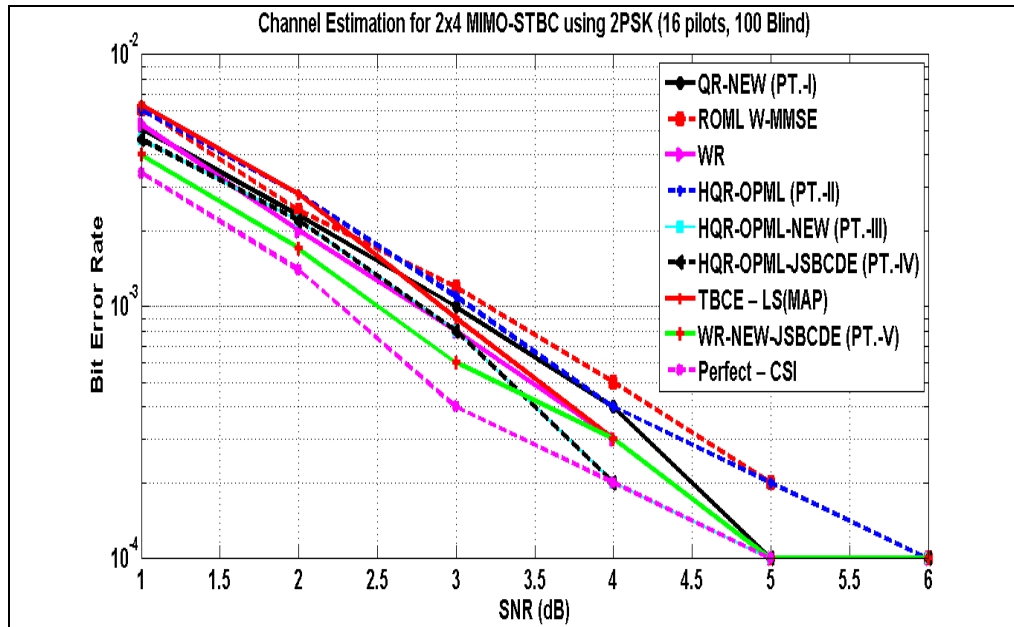


Figure 5.18: Channel Estimation for 2 Transmitters and 4 Receivers MIMO-STBC Using 2-PSK (16 Pilots, 100 Blind) for Rayleigh Fading Channel Model

➤ **Estimation for 2x6 MIMO-STBC using BPSK (16 pilots,100 Blind)**

Table 5.19

Channel Estimation for 2x6 MIMO-STBC using 2-PSK (16 pilots, 100 blind)

CE Algorithms	BER						
QR-NEW (Proposed Tech.-I):	1.0e-003 *	0.7250	0.2000	0.1000	0	0	0
ROML W-MMSE	1.0e-003 *	0.8500	0.2500	0.1000	0	0	0
WR	1.0e-003 *	0.6750	0.2250	0.1000	0	0	0
HQR-OPML (Proposed Tech.-II)		0.0010	0.0004	0.0001	0	0	0
HQR-OPML-NEW (Proposed Tech.-III)	1.0e-003 *	0.8500	0.2000	0.0500	0	0	0
HQR-OPML-JSBCDE (Proposed Tech.-IV)	1.0e-003 *	0.8500	0.2000	0.0500	0	0	0
TBCE – LS		0.0011	0.0003	0.0001	0	0	0
TBCE - MAP		0.0011	0.0003	0.0001	0	0	0
WR-NEW-JSBCDE (Proposed Tech.-V)	1.0e-003 *	0.4000	0.1000	0.0750	0	0	0
Perfect – CSI	1.0e-003 *	0.4500	0.1000	0.0250	0	0	0

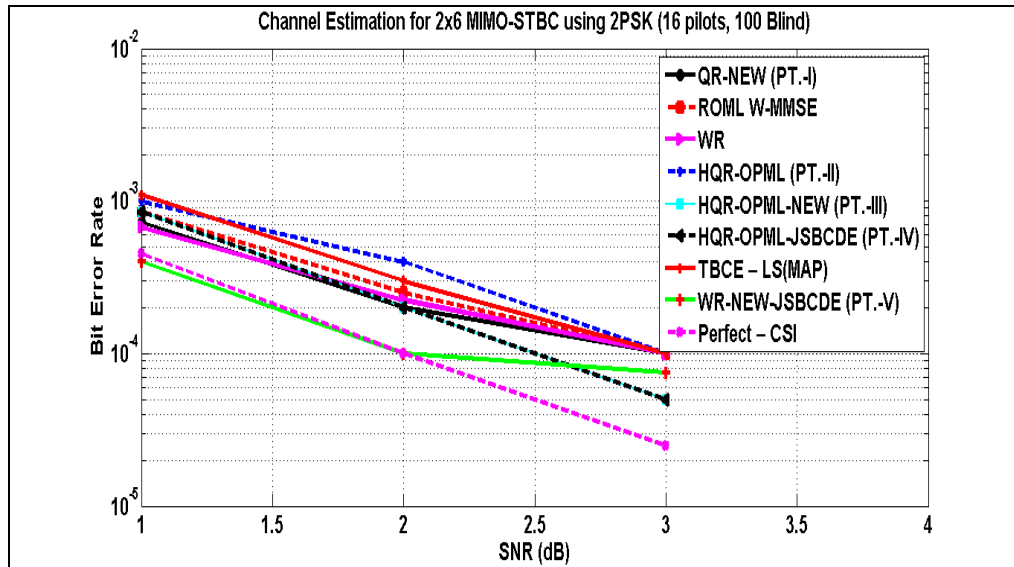


Figure 5.19: Channel Estimation for 2 Transmitters and 6 Receivers MIMO-STBC Using 2-PSK (16 Pilots, 100 Blind) for Rayleigh Fading Channel Model

➤ **Estimation for 2x6 MIMO-STBC using 4PSK (16 pilots, 100 Blind)**

Table 5.20

Channel Estimation for 2x6 MIMO-STBC using 4-PSK (16 pilots, 100 blind)

CE Algorithms	BER					
	QR-NEW (Proposed Tech.-I):	0.0199	0.0100	0.0039	0.0016	0.0004
ROML W-MMSE	0.0209	0.0098	0.0038	0.0015	0.0005	0.0003
WR	0.0180	0.0081	0.0033	0.0013	0.0003	0.0001
HQR-OPML (Proposed Tech.-II)	0.0219	0.0105	0.0039	0.0017	0.0004	0.0002
HQR-OPML-NEW (Proposed Tech.-III)	0.0169	0.0081	0.0024	0.0009	0.0003	0.0001
HQR-OPML-JSBCDE (Proposed Tech.-IV)	0.0169	0.0081	0.0024	0.0009	0.0003	0.0001
TBCE – LS	0.0200	0.0102	0.0039	0.0015	0.0003	0.0002
TBCE - MAP	0.0200	0.0102	0.0039	0.0015	0.0003	0.0002
WR-NEW-JSBCDE (Proposed Tech.-V)	0.0135	0.0066	0.0020	0.0008	0.0002	0.0001
Perfect – CSI	0.0109	0.0055	0.0016	0.0007	0.0001	0.0000

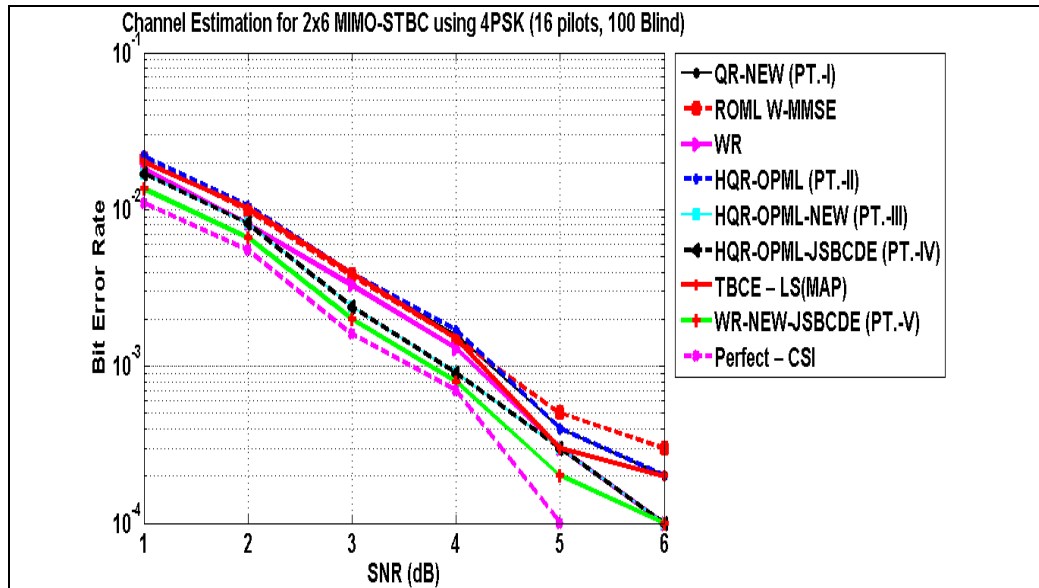


Figure 5.20: Channel Estimation for 2 Transmitters and 6 Receivers MIMO-STBC Using 4-PSK (16 Pilots, 100 Blind) for Rayleigh Fading Channel Model

➤ **Estimation for 2x4 MIMO-STBC using 4PSK (16 pilots, 100 Blind**

Table 5.21

Channel Estimation for 2x4 MIMO-STBC using 4-PSK (16 pilots, 100 blind)

CE Algorithms	BER					
	QR-NEW (Proposed Tech.-I):	0.0586	0.0357	0.0197	0.0098	0.0051
ROML W-MMSE	0.0640	0.0379	0.0220	0.0114	0.0070	0.0031
WR	0.0551	0.0318	0.0177	0.0085	0.0046	0.0017
HQR-OPML (Proposed Tech.-II)	0.0620	0.0371	0.0193	0.0097	0.0052	0.0020
HQR-OPML-NEW (Proposed Tech.-III)	0.0490	0.0283	0.0142	0.0072	0.0032	0.0014
HQR-OPML-JSBCDE (Proposed Tech.-IV)	0.0490	0.0283	0.0142	0.0072	0.0032	0.0014
TBCE – LS	0.0602	0.0349	0.0184	0.0091	0.0050	0.0018
TBCE - MAP	0.0602	0.0349	0.0184	0.0091	0.0050	0.0018
WR-NEW-JSBCDE (Proposed Tech.-V)	0.0438	0.0255	0.0134	0.0067	0.0028	0.0014
Perfect – CSI	0.0395	0.0226	0.0118	0.0053	0.0026	0.0013

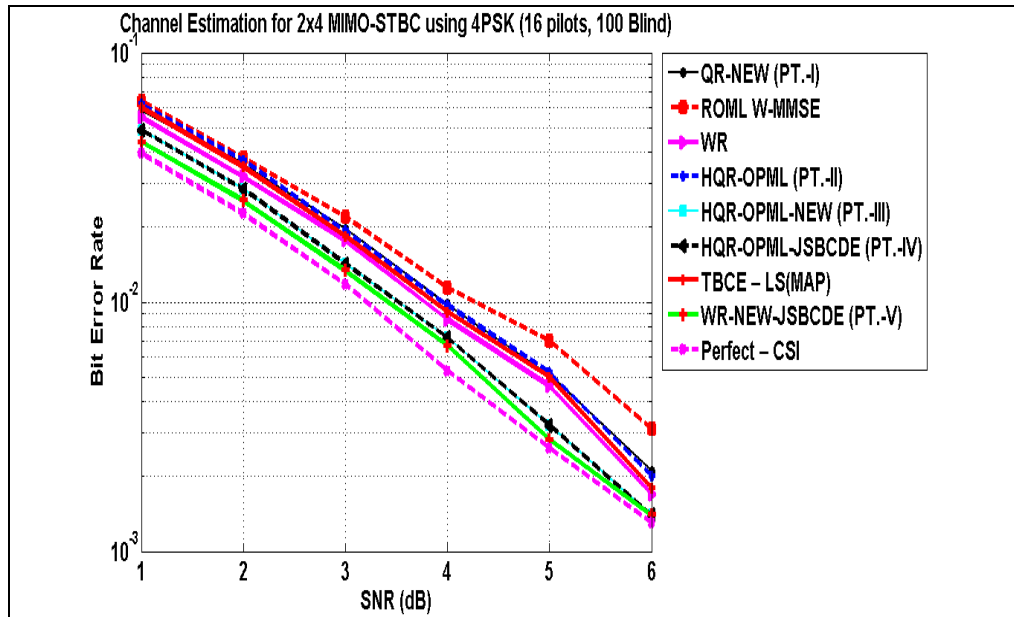


Figure 5.21: Channel Estimation for 2 Transmitters and 4 Receivers MIMO-STBC Using 4-PSK (16 Pilots, 100 Blind) for Rayleigh Fading Channel Model

➤ **Estimation for 2x8 MIMO-STBC using 4PSK (16 pilots, 100 Blind**

Table 5.22

Channel Estimation for 2x8 MIMO-STBC using 4-PSK (16 pilots, 100 blind)

CE Algorithms	BER					
	QR-NEW (Proposed Tech.-I):	0.0067	0.0027	0.0011	0.0004	0.0001
ROML W-MMSE	0.0060	0.0021	0.0010	0.0002	0.0001	0.0000
WR	0.0055	0.0022	0.0008	0.0001	0.0000	0.0000
HQR-OPML (Proposed Tech.-II)	0.0075	0.0031	0.0012	0.0002	0.0001	0.0000
HQR-OPML-NEW (Proposed Tech.-III)	0.0051	0.0017	0.0008	0.0001	0	0
HQR-OPML-JSBCDE (Proposed Tech.-IV)	0.0051	0.0017	0.0008	0.0001	0	0
TBCE – LS	0.0073	0.0025	0.0008	0.0002	0	0
TBCE - MAP	0.0073	0.0025	0.0008	0.0002	0	0
WR-NEW-JSBCDE (Proposed Tech.-V)	0.0039	0.0014	0.0006	0.0001	0.0000	0.0000
Perfect – CSI	0.0032	0.0011	0.0004	0.0001	0	0

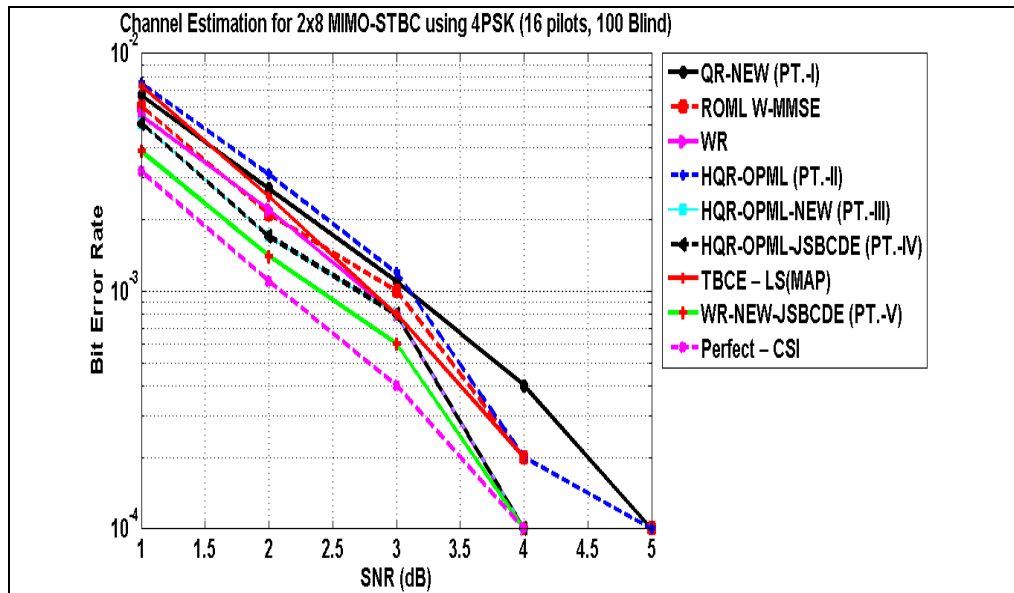


Figure 5.22: Channel Estimation for 2 Transmitters and 8 Receivers MIMO-STBC Using 4-PSK (16 Pilots, 100 Blind) for Rayleigh Fading Channel Model

➤ **Estimation for 2x2 MIMO-STBC using 4PSK (16 pilots, 100 Blind)**

Table 5.23

Channel Estimation for 2x2 MIMO-STBC using 4-PSK (16 pilots, 100 blind)

CE Algorithms	BER					
	QR-NEW (Proposed Tech.-I):	0.1766	0.1369	0.1009	0.0721	0.0489
ROML W-MMSE	0.2065	0.1643	0.1272	0.0972	0.0722	0.0524
WR	0.1780	0.1355	0.0982	0.0696	0.0471	0.0304
HQR-OPML (Proposed Tech.-II)	0.1780	0.1355	0.0982	0.0696	0.0471	0.0304
HQR-OPML-NEW (Proposed Tech.-III)	0.1518	0.1143	0.0804	0.0558	0.0377	0.0232
HQR-OPML-JSBCDE (Proposed Tech.-IV)	0.1518	0.1143	0.0804	0.0558	0.0377	0.0232
TBCE – LS	0.1779	0.1362	0.0988	0.0706	0.0472	0.0311
TBCE - MAP	0.1779	0.1362	0.0988	0.0706	0.0472	0.0311
WR-NEW-JSBCDE (Proposed Tech.-V)	0.1547	0.1167	0.0838	0.0586	0.0385	0.0262
Perfect – CSI	0.1440	0.1095	0.0769	0.534	0.0360	0.0227

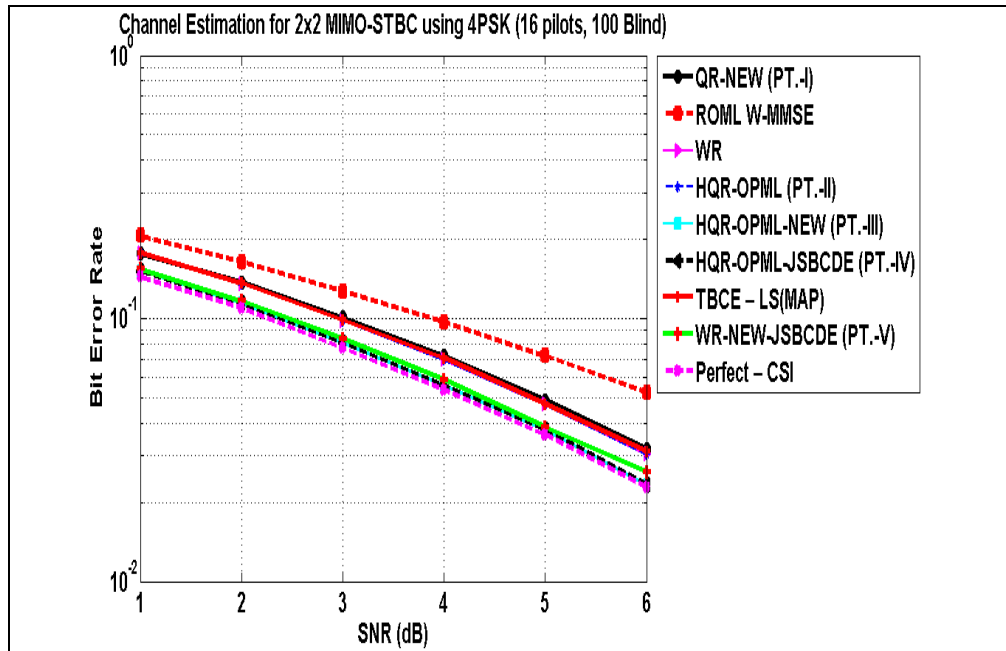


Figure 5.23: Channel Estimation for 2 Transmitters and 2 Receivers MIMO-STBC Using 4-PSK (16 Pilots, 100 Blind) for Rayleigh Fading Channel Model

- **Channel Estimation of QR-NEW (Proposed Tech.-I) for 2x4 MIMO-STBC presented under 4PSK (4 pilots, 100 Blind) using Rician channel model**

Table 5.24

Channel Estimation of QR-NEW (P.T.-I) for 2x4 MIMO-STBC using 4-PSK (4 pilots, 100 blind) for different Rice factors.

Rice factors	BER					
K= 0 (Rayleigh fading)	0.1033	0.0661	0.0419	0.0239	0.0132	0.0056
K=5	0.0798	0.0478	0.0274	0.0129	0.0058	0.0019
K=10	0.0742	0.0433	0.0239	0.0114	0.0043	0.0015
K=15	0.0722	0.0420	0.0221	0.0103	0.0037	0.0013

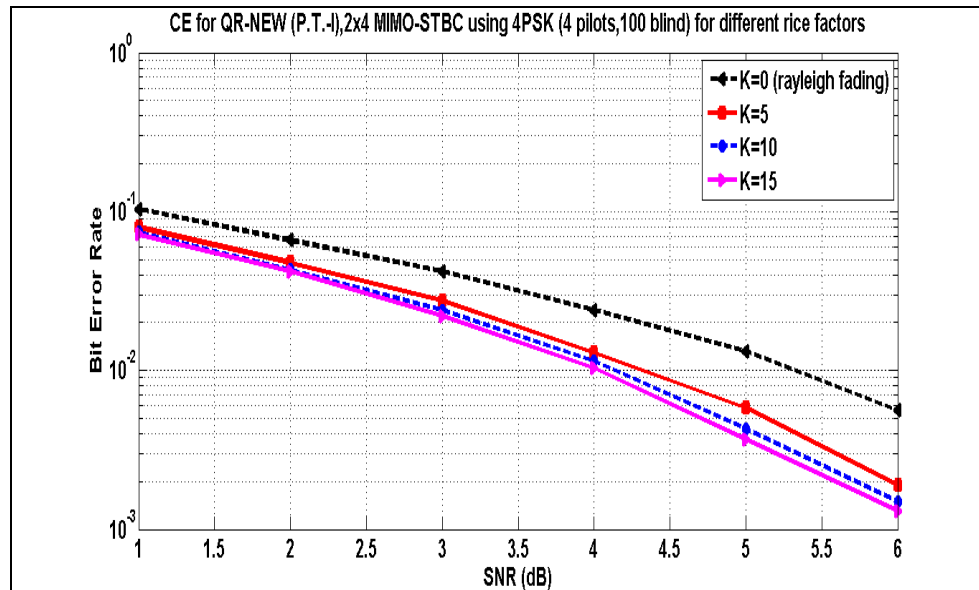


Figure 5.24: Channel Estimation of QR-NEW (P.T.-I) for 2x4 MIMO-STBC Presented Under 4-PSK (4 Pilots, 100 Blind) for Different Rice Factors Presented Using Rician Fading Channel Model.

- **Channel Estimation of HQR-OPML (Proposed Tech.-II) for 2x4 MIMO-STBC presented under 4PSK (4 pilots, 100 Blind) using Rician channel model**

Table 5.25

Channel Estimation of HQR-OPML (P.T.-II) for 2x4 MIMO-STBC using 4-PSK (4 pilots, 100 blind) for different Rice factors.

Rice factors	BER					
K= 0 (Rayleigh fading)	0.1053	0.0676	0.0415	0.0236	0.0123	0.0053
K=5	0.0832	0.0487	0.0270	0.0126	0.0055	0.0018
K=10	0.0780	0.0447	0.0239	0.0111	0.0041	0.0013
K=15	0.0758	0.0435	0.0226	0.0100	0.0036	0.0013

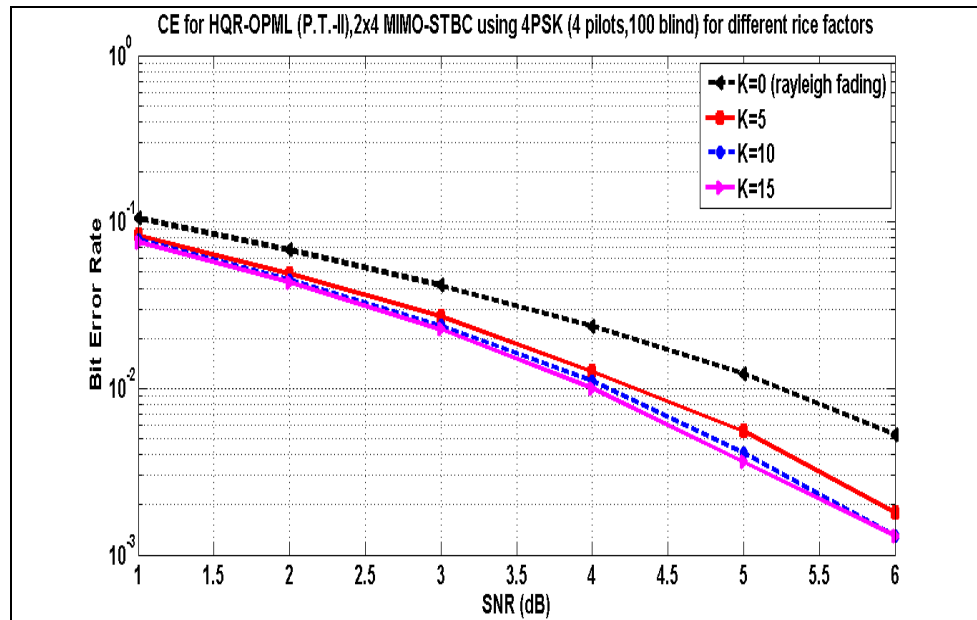


Figure 5.25: Channel Estimation of HQR-OPML (P.T.-II) for 2x4 MIMO-STBC Presented Under 4-PSK (4 Pilots, 100 Blind) for Different Rice Factors Presented Using Rician Fading Channel Model.

- **Channel Estimation of HQR-OPML-NEW (Proposed Tech.-III) for 2x4 MIMO-STBC presented under 4PSK (4 pilots, 100 Blind) using Rician channel model**

Table 5.26

Channel Estimation of HQR-OPML-NEW (P.T.-III) for 2x4 MIMO-STBC using 4-PSK (4 pilots, 100 blind) for different Rice factors.

Rice factors	BER					
K= 0 (Rayleigh fading)	0.0508	0.0283	0.0158	0.0080	0.0034	0.0018
K=5	0.0344	0.0181	0.0087	0.0033	0.0010	0.0004
K=10	0.0315	0.0157	0.0069	0.0026	0.0006	0.0003
K=15	0.0301	0.0149	0.0063	0.0024	0.0005	0.0002

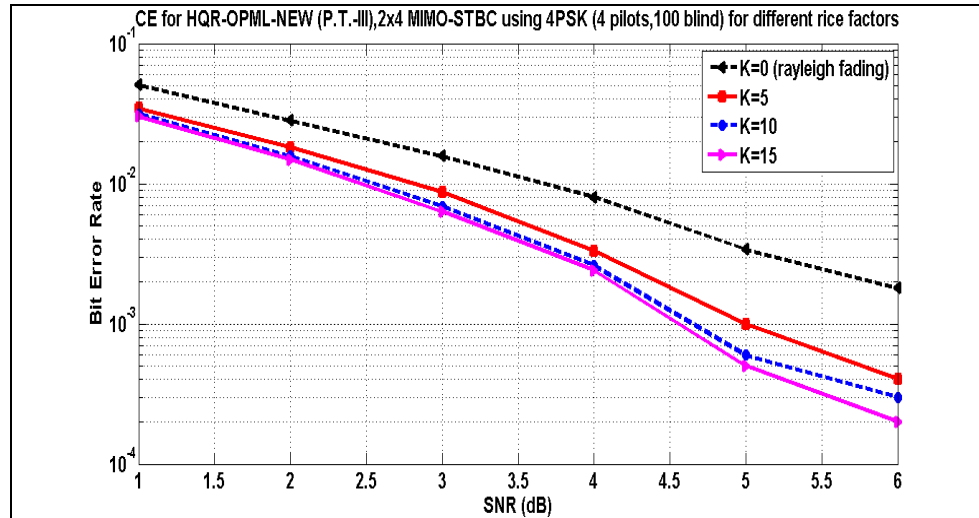


Figure 5.26: Channel Estimation of HQR-OPML-NEW (P.T.-III) for 2x4 MIMO-STBC Presented Under 4-PSK (4 Pilots, 100 Blind) for Different Rice Factors Presented Using Rician Fading Channel Model.

- **Channel Estimation of HQR-OPML-JSBCDE (Proposed Tech.-IV) for 2x4 MIMO-STBC presented under 4PSK (4 pilots, 100 Blind) using Rician channel model**

Table 5.27

Channel Estimation of HQR-OPML-JSBCDE (P.T.-IV) for 2x4 MIMO-STBC using 4-PSK (4 pilots, 100 blind) for different Rice factors.

Rice factors	BER					
K=0 (Rayleigh fading)	0.0452	0.0244	0.0140	0.0070	0.0032	0.0018
K=5	0.0327	0.0170	0.0080	0.0031	0.0008	0.0004
K=10	0.0306	0.0154	0.0068	0.0025	0.0006	0.0003
K=15	0.0302	0.0147	0.0062	0.0023	0.0005	0.0002

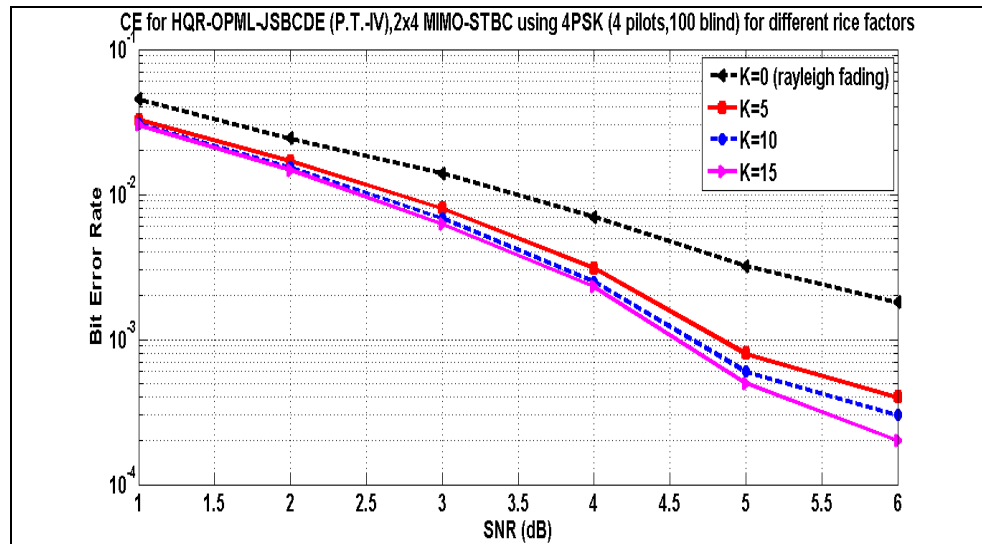


Figure 5.27: Channel Estimation of HQR-OPML-JSBCDE (P.T.-IV) for 2x4 MIMO-STBC Presented Under 4-PSK (4 Pilots, 100 Blind) for Different Rice Factors Presented Using Rician Fading Channel Model.

- **Channel Estimation of WR-NEW-JSBCDE (Proposed Tech.-V) for 2x4 MIMO-STBC presented under 4PSK (4 pilots, 100 Blind) using Rician channel model**

Table 5.28

Channel Estimation of WR-NEW-JSBCDE (P.T.-V) for 2x4 MIMO-STBC using 4-PSK (4 pilots, 100 blind) for different Rice factors.

Rice factors	BER					
K= 0 (Rayleigh fading)	0.0452	0.0244	0.0140	0.0070	0.0032	0.0018
K=5	0.0327	0.0170	0.0080	0.0031	0.0008	0.0004
K=10	0.0306	0.0154	0.0068	0.0025	0.0006	0.0003
K=15	0.0302	0.0147	0.0062	0.0023	0.0005	0.0002

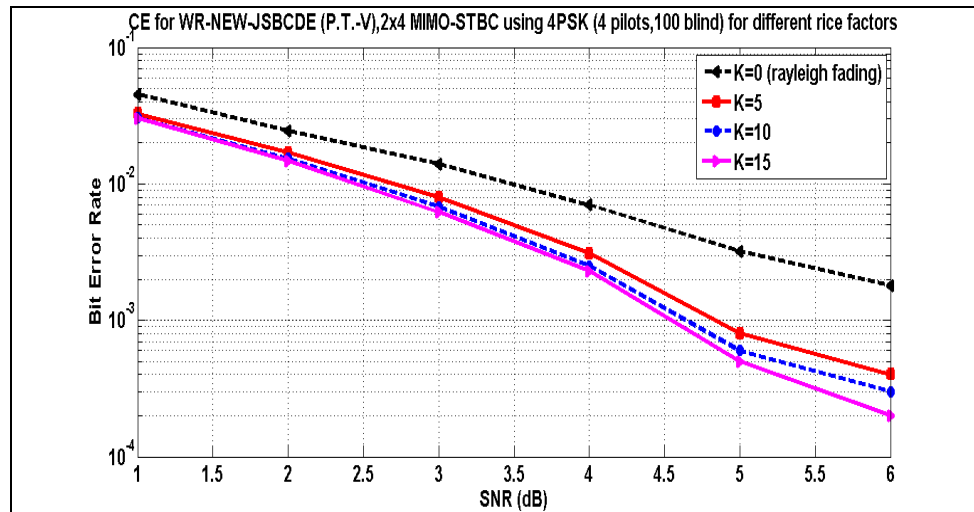


Figure 5.28: Channel Estimation of WR-NEW-JSBCDE (P.T.-V) for 2x4 MIMO-STBC Presented Under 4-PSK (4 Pilots, 100 Blind) for Different Rice Factors Presented Using Rician Fading Channel Model.

- **Channel Estimation of QR-NEW (Proposed Tech.-I) for 2x6 MIMO-STBC presented under 4PSK (4 pilots, 100 Blind) using Rician channel model**

Table 5.29

Channel Estimation of QR-NEW (P.T.-I) for 2x6 MIMO-STBC using 4-PSK (4 pilots, 100 blind) for different Rice factors.

Rice factors	BER					
	0.0403	0.0243	0.0116	0.0049	0.0018	0.0007
K=0 (Rayleigh fading)	0.0403	0.0243	0.0116	0.0049	0.0018	0.0007
K=5	0.0293	0.0142	0.0062	0.0023	0.0006	0.0001
K=10	0.0261	0.0120	0.0049	0.0018	0.0005	0.0001
K=15	0.0250	0.0114	0.0043	0.0016	0.0004	0.0001

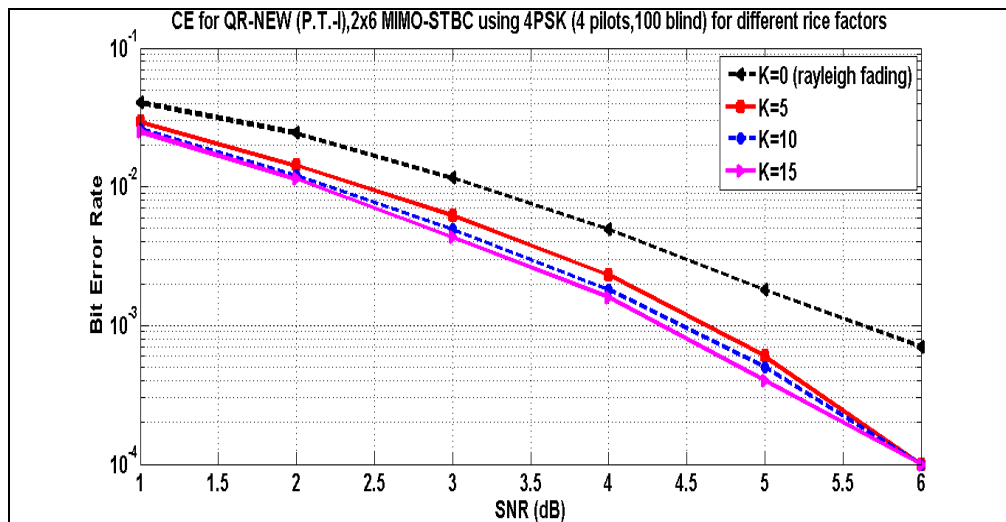


Figure 5.29: Channel Estimation of QR-NEW (P.T.-I) for 2x6 MIMO-STBC Presented Under 4-PSK (4 Pilots, 100 Blind) for Different Rice Factors Presented Using Rician Fading Channel Model.

- **Channel Estimation of HQR-OPML (Proposed Tech.-II) for 2x6 MIMO-STBC presented under 4PSK (4 pilots, 100 Blind) using Rician channel model**

Table 5.30

Channel Estimation of HQR-OPML (P.T.-II) for 2x6 MIMO-STBC using 4-PSK (4 pilots, 100 blind) for different Rice factors.

Rice factors	BER					
K= 0 (Rayleigh fading)	0.0437	0.0247	0.0111	0.0045	0.0019	0.0005
K=5	0.0304	0.0147	0.0063	0.0022	0.0006	0.0001
K=10	0.0275	0.0124	0.0051	0.0018	0.0005	0.0001
K=15	0.0263	0.0117	0.0046	0.0015	0.0004	0.0001

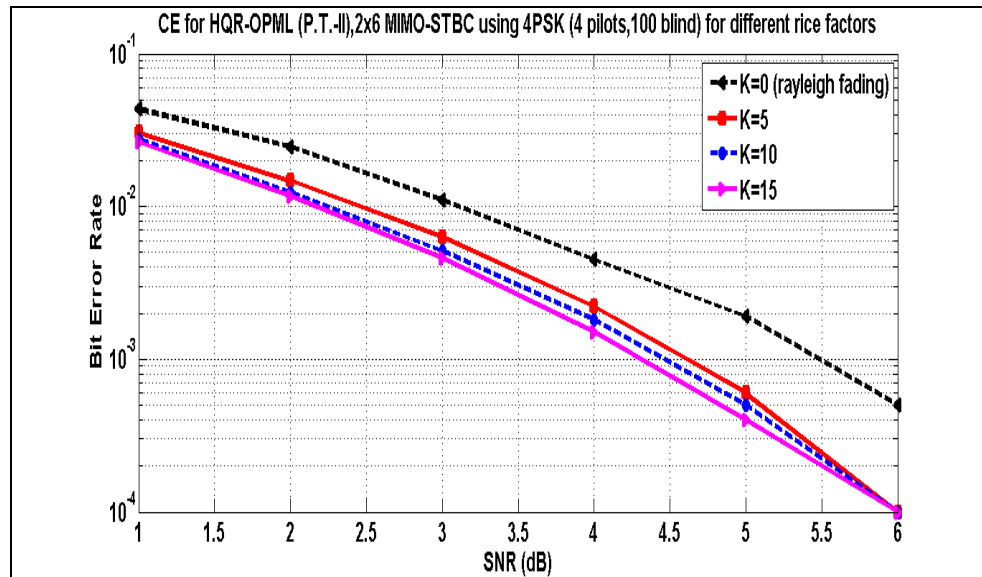


Figure 5.30: Channel Estimation of HQR-OPML (P.T.-II) for 2x6 MIMO-STBC Presented Under 4-PSK (4 Pilots, 100 Blind) for Different Rice Factors Presented Using Rician Fading Channel Model.

- **Channel Estimation of HQR-OPML-NEW (Proposed Tech.-III) for 2x6 MIMO-STBC presented under 4PSK (4 pilots, 100 Blind) using Rician channel model**

Table 5.31

Channel Estimation of HQR-OPML-NEW (P.T.-III) for 2x6 MIMO-STBC using 4-PSK (4 pilots, 100 blind) for different Rice factors.

Rice factors	BER					
K= 0 (Rayleigh fading)	0.0155	0.0083	0.0034	0.0008	0.0004	0.0001
K=5	0.0099	0.0034	0.0013	0.0004	0.0000	0
K=10	0.0084	0.0026	0.0010	0.0003	0.0000	0
K=15	0.0079	0.0025	0.0008	0.0002	0.0000	0

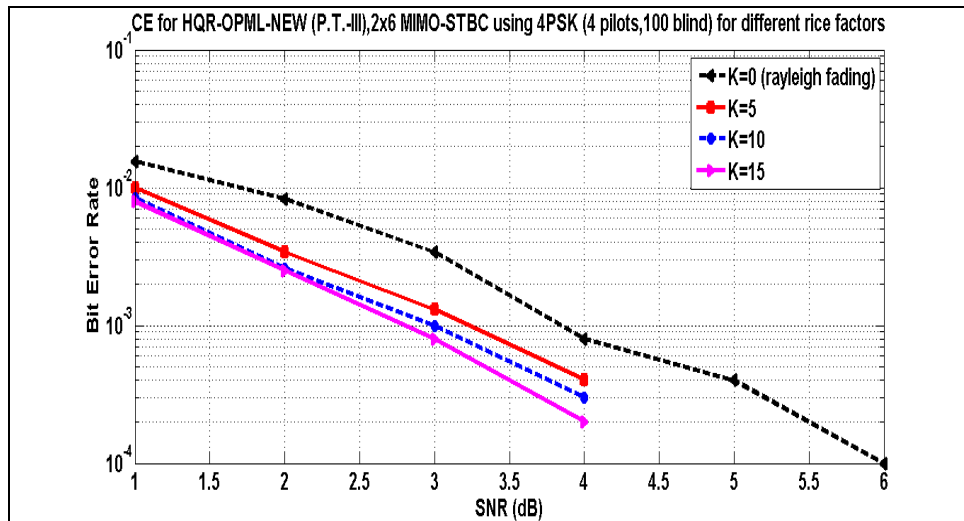


Figure 5.31: Channel Estimation of HQR-OPML-NEW (P.T.-III) for 2x6 MIMO-STBC Presented Under 4-PSK (4 Pilots, 100 Blind) for Different Rice Factors Presented Using Rician Fading Channel Model.

- **Channel Estimation of HQR-OPML-JSBCDE (Proposed Tech.-IV) for 2x6 MIMO-STBC presented under 4PSK (4 pilots, 100 Blind) using Rician channel model**

Table 5.32

Channel Estimation of HQR-OPML-JSBCDE (P.T.-IV) for 2x6 MIMO-STBC using 4-PSK (4 pilots, 100 blind) for different Rice factors.

Rice factors	BER					
K= 0 (Rayleigh fading)	0.0152	0.0083	0.0033	0.0009	0.0003	0.0001
K=5	0.0093	0.0033	0.0016	0.0004	0.0000	0
K=10	0.0082	0.0026	0.0010	0.0003	0.0000	0
K=15	0.0076	0.0026	0.0009	0.0002	0.0000	0

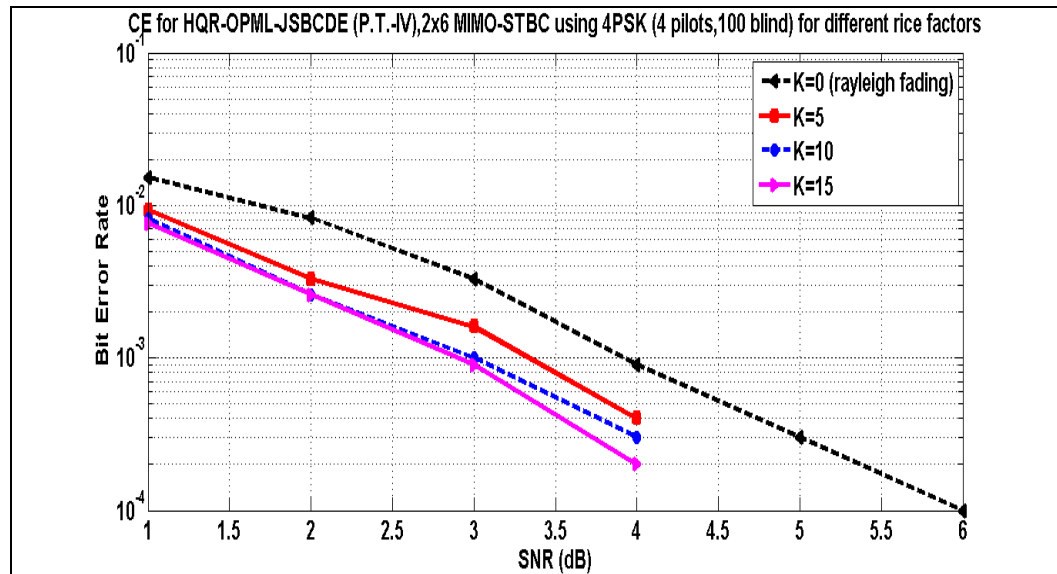


Figure 5.32: Channel Estimation of HQR-OPML-JSBCDE (P.T.-IV) for 2x6 MIMO-STBC Presented Under 4-PSK (4 Pilots, 100 Blind) for Different Rice Factors Presented Using Rician Fading Channel Model.

- **Channel Estimation of WR-NEW-JSBCDE (Proposed Tech.-V) for 2x6 MIMO-STBC presented under 4PSK (4 pilots, 100 Blind) using Rician channel model**

Table 5.33

Channel Estimation of WR-NEW-JSBCDE (P.T.-V) for 2x6 MIMO-STBC using 4-PSK (4 pilots, 100 blind) for different Rice factors.

Rice factors	BER					
K=0 (Rayleigh fading)	0.0118	0.0071	0.0024	0.0008	0.0003	0.0001
K=5	0.0087	0.0031	0.0013	0.0004	0.0000	0
K=10	0.0078	0.0026	0.0010	0.0003	0.0000	0
K=15	0.0074	0.0026	0.0010	0.0002	0.0000	0

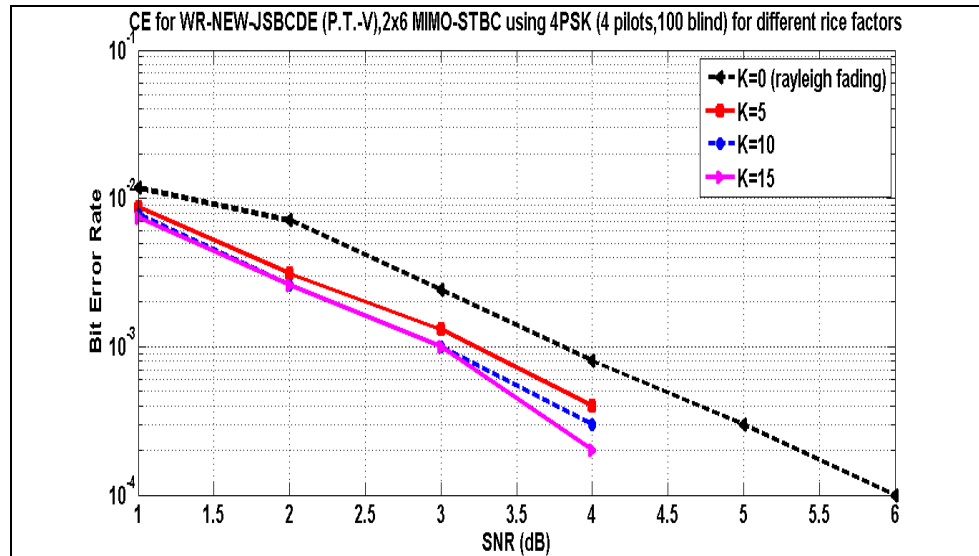


Figure 5.33: Channel Estimation of WR-NEW-JSBCDE (P.T.-V) for 2x6 MIMO-STBC Presented Under 4-PSK (4 Pilots, 100 Blind) for Different Rice Factors Presented Using Rician Fading Channel Model.

- **Channel Estimation of QR-NEW (Proposed Tech.-I) for 2x8 MIMO-STBC presented under 4PSK (4 pilots, 100 Blind) using Rician channel model**

Table 5.34

Channel Estimation of QR-NEW (P.T.-I) for 2x8 MIMO-STBC using 4-PSK (4 pilots, 100 blind) for different Rice factors.

Rice factors	BER					
K= 0 (Rayleigh fading)	0.0182	0.0089	0.0036	0.0010	0.0003	0.0001
K=5	0.0135	0.0048	0.0015	0.0004	0.0001	0
K=10	0.0118	0.0040	0.0012	0.0003	0	0
K=15	0.0112	0.0037	0.0010	0.0002	0	0

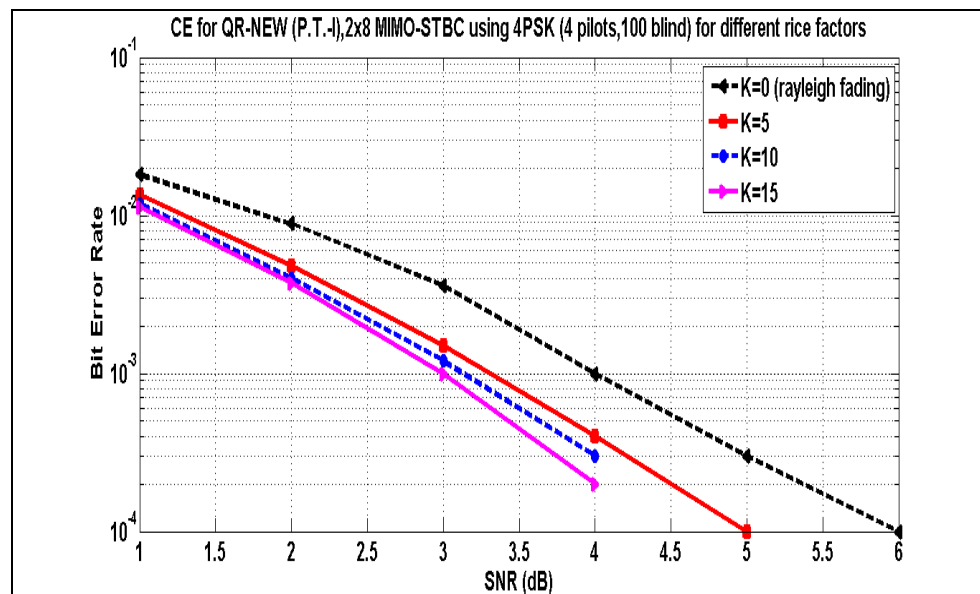


Figure 5.34: Channel Estimation of QR-NEW (P.T.-I) for 2x8 MIMO-STBC Presented Under 4-PSK (4 Pilots, 100 Blind) for Different Rice Factors Presented Using Rician Fading Channel Model.

- **Channel Estimation of HQR-OPML (Proposed Tech.-II) for 2x8 MIMO-STBC presented under 4PSK (4 pilots, 100 Blind) using Rician channel model**

Table 5.35

Channel Estimation of HQR-OPML (P.T.-II) for 2x8 MIMO-STBC using 4-PSK (4 pilots, 100 blind) for different Rice factors.

Rice factors	BER					
	0.0190	0.0098	0.0039	0.0010	0.0003	0
K=0 (Rayleigh fading)	0.0190	0.0098	0.0039	0.0010	0.0003	0
K=5	0.0141	0.0046	0.0017	0.0004	0.0001	0
K=10	0.0123	0.0039	0.0013	0.0003	0	0
K=15	0.0117	0.0036	0.0011	0.0002	0	0

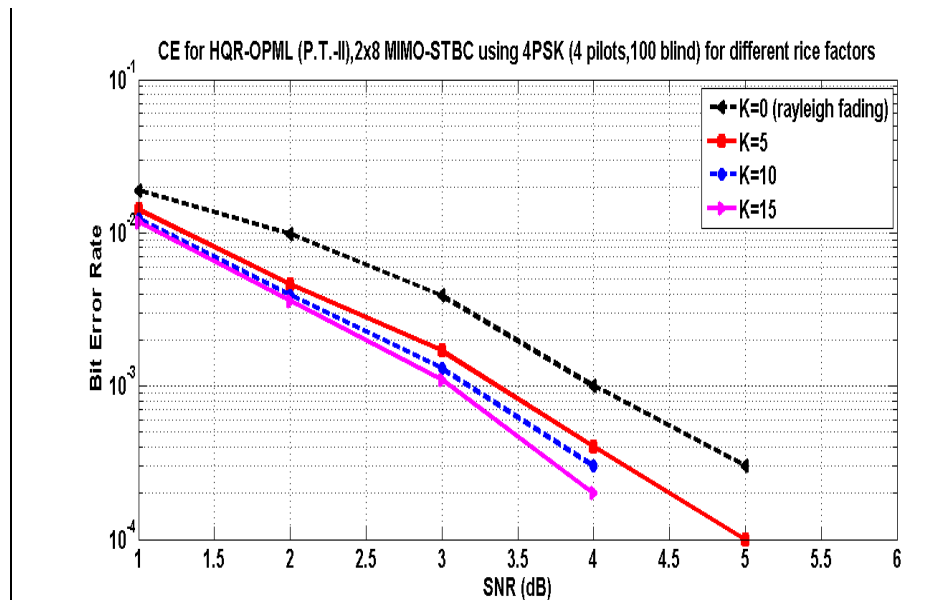


Figure 5.35: Channel Estimation of HQR-OPML (P.T.-II) for 2x8 MIMO-STBC Presented Under 4-PSK (4 Pilots, 100 Blind) for Different Rice Factors Presented Using Rician Fading Channel Model.

- **Channel Estimation of HQR-OPML-NEW (Proposed Tech.-III) for 2x8 MIMO-STBC presented under 4PSK (4 pilots, 100 Blind) using Rician channel model**

Table 5.36

Channel Estimation of HQR-OPML-NEW (P.T.-III) for 2x8 MIMO-STBC using 4-PSK (4 pilots, 100 blind) for different Rice factors.

Rice factors	BER					
K= 0 (Rayleigh fading)	0.0057	0.0026	0.0008	0.0002	0.0000	0
K=5	0.0029	0.0008	0.0003	0	0	0
K=10	0.0025	0.0006	0.0001	0	0	0
K=15	0.0023	0.0006	0.0001	0	0	0

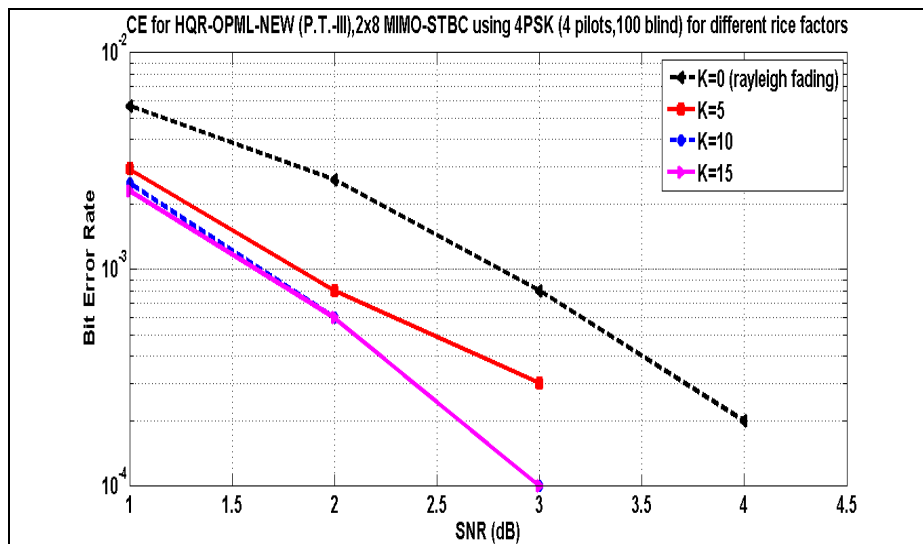


Figure 5.36: Channel Estimation of HQR-OPML-NEW (P.T.-III) for 2x8 MIMO-STBC Presented Under 4-PSK (4 Pilots, 100 Blind) for Different Rice Factors Presented Using Rician Fading Channel Model.

- **Channel Estimation of HQR-OPML-JSBCDE (Proposed Tech.-IV) for 2x8 MIMO-STBC presented under 4PSK (4 pilots, 100 Blind) using Rician channel model**

Table 5.37

Channel Estimation of HQR-OPML-JSBCDE (P.T.-IV) for 2x8 MIMO-STBC using 4-PSK (4 pilots, 100 blind) for different Rice factors.

Rice factors	BER					
K= 0 (Rayleigh fading)	0.0056	0.0024	0.0008	0.0002	0.0000	0
K=5	0.0032	0.0008	0.0004	0.0000	0.0000	0
K=10	0.0026	0.0007	0.0003	0	0	0
K=15	0.0023	0.0007	0.0002	0	0	0

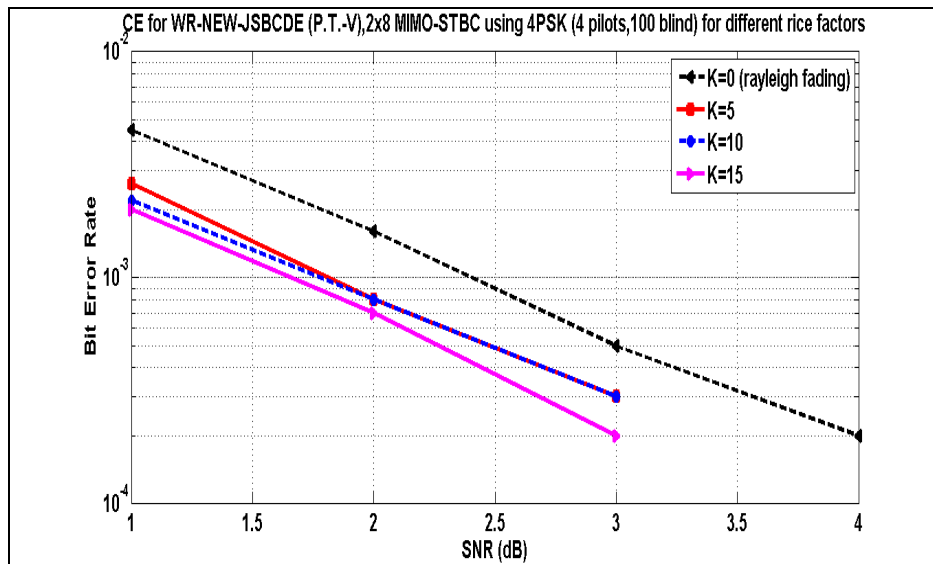


Figure 5.37: Channel Estimation of HQR-OPML-JSBCDE (P.T.-IV) for 2x8 MIMO-STBC Presented Under 4-PSK (4 Pilots, 100 Blind) for Different Rice Factors Presented Using Rician Fading Channel Model.

- **Channel Estimation of WR-NEW-JSBCDE (Proposed Tech.-V) for 2x8 MIMO-STBC presented under 4PSK (4 pilots, 100 Blind) using Rician channel model**

Table 5.38

Channel Estimation of WR-NEW-JSBCDE (P.T.-V) for 2x8 MIMO-STBC using 4-PSK (4 pilots, 100 blind) for different Rice factors.

Rice factors	BER					
K= 0 (Rayleigh fading)	0.0045	0.0016	0.0005	0.0002	0	0
K=5	0.0026	0.0008	0.0003	0.0000	0	0
K=10	0.0022	0.0008	0.0003	0	0	0
K=15	0.0020	0.0007	0.0002	0	0	0

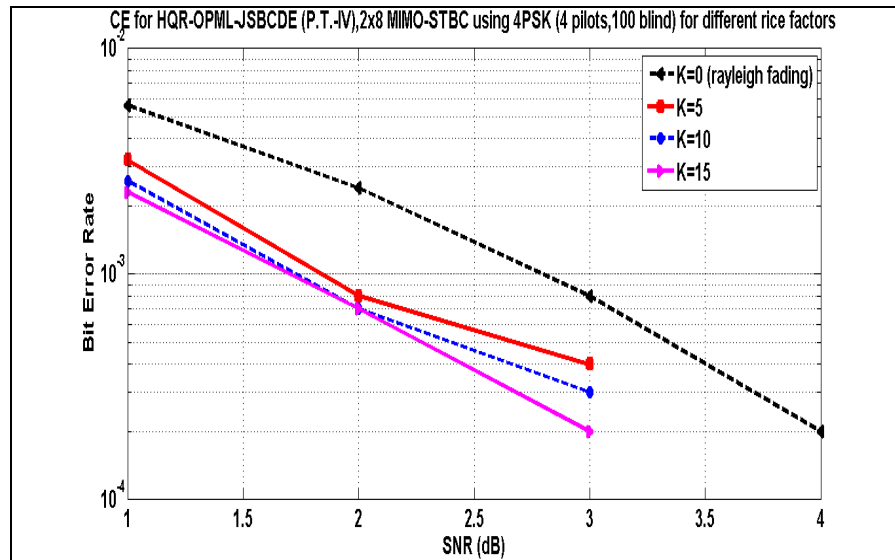


Figure 5.38: Channel Estimation of WR-NEW-JSBCDE (P.T.-V) for 2x8 MIMO-STBC Presented Under 4-PSK (4 Pilots, 100 Blind) for Different Rice Factors Presented Using Rician Fading Channel Model.

5.4 OBSERVATIONS OF SIMULATION RESULTS

As per simulation results presented in previous section, following observations have been carried out.

- Conventional semi-blind channel estimation technique SVD-OPML (WR) shows better results compared to conventional SVD-ROML based semi-blind channel estimation technique, Least Square (LS) and Maximum a Posteriori (MAP) based training channel estimation techniques for all combinations.
- Proposed Tech.-I and II show nearby performances compared to conventional SVD-OPML (WR) technique, while proposed Tech. –III, IV and V outperform others and show near optimal performance by comparing with perfect channel state information (CSI) for all combinations.
- BER performance improves by increasing receiver antennas for any techniques and for any combinations.
- BER performance improves by increasing orthogonal pilot symbols for conventional techniques.
- BER performance degrades by using higher modulation schemes. For any combinations, BER degrades if 8-PSK is used instead of 4-PSK and 4-PSK instead of 2-PSK.
- For Rician fading channel model, BER performance improves with increase of Rice factors (like Rice factors $K=0, 5, 10, 15$). Rice factor $K=0$ is Rayleigh fading case, so performance improves with respect to increasing Rice factors.

5.6 SUMMARY

In this chapter extensive computer simulations have been carried out to investigate and demonstrate performance of novel semi-blind channel estimation techniques for Rayleigh flat fading MIMO channel using various parameters like receiver antennas, modulation schemes (m -PSK, where $m = 2, 4, 8$) and orthogonal pilots (4 pilots, 8 pilots and 16 pilots). Finally analysis of proposed novel techniques

have been performed by using flat fading Rician channel model under 4-PSK modulation scheme for 2 transmitters and various receiver antennas.

CHAPTER 6

CONCLUSIONS AND FUTURE SCOPE

6.1 CONCLUSIONS

It is known that reliability of MIMO systems depends upon knowledge of channel state information (CSI) at the receiver for data detection and decoding. Therefore the accurate and robust estimation of wireless channel is very important part of MIMO communication system.

In this thesis, performance of proposed novel semi-blind channel estimation and data detection has been compared to conventional channel estimation techniques and investigated by taking BER analysis. From extensive computer simulations presented for $2 \times N$ MIMO-STBC systems using flat fading Rayleigh and Rician channels for various parameters like combinations of receiver antennas, modulation schemes (m-PSK, where $m = 2, 4, 8$) and orthogonal pilots (4 pilots, 8 pilots and 16 pilots), following points have been concluded.

- Conventional SVD-OPML (WR) semi-blind channel technique shows better result compared to SVD-ROML based semi-blind channel estimation technique and other training based channel estimation techniques like LS and MAP for all the combinations of receiver antennas, modulation schemes (m-PSK) and orthogonal training (pilot) symbols. For example, 2×6 MIMO-STBC Rayleigh fading model using 4-PSK (4 pilots, 100 blind information symbols) simulation shows; BER at 1 dB, 3 dB and 5 dB SNR are 0.0364, 0.0097 and 0.0017 for SVD-OPML Technique, 0.0500, 0.0153 and 0.0034 for SVD-ROML Technique, 0.0554, 0.0320 and 0.0024 for Training based LS and MAP Techniques. (Refer Table 5.1)
- BER performance improves with increases in number of receiver antennas for all the successive techniques comparatively. Here 2 transmitter antennas and 2, 4, 6 and 8 receiver antennas have been used to investigate

performance of various channel estimation Techniques. For example, MIMO-STBC Rayleigh fading model using 4-PSK (4 pilots, 100 blind information symbols) simulation setup gives BER for SVD-OPML Technique at 1 dB, 3 dB and 5 dB SNR are 0.2541, 0.1592 and 0.0802 using 2 receiver antennas, 0.0948, 0.0369 and 0.0111 using 4 receiver antennas, 0.0364, 0.0097 and 0.0017 using 6 receiver antennas and 0.0156, 0.0033 and 0.0002 using 8 receiver antennas. (Refer Table 5.1 to 5.4)

- In semi-blind channel estimation schemes, 4, 8 and 16 orthogonal pilot symbols have been taken. BER performance improves with an increase in number of orthogonal pilot symbols for particular scheme but it increases complexity of matrix calculations by increasing size of matrix. For example, 2×6 MIMO-STBC Rayleigh fading model using 4-PSK simulation setup shows BER for SVD-OPML at 1 dB, 3 dB and 5 dB SNR are 0.0364, 0.0097 and 0.0017 using 4 orthogonal pilots, 0.0237, 0.0049 and 0.0008 using 8 orthogonal pilots and 0.0180, 0.0033 and 0.0003 using 16 orthogonal pilots. (Refer Table 5.1, 5.10, 5.20)
- Simulation results show that BER performance for same combination degrades with applying higher modulation scheme. For the same combination, 2-PSK performs better compared to 4-PSK and 8-PSK for any technique. For example, 2×6 MIMO-STBC Rayleigh fading model (4 pilots, 100 blind information symbols) simulation setup gives BER for SVD-OPML 1 dB, 3 dB and 5 dB SNR are 0.2511, 0.1480, and 0.0699 using 8-PSK, 0.0364, 0.0097 and 0.0017 using 4-PSK and 0.0021, 0.0001 and 0.0000 using 2-PSK (BPSK). (Refer Table 5.1, 5.7 and 5.9)
- Five novel semi-blind channel estimation techniques have been proposed. Among those, proposed techniques I and II show nearby performances compared to SVD-OPML (WR) based technique and proposed techniques III, IV and V show better performances compared to SVD-OPML and other techniques with 2 to 3 dB improvement and show near optimal performance

by comparing with known channel (perfect Channel state information). Further Proposed techniques III to V shows almost nearby performance, still technique V is marginally better compared to technique III and IV. Proposed technique III and IV uses Householder QR decomposition (H-QRD) which is less computationally complex in comparison with other matrix decomposition techniques because not only it avoids explicit matrix inversions but it converts full rank matrix into a simpler form and it guarantees numerical stability by minimizing errors so that can be suitable techniques for reduced complexity solutions with near optimal performance.

- Finally in the last part of simulations, flat fading Rician channel model have been taken using 4-PSK modulation scheme to simulate proposed techniques for different Rice factors. Simulation results indicate that by increasing Rice factors ($K=0$ (Rayleigh fading), $K=5, 10, 15$), BER performance successively improves for all combinations.(Refer Table 5.24 to 5.38)

6.2 FUTURE SCOPE OF THE WORK

In thesis, novel semi-blind channel estimation and data detection techniques for low complexity and near optimal performance using flat fading Rayleigh and Rician channel models for single carrier MIMO-STBC system have been proposed with its mathematical model. The future work can be suggested as the development of a low complexity adaptive channel estimation technique for MIMO-OFDM based multicarrier system for frequency selective fading environment. Nowadays there is need to calculate channel coefficient for fast frequency selective environment due to vehicular speed. For this, efficient channel estimation techniques are required to deal with such types of time-varying environment where channel coefficients are not fixed but keep changing after every time interval. Further one can use more number of

transmitter antennas with various OSTBC schemes to investigate performance of the same. Further adaptive receiver design can be suggested for time-varying environment.

BIBLIOGRAPHY

- 1 S. M. Alamouti, "A simple transmit diversity technique for wireless communications," *IEEE Jnl. on Selected. Areas in Communication*, Vol. 16, No. 8, pp. 1451-58, Oct. 1998.
- 2 H. Bolcskel, D. Gesbert, C.B. Papadias and A.J. Van Der Veen, "Space-Time Wireless Systems," Cambridge University Press, Cambridge, 2006.
- 3 D. Tse and P. Viswanath, "Fundamentals of Wireless Communications," Cambridge University Press, Cambridge, 2005.
- 4 G. K. Krishnan and V. U. Reddy, "MIMO communications-motivation and a practical realization," *IETE Tech. Rev.*, Vol. 24, No. 4, pp. 203-13, Jul-Aug 2007.
- 5 A. J. Paulraj, D. A. Gore, R. U. Nabar, and H. Bclcskei, "An overview of MIMO communications - A key to gigabit wireless," *Proc. IEEE*, Vol. 92, No. 2, pp. 198-218, 2004.
- 6 M. Kiessling, J. Speidel and Y. Chen, "MIMO channel estimation in correlated fading environments," *In Proceedings of 58th IEEE Vehicular Technology Conference (VTC'03)*, Orlando, Oct 2003, pp. 1187-91.
- 7 G. Xie, X. Fang, A. Yang and Y. Liu, "Channel estimation with pilot symbol and spatial correlation information," *In Proceedings of IEEE International Symposium on Communications and Information Technologies (ISCIT'07)*, Sydney, Oct 2007, pp. 1003-6.
- 8 S. M. Kay, "Fundamentals of Statistical Signal Processing: Estimation Theory". Prentice-Hall, Upper Saddle River, NJ 07458, 1993.
- 9 S. Coleri, M. Ergen, A. Puri, and A. Bahai, "Channel estimation techniques based on pilot arrangement in OFDM systems," *IEEE Tran. on Broadcasting*, vol.48, no. 3, pp. 223-229, Sept. 2002.
- 10 G. K. Krishnan and V. U. Reddy, "MIMO communications-motivation and a practical realization," *IETE Tech. Rev.*, Vol. 24, No. 4, pp. 203-13, Jul-Aug 2007.
- 11 M. Abuthinien, S. Chen, A. Wolfgang, and L. Hanzo, "Joint maximum likelihood channel estimation and data detection for MIMO systems," *In Proceedings of IEEE International Conference on Communications (ICC'07)*, Glasgow, pp. 5354-8, Jun 2007.
- 12 H. Nooralizadeh, S. Shirvani Moghaddam and H. R. Bakhshi, "Optimal training sequences in MIMO channel estimation with spatially correlated Rician flat fading," *In Proceedings of 2009 IEEE Symposium on Industrial Electronics and Applications (ISIEA'09)*, Malaysia, pp. 227-32, Oct. 2009.
- 13 H. Nooralizadeh and S. Shirvani Moghaddam, "A new shifted scaled LS channel estimator for Rician flat fading MIMO channel," *In Proceedings of 2009 IEEE Symposium on Industrial Electronics and Applications (ISIEA'09)*, Malaysia, pp.

- 243-47, Oct 2009.
- 14 H. Nooralizadeh and S. Shirvani Moghaddam, "A novel shifted type of SLS estimator for estimation of Rician flat fading MIMO channels," *Elsevier Signal Processing*, Vol. 90, No. 6, pp. 1886-93, Jun 2010.
 - 15 X. Ma, L. Yang and G. B. Giannakis, "Optimal training for MIMO frequency-selective fading channels," *IEEE Trans. on Wireless Comm.*, Vol. 4, No. 2, pp. 453-66, Mar 2005.
 - 16 M. Biguesh and A. B. Gershman, "Training-based MIMO channel estimation: A study of estimator tradeoffs and optimal training signals," *IEEE Trans. on Signal Process.*, Vol. 54, No. 3, pp. 884-93, Mar 2006.
 - 17 G. Leus and A. J. Van Der Veen, "Optimal training for ML and LMMSE channel estimation in MIMO systems," *In Proceedings of 13th IEEE Workshop on Statistical Signal Processing (SSP'05)*, France, pp. 1354-57, Jul 2005.
 - 18 S. A. Yang and J. Wu, "Optimal binary training sequence design for multiple-antenna systems over dispersive fading channels," *IEEE Trans. on Vehicular Tech.*, Vol. 51, No. 5, pp. 1271-6, Sep 2002.
 - 19 S. Chen, X. C. Yang, L. Chen and L. Hanzo, "Blind joint maximum likelihood channel estimation and data detection for SIMO systems," *Int. J. Auto. Comput.*, Vol. 4, No. 1, pp. 47-51, Jan 2007.
 - 20 K. Sabri, M. El Badaoui, F. Guillet, A. Adib and D. Aboutajdine, "A frequency domain-based approach for blind MIMO system identification using second-order cyclic statistics," *Elsevier Signal Processing*, Vol. 89, No. 1, pp. 77-86, Jan 2009.
 - 21 I. M. Panahi and K. Venkat, "Blind identification of multi-channel systems with single input and unknown orders," *Elsevier Signal Processing*, Vol. 89, No. 7, pp. 1288-310, Jul 2009.
 - 22 L. Tong and S. Perreau, "Multichannel blind identification: From subspace to maximum likelihood methods," *Proc. IEEE*, Vol. 86, No. 10, pp. 1951-68, 1998.
 - 23 J. Fang, A. R. Leyman, and Y. H. Chew, "A new closed-form solution for blind MIMO FIR channel estimation with colored sources," *In Proceedings of IEEE International Conference on Acoustics, Speech, and Signal Processing (ICASSP'05)*, Philadelphia, Mar. 2005, pp. 1049-52.
 - 24 S. Chen, X. C. Yang, and L. Hanzo, "Blind joint maximum likelihood channel estimation and data detection for single-input multiple-output systems," *In Proceedings of 6th IEEE International Conference of 3G and Beyond*, London, Nov 2005, pp. 57-61.
 - 25 C. Q. Chang, S. F. Yau, P. Kwok, F. K. Lam, and F. H. Chan, "Sequential approach to blind source separation using second order statistics," *In Proceedings of 1st International Conference on Information, Communication, and Signal Processing (ICICS'97)*, Sep. 1997, pp. 1608-12.

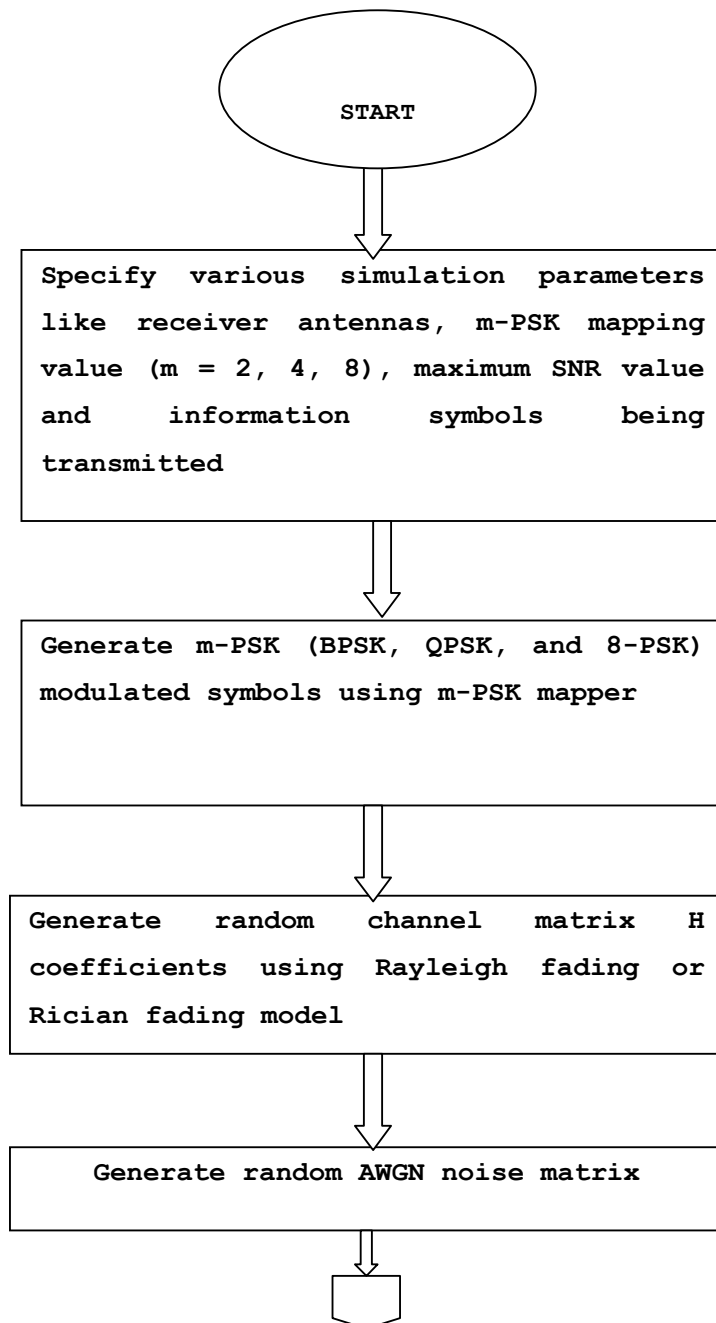
- 26 K. Abed-Meraim, Y. Xiang, J. H. Manron, and Y. B. Hua, "A new approach to blind separation of cyclostationary sources," *In Proceedings of 2nd IEEE Workshop on Signal Processing Advances in Wireless Communications*, Annapolis, May 1999, pp. 114-7.
- 27 J. Fang, A. R. Leyman, Y. H. Chew, and H. Duan, "Some further results on blind identification of MIMO FIR channels via second-order statistics," *Elsevier Signal Processing*, Vol. 87, No. 6, pp. 1434-47, Jun 2007.
- 28 J. F. Cardoso, "Source separation using higher ordered moments," *In Proceedings of IEEE International Conference on Acoustics, Speech, and Signal Processing (ICASSP'89)*, Glasgow, 1989, pp. 2109-12.
- 29 P. Comon, "Independent component analysis: A new concept?" *Elsevier Signal Processing*, Vol. 36, No. 3, pp. 287-314, 1994.
- 30 C.Y. Chi, C. Y. Chen, C. H. Chen, and C. C. Feng, "Batch processing algorithms for blind equalization using higher-order statistics," *IEEE Signal Process. Mag.*, Vol. 20, No. 1, pp. 25-49, 2003.
- 31 T. Wo and P. A. Hoehner, "Semi-blind channel estimation for frequency-selective MIMO systems," *In IST Mobile Summit*, Dresden, Jun 2005, pp.23-27.
- 32 T. Cui and C. Tellambura, "Semiblind channel estimation and data detection for OFDM systems with optimal pilot design," *IEEE Trans. on Commun.*, Vol. 55, No. 5, pp. 1053-62, May 2007.
- 33 T. Wo, P. A. Hoehner, A. Scherb and K. D. Kammeyer, "Performance analysis of maximum-likelihood semi-blind estimation of MIMO channels," *In Proceedings of 63rd IEEE Vehicular Technology Conference (VTC)*, Melbourne, May 2006, pp. 1738-42,
- 34 M. A. Khalighi and S. Bourennane, "Semi-blind single-carrier MIMO channel estimation using overlay pilots," *IEEE Trans. on Vehicular Tech.*, Vol. 57, No. 3, pp. 1951-6, May 2008.
- 35 S. Shirvani Moghaddam and H. Saremi, "Performance evaluation of LS algorithm in both training-based and semi-blind channel estimations for MIMO systems," *In Proceedings of 1st IFIP/IEEE Wireless Days (WD) Conference*, Dubai, Nov 2008, pp. 1-5.
- 36 A. Medles and D. T. Slock, "Semiblind channel estimation for MIMO spatial multiplexing systems," *In Proceedings of 54th IEEE Vehicular Technology Conference (VTC'01)*, Oct 2001, pp.1240-44.
- 37 A. K. Jagannatham, C. R. Murthy, and B. D. Rao, "Semi-blind MIMO channel estimation scheme for MRT," *In Proceedings of International Conference on Acoustics, Speech, Signal Processing (ICASSP'05)*, Philadelphia, Mar 2005, pp. 585-8.
- 38 A. K. Jagannatham and B. D. Rao, "Constrained ML algorithms for semi-blind MIMO channel estimation," *In Proceedings of IEEE Global Telecommun. Conf.*

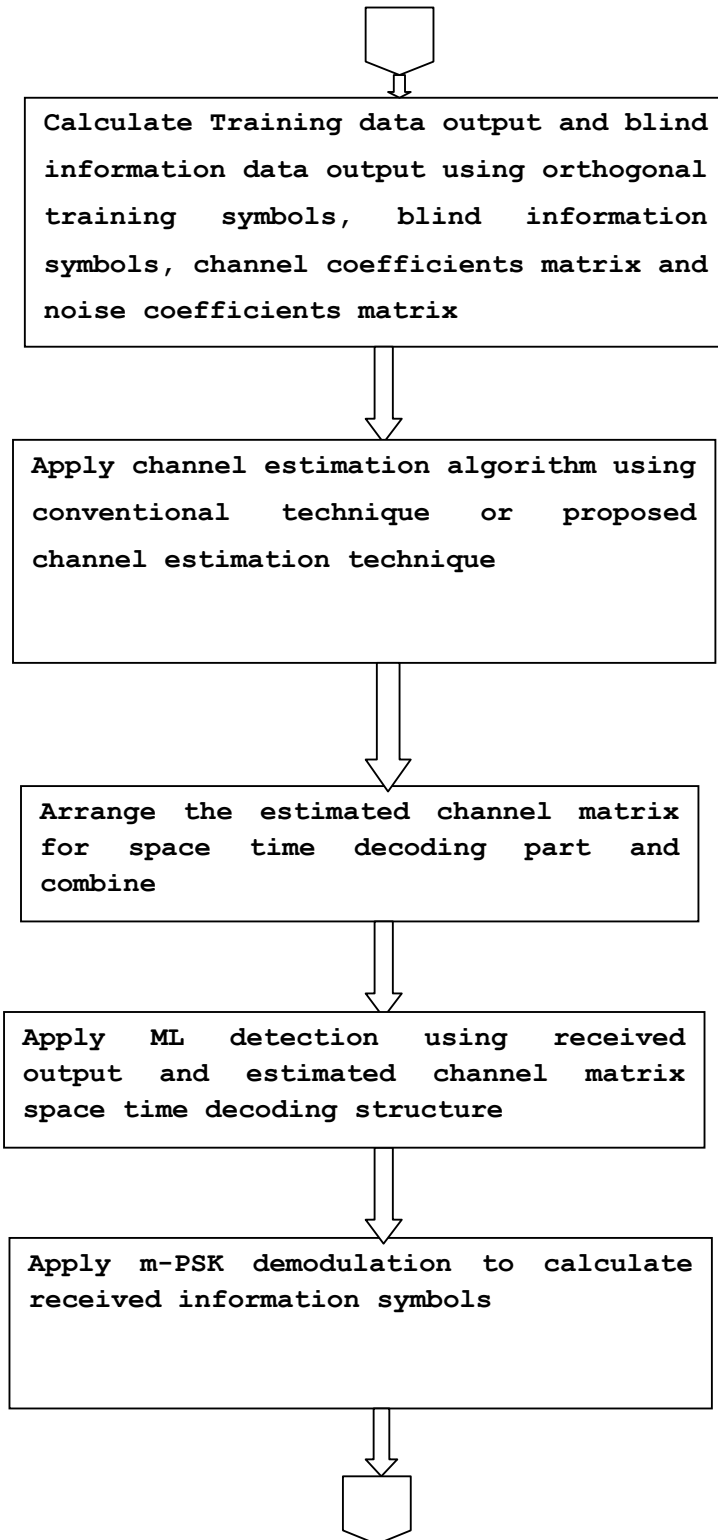
- (*GLOBECOM'04*), Dallas, Dec. 2004, pp. 2457-79.
- 39 C. R. Murthy, A. K. Jagannatham, and B. D. Rao, "Training-based and semiblind channel estimation for MIMO systems with maximum ratio transmission," *IEEE Trans. on Signal Process.*, Vol. 54, No. 7, pp. 2546-58, 2006.
 - 40 A. K. Jagannatham and B. D. Rao, "A semi-blind technique for MIMO Channel matrix estimation," *In Proceedings. of IEEE Workshop on Signal Processing Advances in Wireless Communications (SPAWC 2003)*, Rome, Italy , 2004, pp. 304-308.
 - 41 Xia Liu, Feng Wang and Marek E. Bialkowski "Investigation into a Whitening-Rotation-Based Semi-blind MIMO Channel Estimation for Correlated" *International Conference on Signal Processing and Communication Systems, ICSPCS 2008*, pp. no. 1-4.
 - 42 Qingwu Zhang, Wei-Ping Zhu, Qingmin Meng, "Whitening-rotation-based semi-blind estimation of MIMO FIR channels," *International Conference on Wireless Communications & Signal Processing, WCSP 2009*, pp. 1-4.
 - 43 Feng Wan, Wei-Ping Zhu and M.N.S. Swamy, "Perturbation Analysis of Whitening-Rotation-based Semi-Blind MIMO Channel Estimation," *IEEE International Midwest Symposium on Circuits and Systems, MWSCAS '09*, 2009, pp. 240-243.
 - 44 A. K. Jagannatham and B. D. Rao, "Whitening-rotation-based semiblind MIMO channel estimation," *IEEE Trans. on Signal Processing*, vol. 54, no. 3, pp. 861–869, 2006.
 - 45 J. Akhtman and L. Hanzo, "Reduced-complexity maximum likelihood detection in multiple-antenna-aided multicarrier system," *In Proceedings of 5th International Workshop on Multi-Carrier Spread-Spectrum*, Sep 2005, Germany, pp. 21-8.
 - 46 S. K. Jayaweera and H. V. Poor, "On the capacity of multiple-antenna systems in Rician fading," *IEEE Trans. on Wireless Comm*, Vol. 4, No. 3, pp. 1102-11, May 2005.

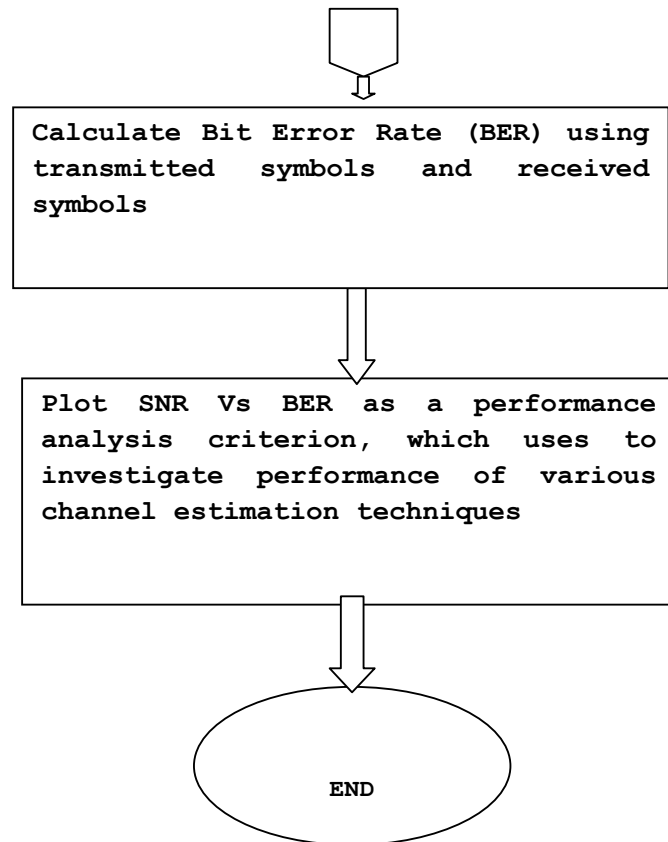
APPENDIX- A

List of Research Papers Published

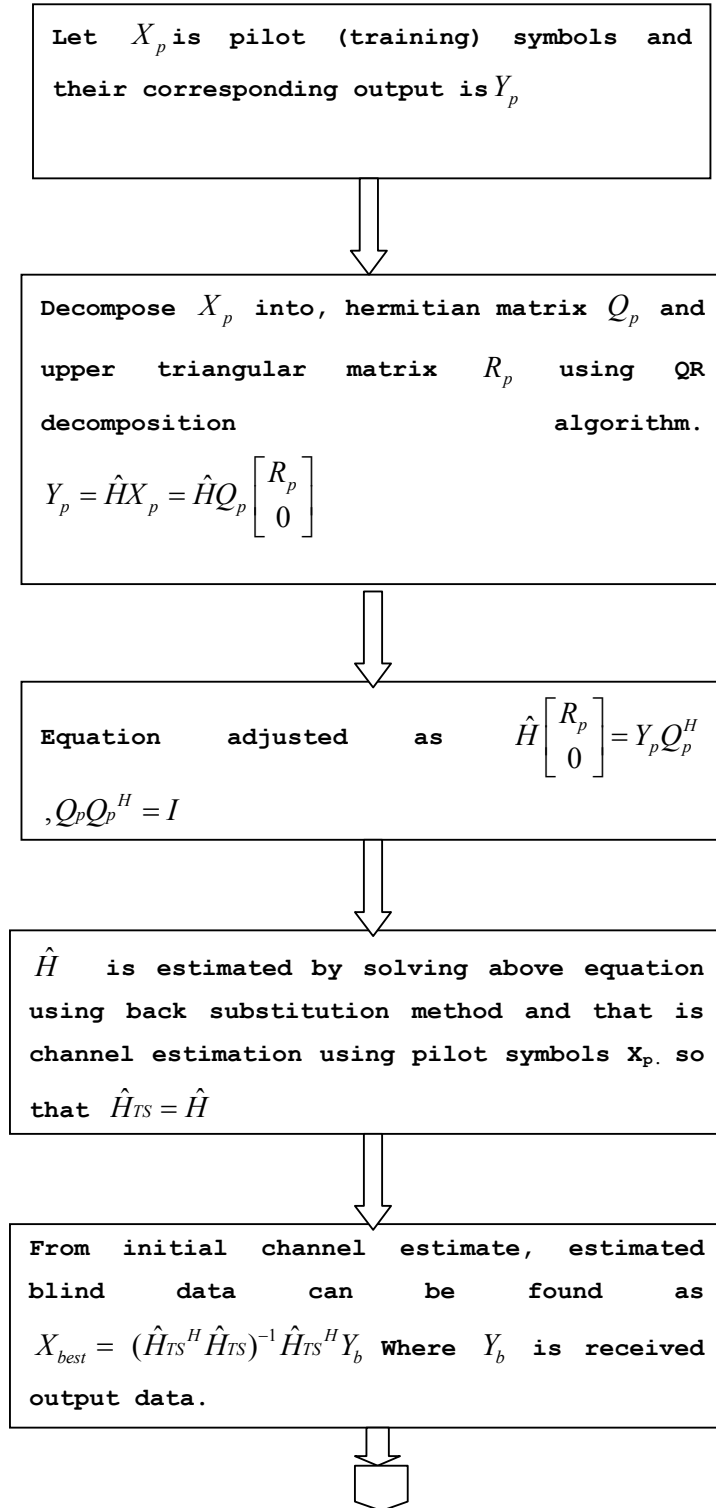
- 1 Bhalani, J. K., D. Chauhan, Y. P. Kosta, and A. I. Trivedi. "Near optimal performance joint semi-blind channel estimation and data detection techniques for Alamouti coded single-carrier (SC) MIMO communication systems." *Physical Communication-Journal* (2013), Elsevier
- 2 J. Bhalani, D. Chauhan, Y.P.Kosta, A.I.Trivedi, "Novel Semi-blind Channel Estimation Schemes for Rician Fading MIMO Channels," *International Journal of Radioelectronics and Communications Systems*, Springer, Vol. 55, No. 4, pp. 149-156, April 2012.
- 3 Jaymin Bhalani, A.I.Trivedi, "Orthogonal Matrix Triangularization based Novel Joint Semi-blind Channel and Data Estimation Technique for MIMO Communication System," *2011 IEEE International conference on Computational Intelligence and Computing Research*, Kanyakumari Dec. 2011, pp. 441-445.
- 4 Jaymin Bhalani, A.I.Trivedi, "Modified Whitening Rotation based Joint Semi-blind Channel and Data Estimation Scheme for Rayleigh Flat Fading MIMO channels," *ACEEE International conference on Advances in Engineering and Technology- AET 2011*, Noida ,Dec. 2011, pp. 90-94.
- 5 Jaymin Bhalani, D. Chauhan, Y.P.Kosta, A.I.Trivedi, "Novel Semi-blind Channel Estimation Schemes for Rayleigh Flat Fading MIMO Channels," *International Journal of Communications, Network and System Sciences (IJCNS) USA*, Vol. 4, No. 9, pp. 578-584, September 2011.
- 6 Jaymin Bhalani, D. Chauhan, A.I.Trivedi, "Performance Investigation of OPML Semi-Blind MIMO Channel Estimation Technique under Various Modulation Schemes and Different Receiver Antennas," *CiiT International Journal of Digital Signal Processing*, Vol.3, No.6, pp. 268-270, July 2011.
- 7 Jaymin Bhalani, D Chauhan, A.I.Trivedi, "Performance Comparison of Orthogonal Pilot and Rotation Optimization Maximum Likelihood Estimator for Semi-Blind Multiple Input Multiple Output Channel Estimation," *International Conference on Advances in Communication, Network, and Computing*, Kozhikode, Kerela, October-2010, pp 317-320.
- 8 Jaymin Bhalani, A.I.Trivedi, Y.P.Kosta, "Performance Evaluation of Orthogonal Pilot ML and Rotation Optimization ML Semi-Blind Channel Estimation for MIMO Communication System" *International Journal of Advances in Wireless and Mobile Communications (AWMC)*, Vol.3, No.2, pp. 93-100, 2010.
- 9 Jaymin Bhalani, A.I.Trivedi, Y.P.Kosta, "Performance Comparison of Semi-blind Channel Estimation Methods of MIMO Communication Systems," *First IEEE/IFIP Asian Himalayas International Conference on Internet*, Nepal, Nov. 3-5, 2009, pp 1-5.

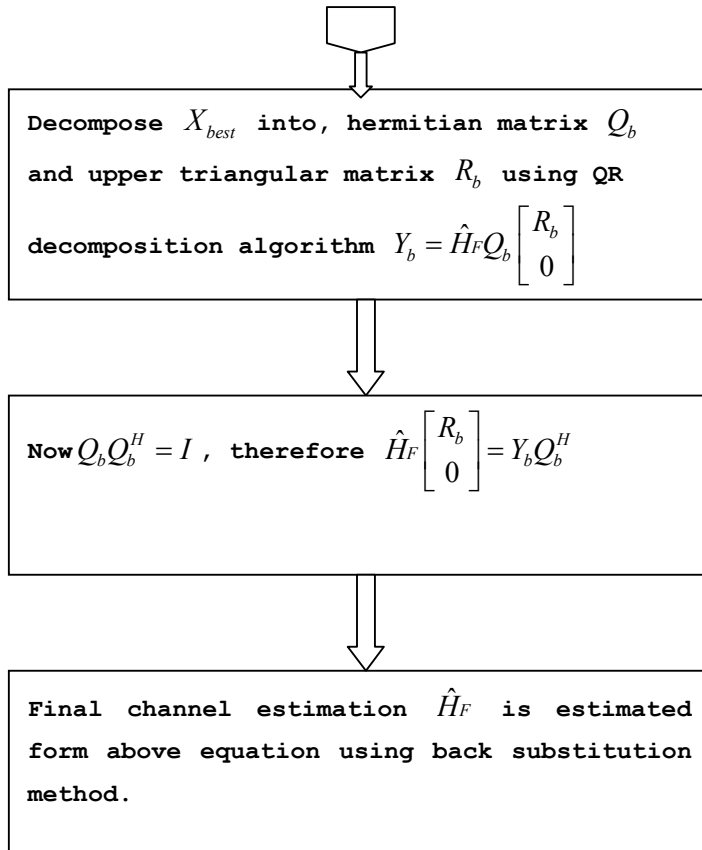
APPENDIX- B**Overall Work flow diagram:**



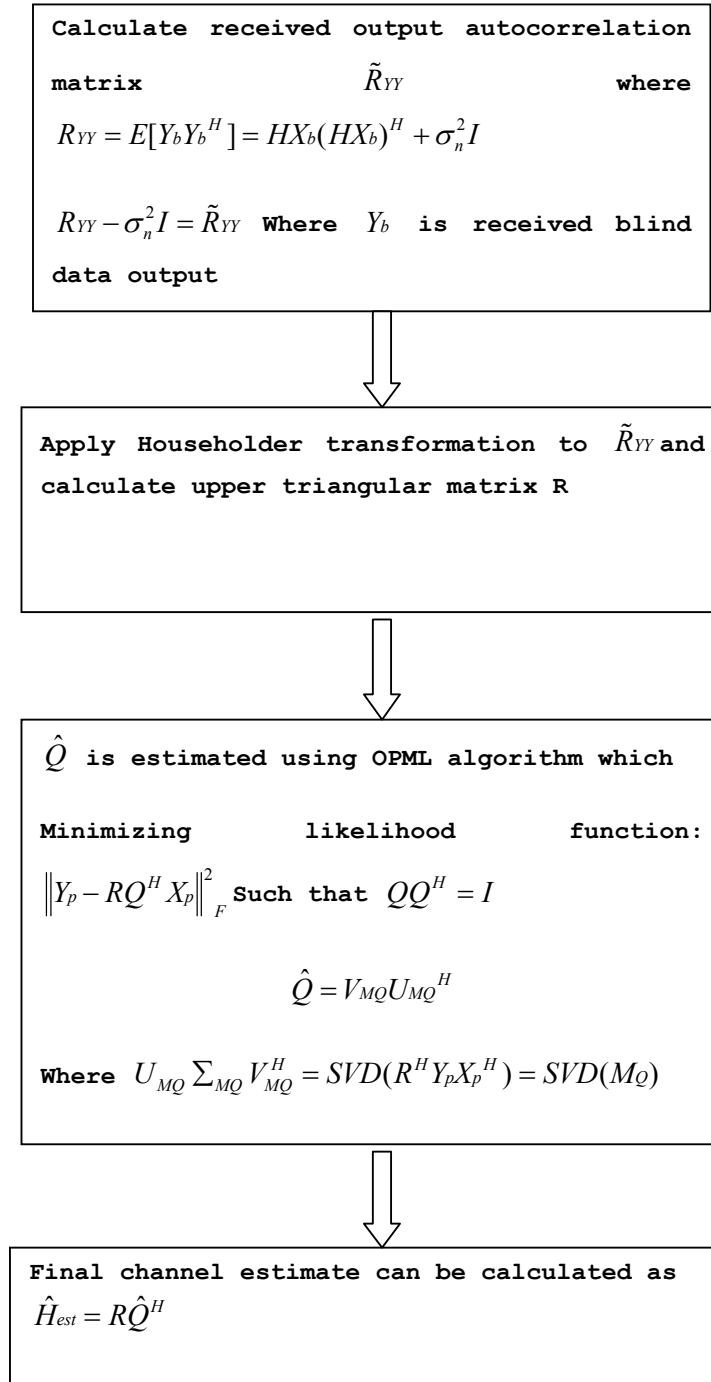


**Flow diagram of Joint Channel Estimation and Data Detection QR-NEW
(Proposed Technique-I):**

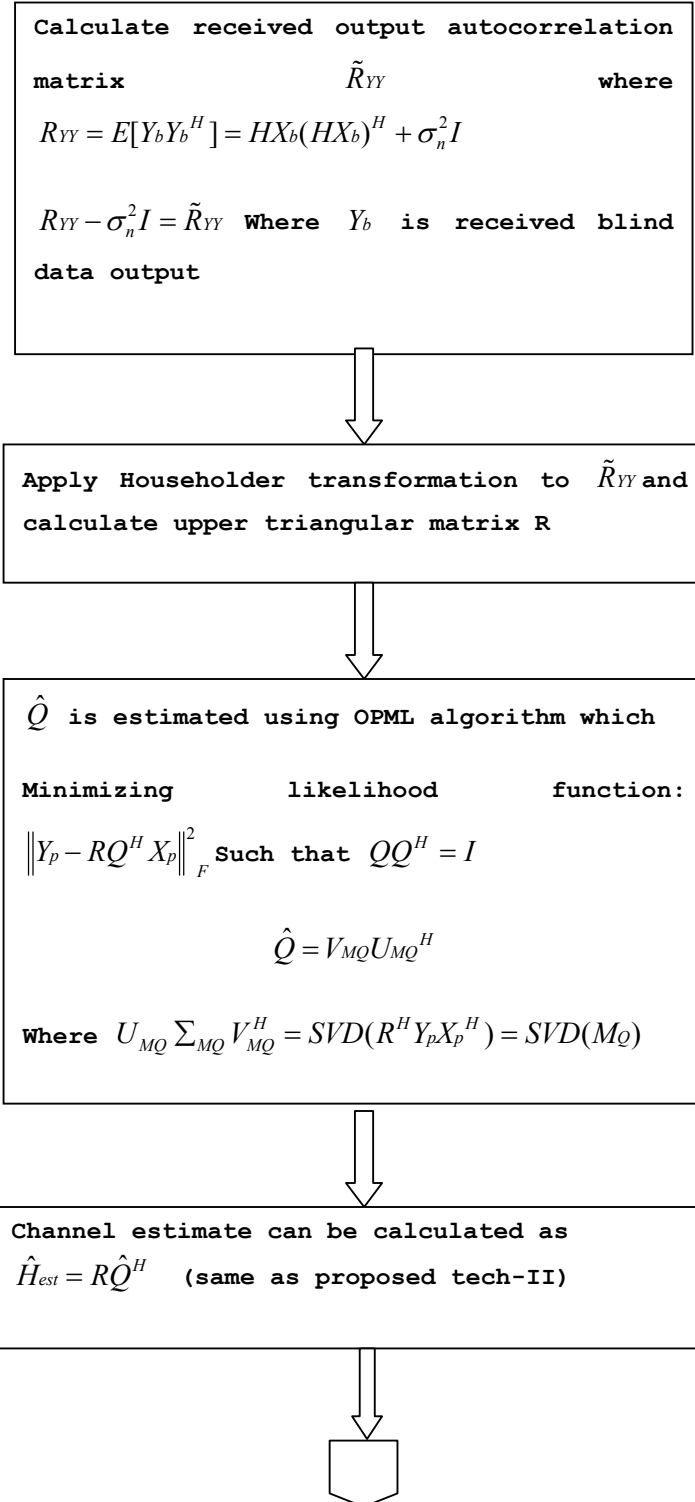




Flow diagram of Householder QR-OPML (Proposed Technique-II):



Flow diagram of Householder QR-OPML-NEW (Proposed Technique-III):





Given channel knowledge (estimate), find error covariance matrix of estimated channel

$$\arg \min E \left\| H - \hat{H}_{est} \right\|^2 \text{ and, } \Re e_h = \sigma_n^2 E(H^H \hat{H}_{est})$$

$X_{pnew} = (\Re e_h X_P)$ where X_P are conventional orthogonal pilot symbols



Again perform OPML algorithm to minimize given cost function represented as

$$\left\| Y_P - R \hat{Q}_b^H X_{pnew} \right\|_F^2$$

$$\hat{Q}_b = V_{MQnew} U_{MQnew}^H \text{ where}$$

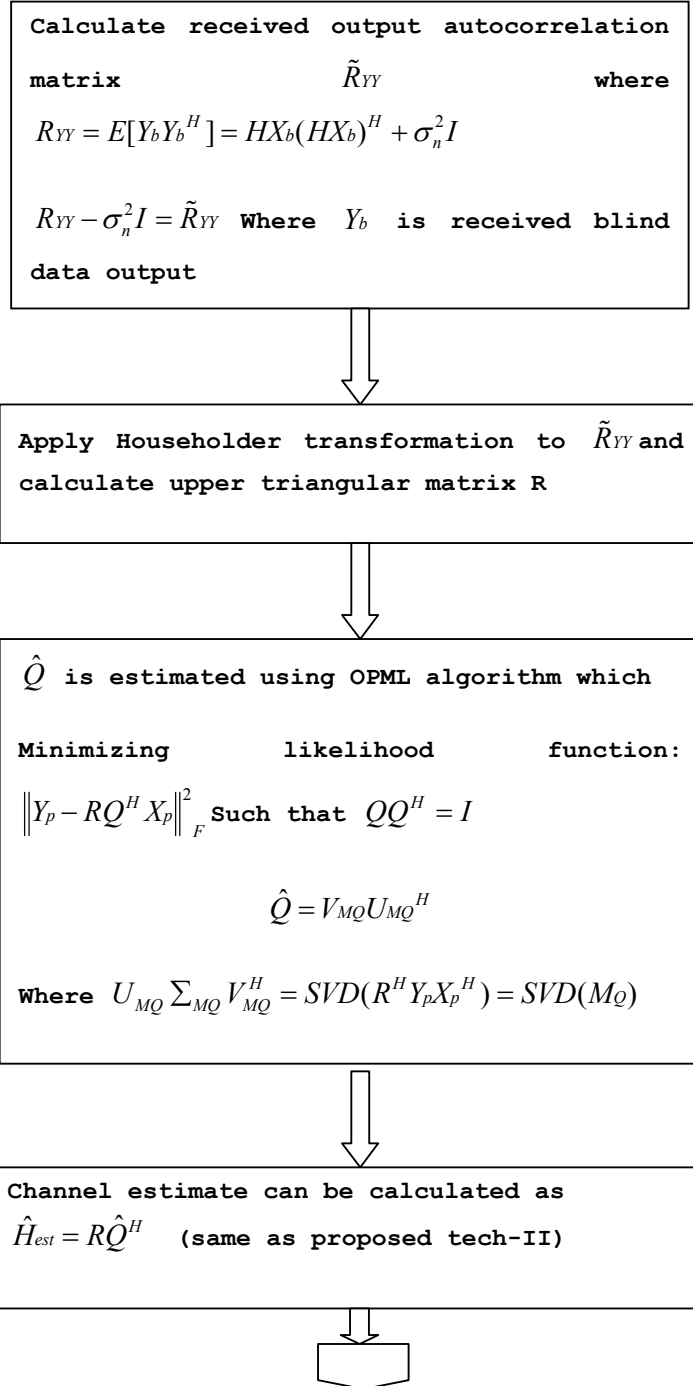
$$U_{MQnew} \sum_{MQnew} V_{MQnew}^H = SVD(R^H Y_P X_{pnew}^H) = SVD(M_{Qnew})$$



Final channel matrix H is then estimated as

$$\hat{H} = R \hat{Q}_b^H$$

Flow diagram of Householder QR-OPML- Joint Semi-Blind Channel Estimation and Data Detection (JSBCDE) (Proposed Technique-IV):





Given channel knowledge (estimate), perform data detection as

$$X_{besti} = \hat{H}_{est}^\dagger Y_b = (\hat{H}_{est}^H \hat{H}_{est})^{-1} \hat{H}_{est}^H Y_b$$

Find error covariance matrix of estimated data

$$\arg \min E \|X_b - X_{besti}\|^2 = \arg \min E \|H^\dagger Y_b - \hat{H}_{est}^\dagger Y_b\|^2$$

$\mathfrak{R}e_i = \sigma_n^2 E(X_b X_{besti}^H)$ and new pilot symbols are derived as $X_{pnewi} = (\mathfrak{R}e_i X_P)$ where X_P are conventional orthogonal pilot symbols



Again perform OPML algorithm using new pilot symbols to minimize given cost function represented as

$$\|Y_P - R \hat{Q}_{bi}^H X_{pnewi}\|_F^2$$

$$\hat{Q}_{bi} = V_{MQnewi} U_{MQnewi}^H \text{ where}$$

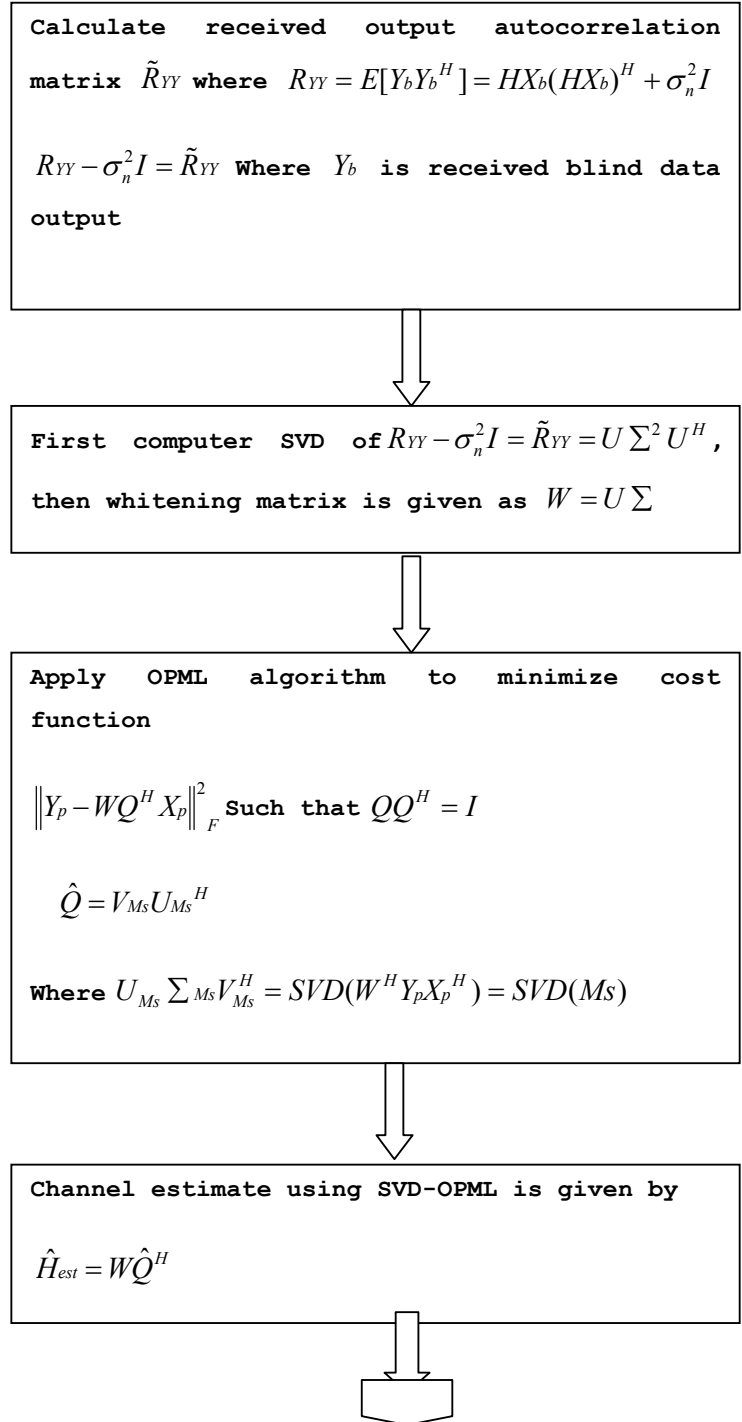
$$U_{MQnewi} \Sigma_{MQnewi} V_{MQnewi}^H = SVD(R^H Y_P X_{pnewi}^H) = SVD(M_{Qnewi})$$

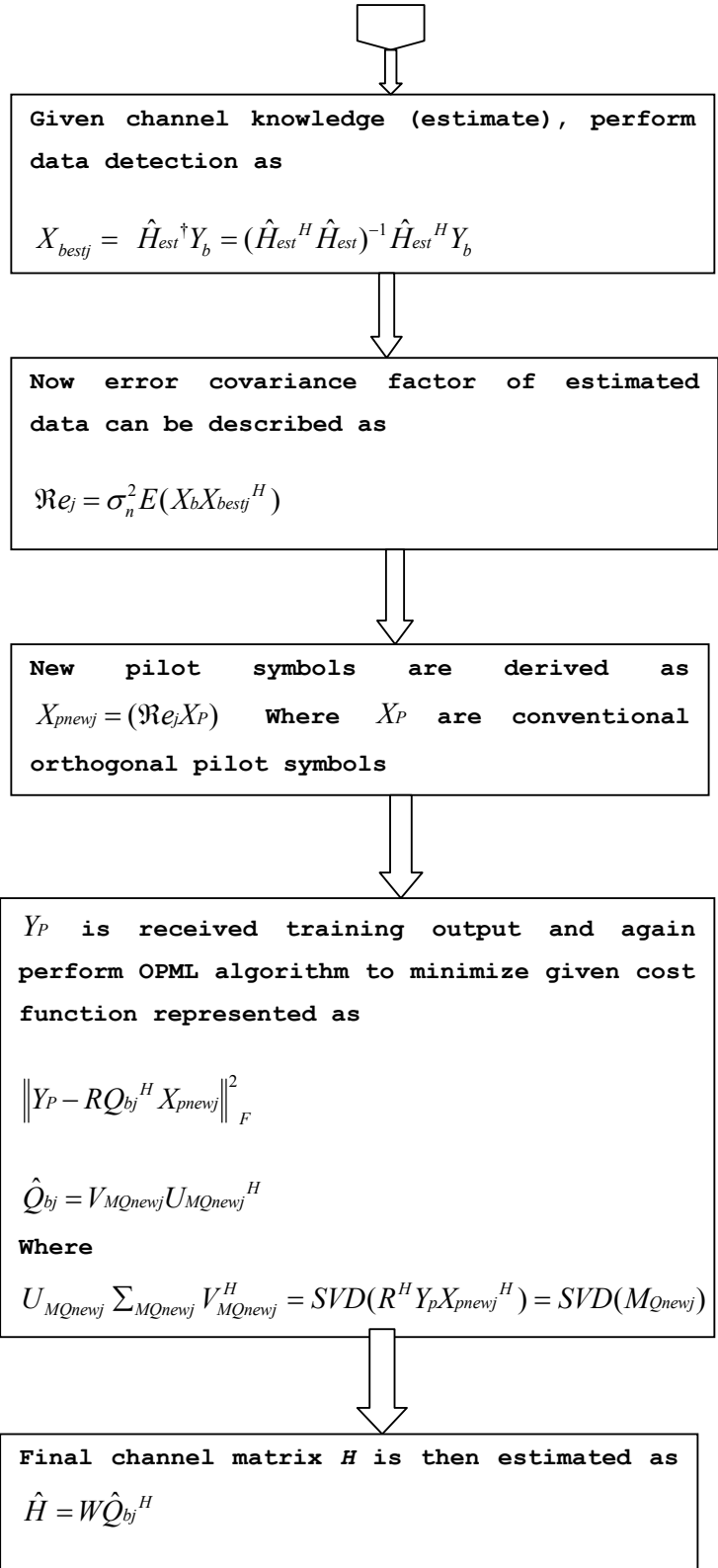


Final channel matrix H is then estimated as

$$\hat{H} = R \hat{Q}_{bi}^H$$

Flow diagram of Modified Whitening Rotation (SVD-OPML) based Joint Semi-Blind Channel Estimation and Data Detection (Proposed Technique -V):





APPENDIX- C
Explanation of Equation 4.78-4.83 of Chapter no. 4 in detail:

Equation 4.78 of OPML algorithm is given below

$$\|Y_P - WQ_{bj}^H X_{pnewj}\|_F^2 \quad \text{Such that } Q_{bj}Q_{bj}^H = I \quad \dots (C1)$$

Where Y_P is received training output, X_{pnewj} is newly derived pilot symbols from error covariance factor and channel matrix is $H = WQ_{bj}^H$

(Refer section 4.5.5 in thesis.)

Now from the WR (SVD-OPML) technique which mentioned in section 4.3, We know that MIMO channel $H \in C^{N \times M}$ which has at least as many receive antennas as transmit antennas i.e. $N \geq M$. Then, the channel matrix H can be decomposed as $H = WQ^H$ where $W \in C^{N \times M}$ is also known as the whitening matrix which can be estimated blindly from the autocorrelation matrix of received data alone and $Q \in C^{M \times M}$, termed as the rotation matrix, that is unitary i.e. $Q^H Q = Q Q^H = I$ which can be estimated using orthogonal pilot symbols using OPML algorithm.

Hence as a part of semi-blind channel estimation, estimated channel matrix is given by equation 4.14 as

$$\hat{H} = W\hat{Q}^H \quad \dots(C2)$$

Explanation of OPML algorithm in detail:

Now as a part of OPML algorithm, cost minimization function is given as

$$\|Y_p - HX_p\|_F^2 = \|Y_p - WQ^H X_p\|_F^2 \quad \text{Such that } QQ^H = I \quad \dots (C3)$$

Upper problem is *mean of squared Frobenius norm* which is explained as

$$\|A\|_F^2 = \text{trace}(AA^H) \quad \dots (C4)$$

When trace of matrix is sum of diagonal entries of matrix.

So from that we can write using mathematical background

$$\begin{aligned} \|Y_p - WQ^H X_p\|_F^2 &= \text{tr}(Y_p Y_p^H) + \text{tr}(WW^H QQ^H X_p X_p^H) - 2\text{tr}((Q^H X_p)^H W^H Y_p) \\ &= \text{tr}(Y_p Y_p^H) + \text{tr}(WW^H) - 2\text{tr}((Q^H X_p)^H W^H Y_p) \quad \dots (C5) \end{aligned}$$

, provided $QQ^H = I = X_p X_p^H$

Now for minimizing that cost function occurs by maximizing $\text{tr}((Q^H X_p)^H W^H Y_p)$

From that maximizing Q can be found by calculating SVD of $(W^H Y_p X_p^H = Ms)$

$$U_{M_s} \sum_{M_s} V_{M_s}^H = \text{SVD}(W^H Y_p X_p^H) = \text{SVD}(Ms) \quad \dots (C6)$$

$$\text{So } U_{M_s} \sum_{M_s} V_{M_s}^H = W^H Y_p X_p^H \quad \dots (C7)$$

$$\text{Further } U_{M_s}^H (W^H Y_p X_p^H) V_{M_s} = \sum_{M_s} = \text{diag}(\sigma_1, \sigma_2, \dots, \sigma_L) \quad \dots \text{ (C8)}$$

$$\text{Now } \text{tr}(Q W^H Y_p X_p^H) = \text{tr}(Q U_{M_s} \sum_{M_s} V_{M_s}^H) = \text{tr}(Z \sum_{M_s}) \quad \dots \text{ (C9)}$$

$$\text{Where } Z = Q U_{M_s} V_{M_s}^H \quad \dots \text{ (C10)}$$

Here upper bound is attained by setting $Z = I$ where I is identity matrix.

Hence

$$Z = Q U_{M_s} V_{M_s}^H = I \quad \dots \text{ (C11)}$$

$$\text{So } \hat{Q} = V_{M_s} U_{M_s}^H \quad \dots \text{ (C12)}$$

Which is equivalent framework shown in equation 4.81. Thus it proves.

Actually this gives relationship between two subspaces. That is rotation of subspaces as a part of mathematical background.

And finally $\hat{H} = W \hat{Q}^H$ shows final semi-blind channel estimate which is explained in equation no 4.83.